

HUMAN-SERINE HYDROXYMETHYLTRANSFERASE (hSHMT)

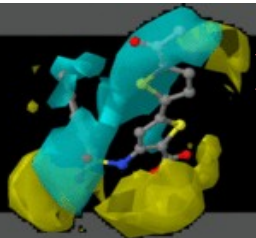


SAPIENZA
UNIVERSITÀ DI ROMA

**Facoltà di Farmacia e Medicina
Corso di Laurea in Farmacia
Tesi Sperimentale in Chimica Farmaceutica
a.a. 2019/2020**

**Laureanda: Giorgos Episkopou
Matricola: 1925359**

Relatore: prof. Rino Ragno



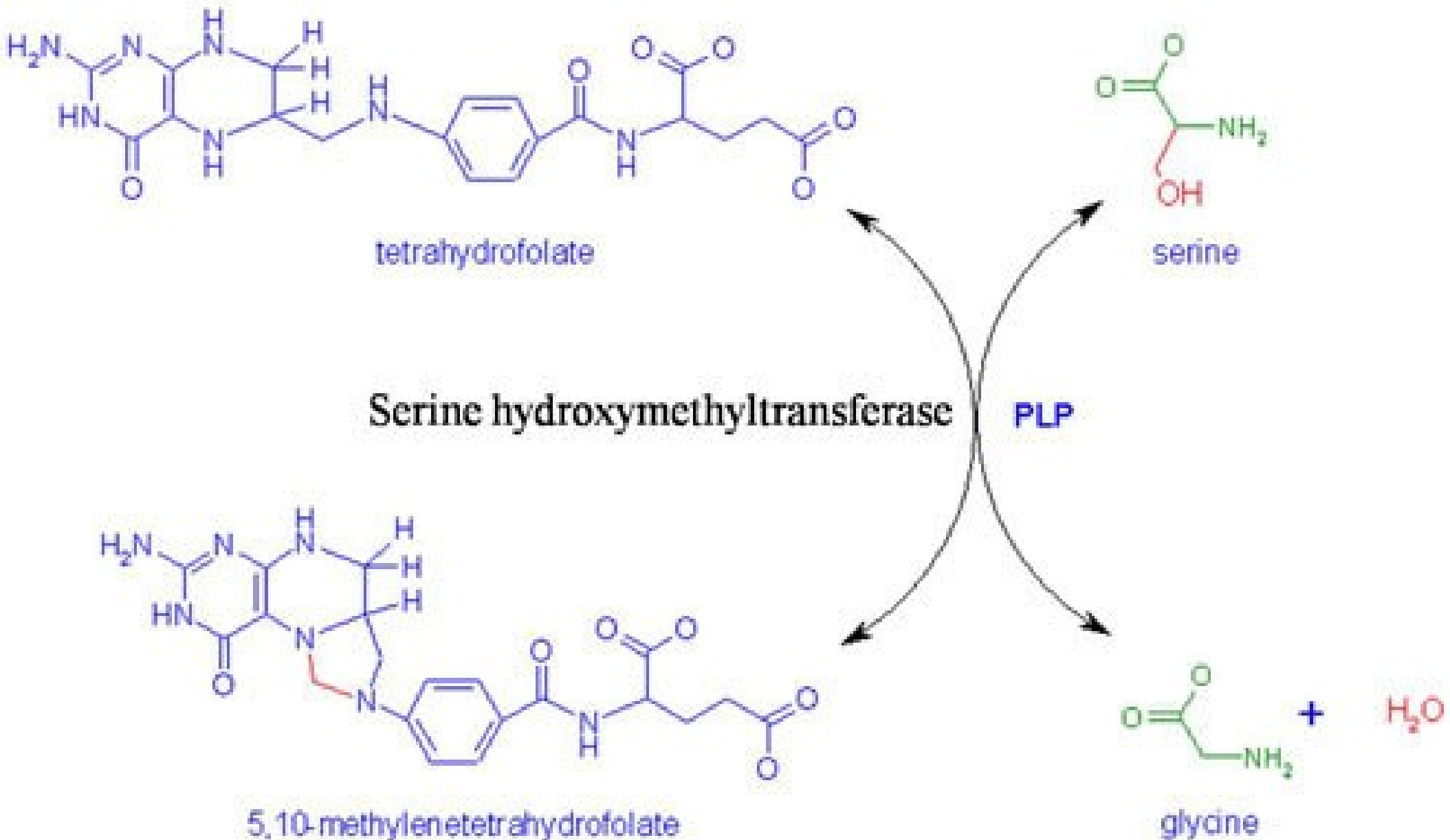
HUMAN-SERINE HYDROXYMETHYLTRANSFERASE (hSHMT)

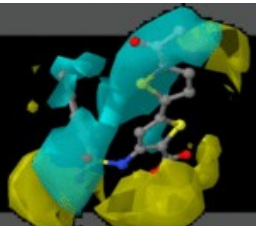
by www.RCMD.it

Serine hydroxymethyltransferase is a pyridoxal-5'-phosphate-dependent enzyme and catalyses the reversible reaction of serine cleavage to glycine, where the resulting hydroxymethyl group is transferred to tetrahydrofolate (THF), generating 5,10-methyleneTHF and H₂O.

SHMT Reaction

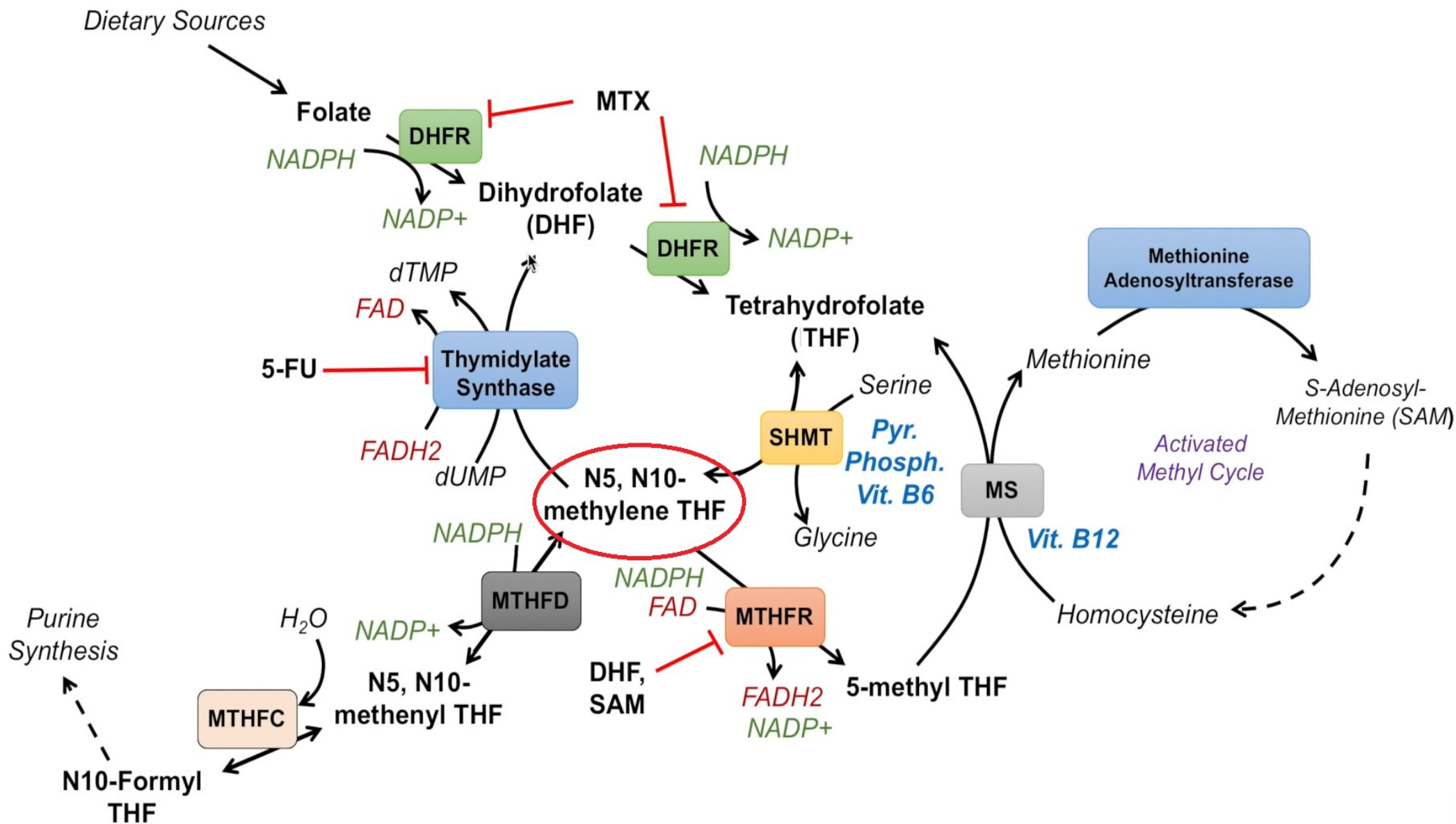
by www.RCMD.it





SHMT Biochemical Pathway

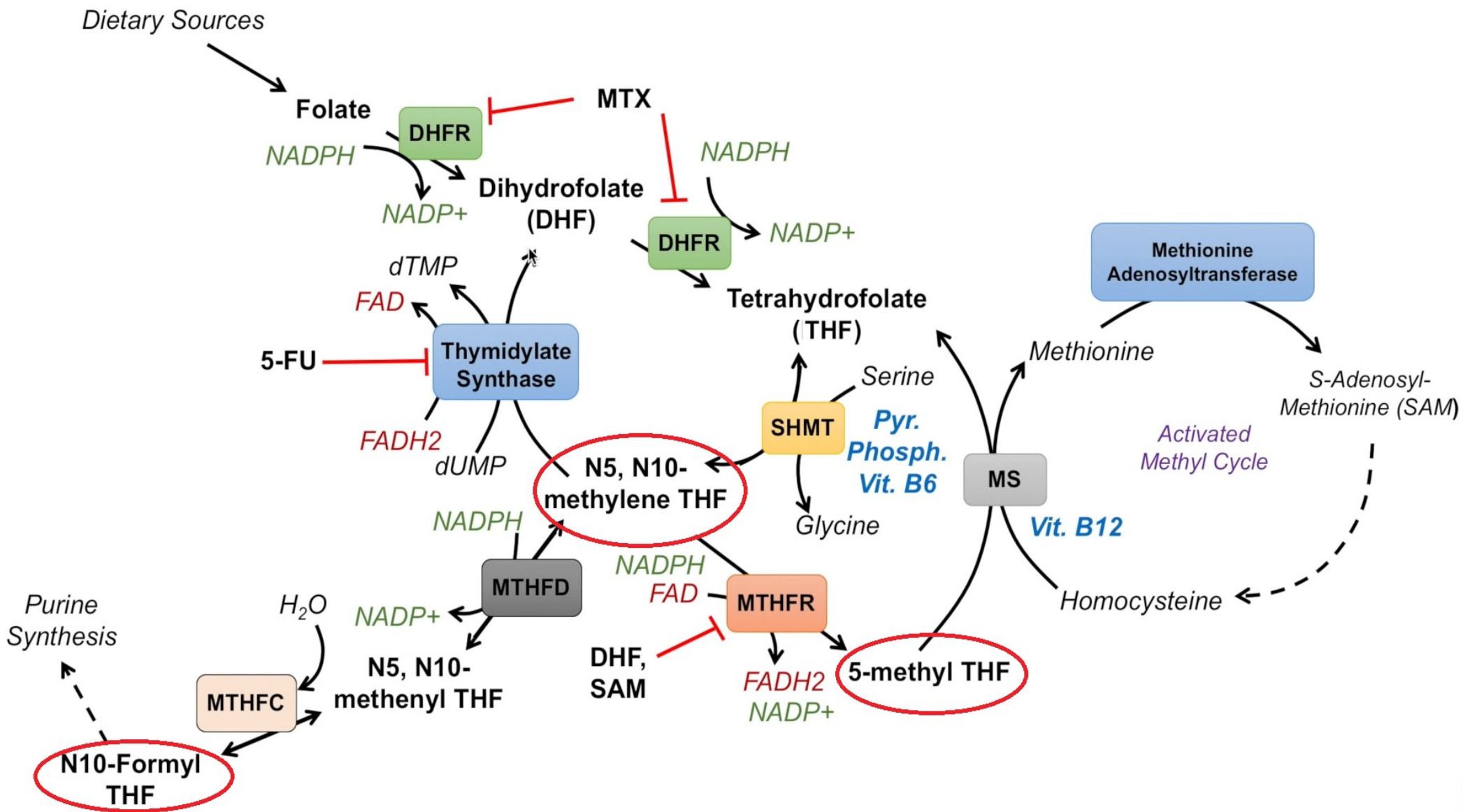
by www.rcmd.it

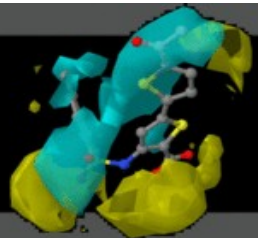




SHMT Biochemical Pathway

by www.RCMD.it

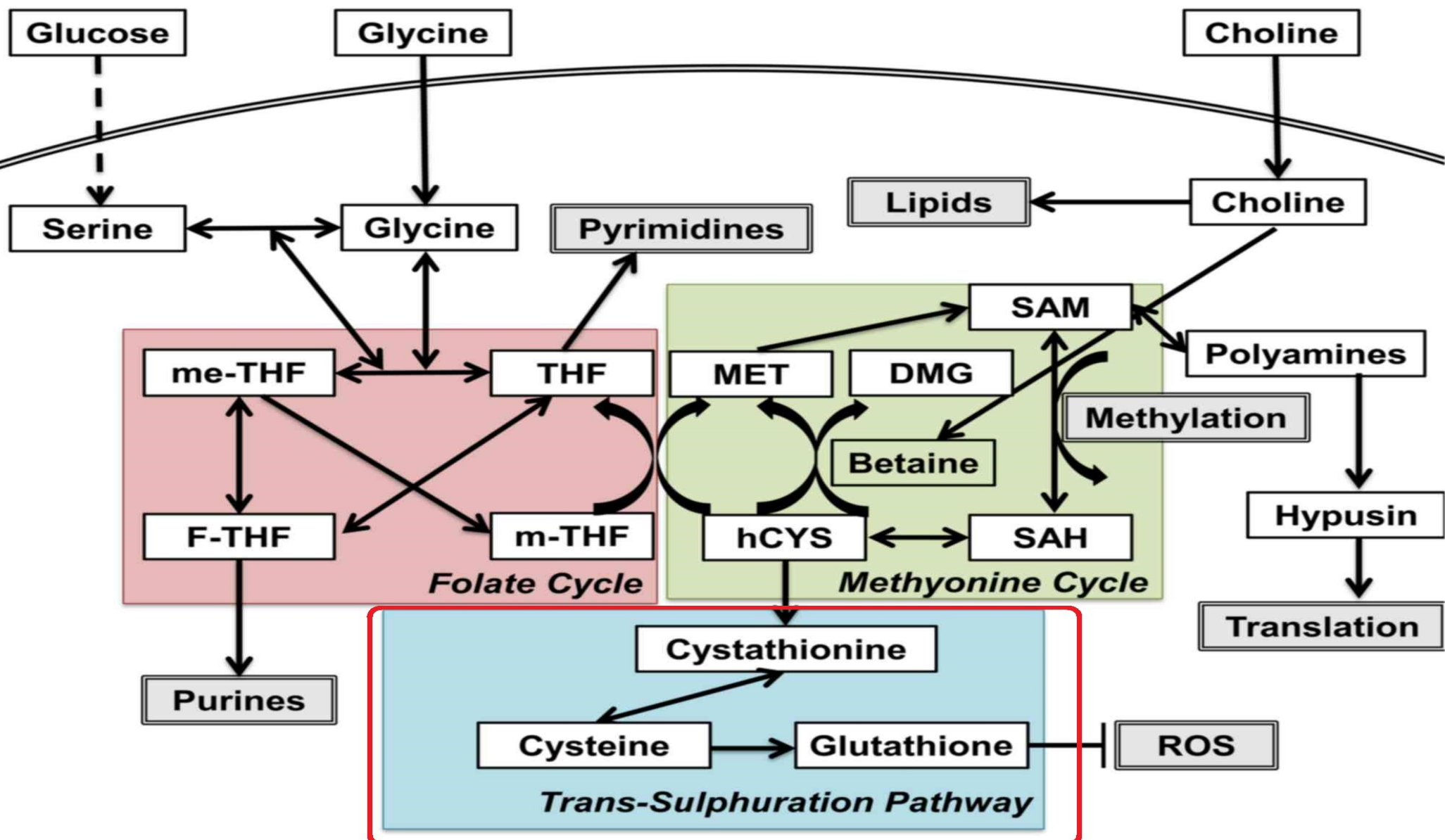


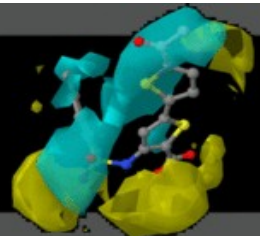


One carbon Metabolism

by www.RCMD.it

- One-carbon (C1) metabolism encompasses a complex metabolic network based on the chemical reaction of folate compounds.
- The folate cycle **couples with the methionine cycle** to form a bicyclic metabolic pathway that circulates carbon units as part of a process referred to as the C1 metabolism .
- These two cycles **also link with the trans-sulfuration pathway**, which plays a critical role in the regulation of the redox state by producing glutathione and SAM.

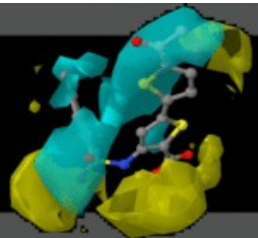




Role of One Carbon Metabolism

by www.RCMD.it

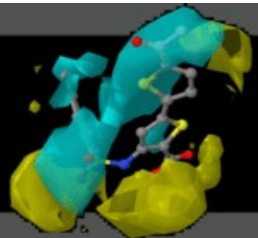
- The output of one-carbon metabolism includes a myriad of components essential to the synthesis of all macromolecules, **such as proteins, lipids, and nucleic acids.**
- C1 metabolism is critical for the **maintenance of genomic stability** through nucleotide metabolism as well as for the **epigenetic control of DNA and histones**, altered expression of which is a characteristic attribute of tumor cells.
- The methionine cycle is required for the **synthesis of phosphatidylcholine**, which contributes 50% of lipid membrane content . Methionine itself is required for protein synthesis, but the adenylation of methionine produces S-adenosylmethionine (SAM). **SAM functions as a methyl donor** for other metabolic pathways that require methyl moieties. Glutathione is also important for the maintenance of the NADP⁺/NADPH ratio and is the **major contributor to redox balance.**



SHMT ISOFORMS

by www.RCMD.it

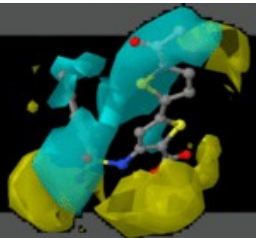
- In humans and other higher organisms, two SHMT genes are found (SHMT1 and SHMT2), encoding the cytoplasmic (hcSHMT) and mitochondrial (hmSHMT) isozymes.
- SHMT2 encodes a second transcript (hcSHMTa), lacking a short exon, that is only required for efficient import into mitochondria.
- This third isozyme (hcSHMTa) is identical to hmSHMT but localizes in the cytoplasm together with hcSHMT.



SHMT2 Isoform

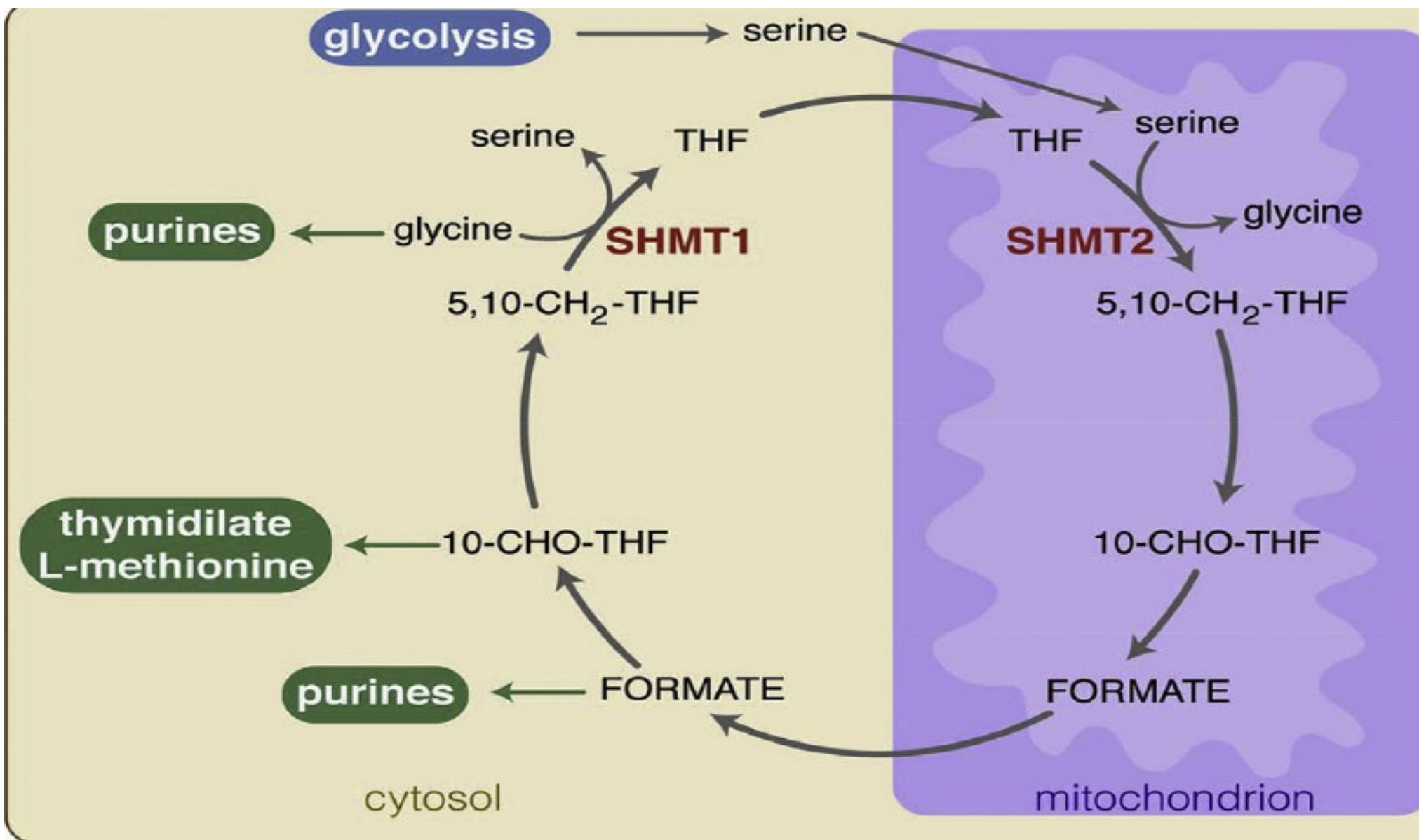
by www.RCMD.it

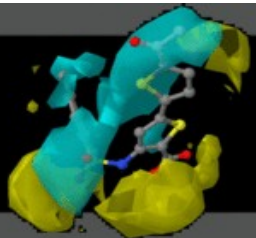
- Serine hydroxymethyltransferase 2 (SHMT2) regulates one-carbon transfer reactions that are essential for amino acid and nucleotide metabolism, and uses pyridoxal-5'-phosphate (PLP) as a cofactor.
- Apo SHMT2 exists as a dimer with unknown functions, whereas PLP binding stabilizes the active tetrameric state.
- **SHMT2 also promotes inflammatory cytokine signalling** by interacting with the deubiquitylating BRCC36 isopeptidase complex (BRISC), although it is unclear whether this function relates to metabolism.



Compartmentalisation

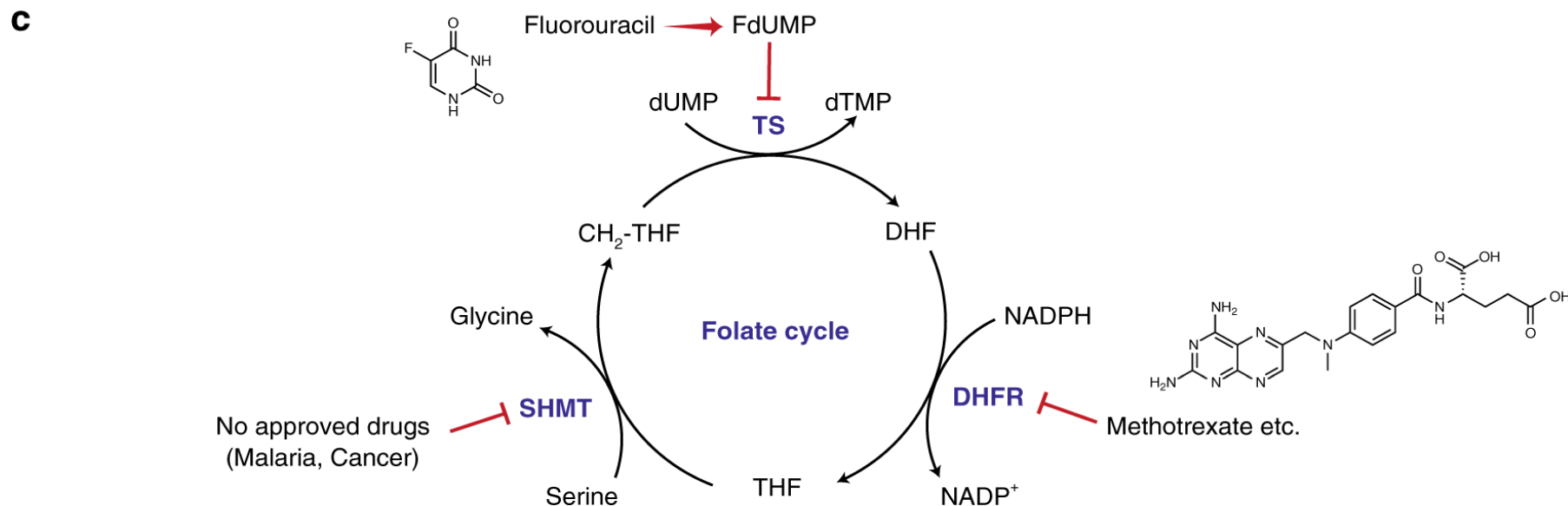
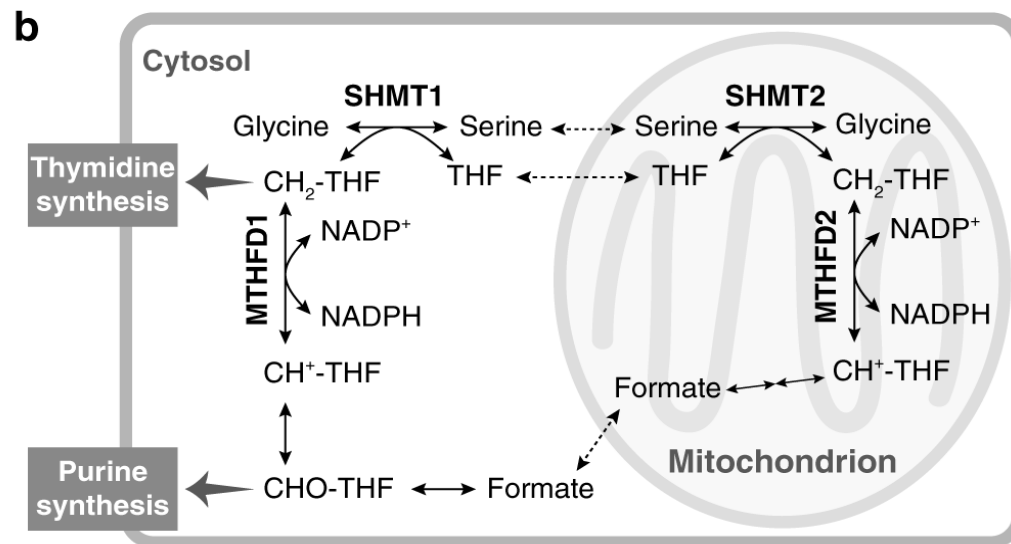
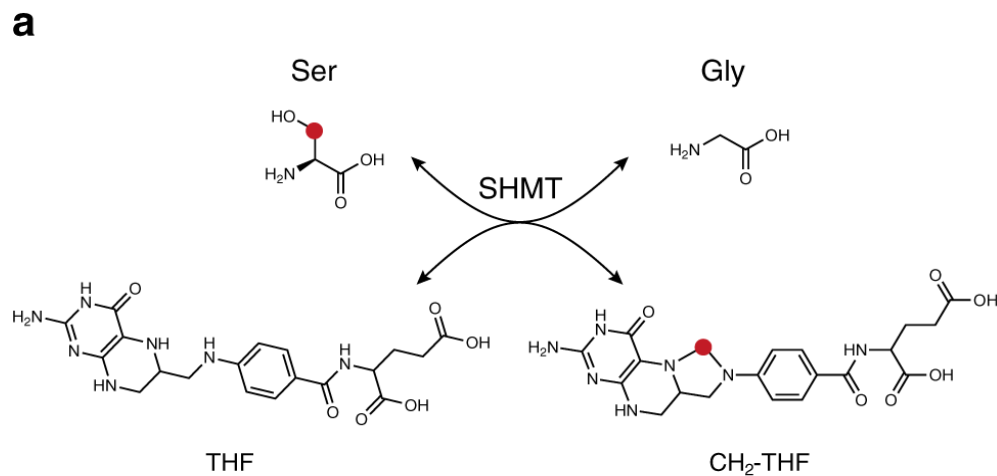
by www.RCMD.it

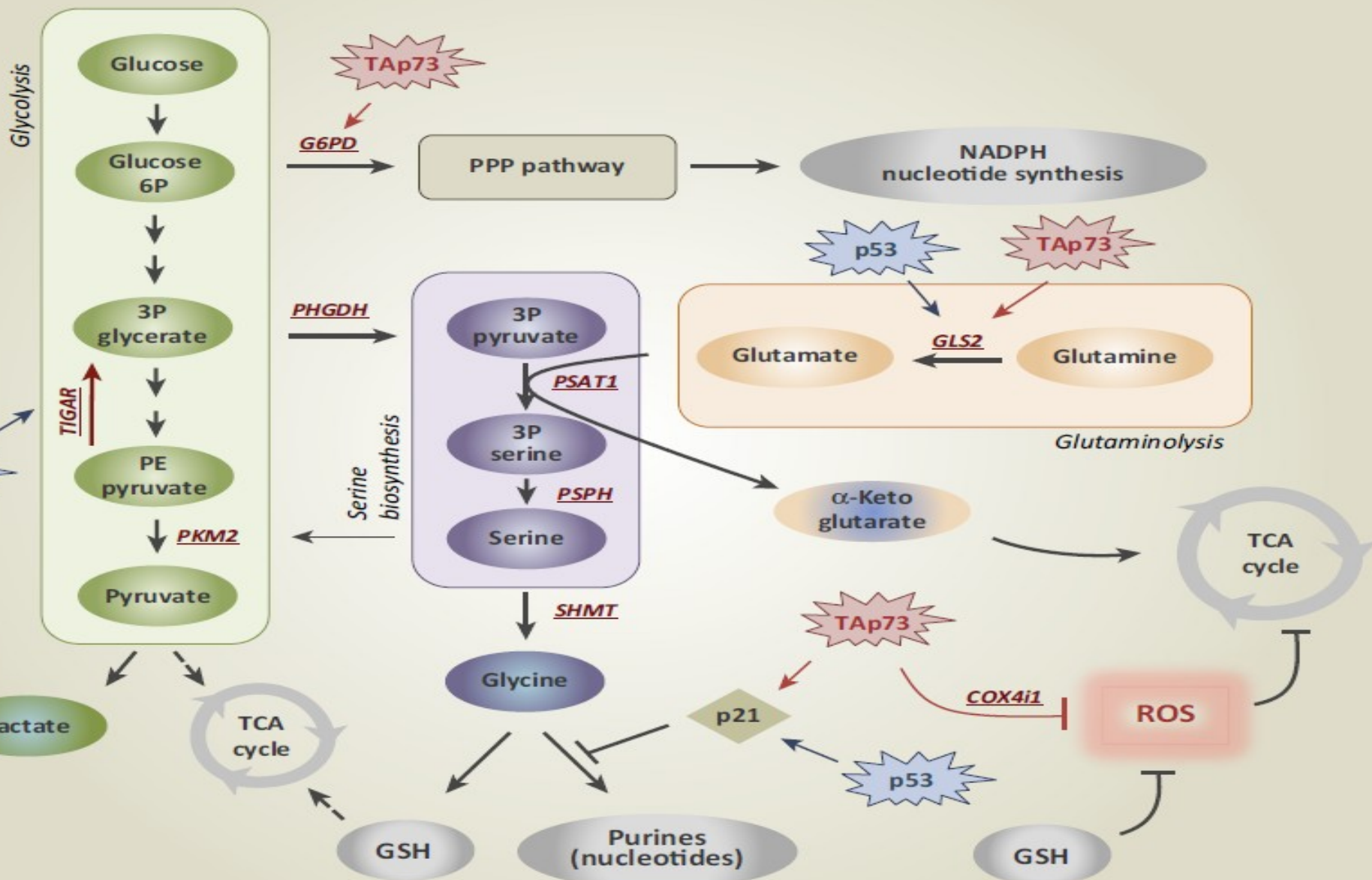


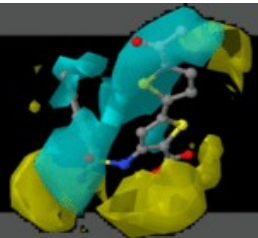


A brief synopsis of SHMT

by www.RCMD.it



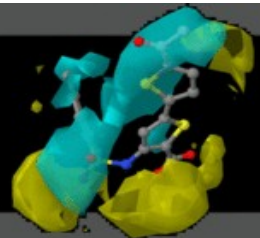




STRUCTURE

by www.RCMD.it

- The structure of the SHMT monomer is similar across prokaryotes and eukaryotes, but **the active enzyme is a dimer in prokaryotes and exists as a tetramer in eukaryotic cells.**
- The eukaryotic SHMT tetramer resembles two prokaryotic dimers that have packed together, forming what has been described as a “dimer of dimers”.
- **SHMT has been assigned to the fold type I (α class) of PLP enzymes,** but it exhibits only very low sequence identity with other members of this family (e.g. aspartate aminotransferase-AAT)
- **His135** in the human cytosolic enzyme, **is involved in tetramer formation.** His135 in the human enzyme is positioned in the **very centre of the tetramer.** The imidazole sidechain ring of a particular subunit stacks onto the equivalent ring of another subunit, that is, the interactions are His135(A)–His135(B) and His135(C)–His135(D).



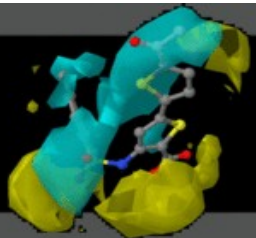
SHMT Tetramer

by www.rcmd.it



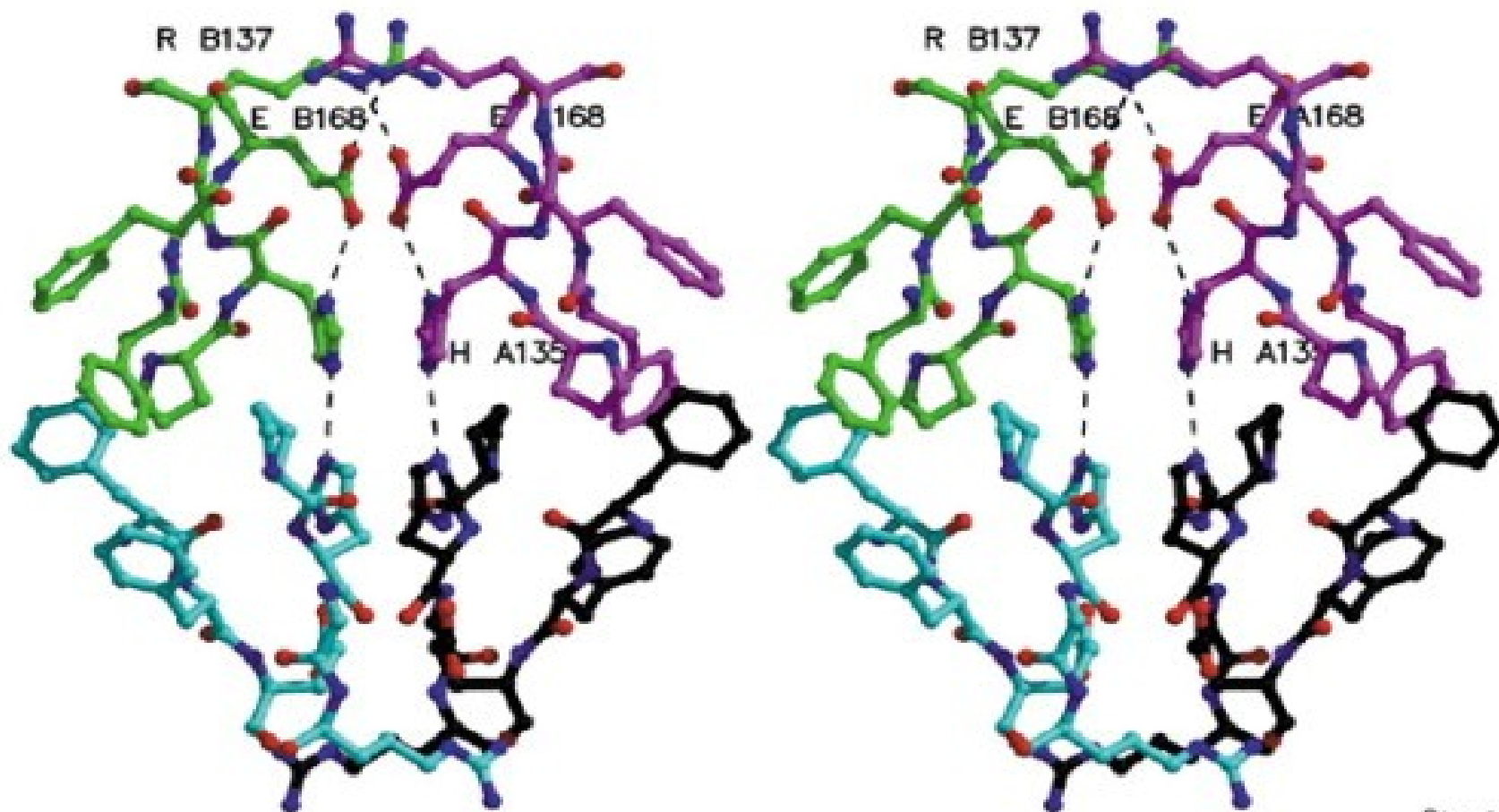
Structure

Stereoview cartoon representation of the SHMT tetramer. Subunit A is coloured in cyan, B in brown, C in green and D in purple. A–D and B–C form the ‘tight’ dimers, which are related by a horizontal twofold axis. Bound PLP cofactor is shown in space-filling representation.



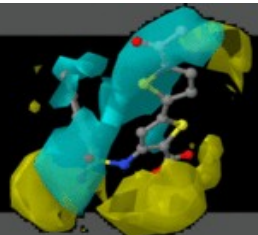
HISTIDINES-CLUSTER

by www.RCMD.it



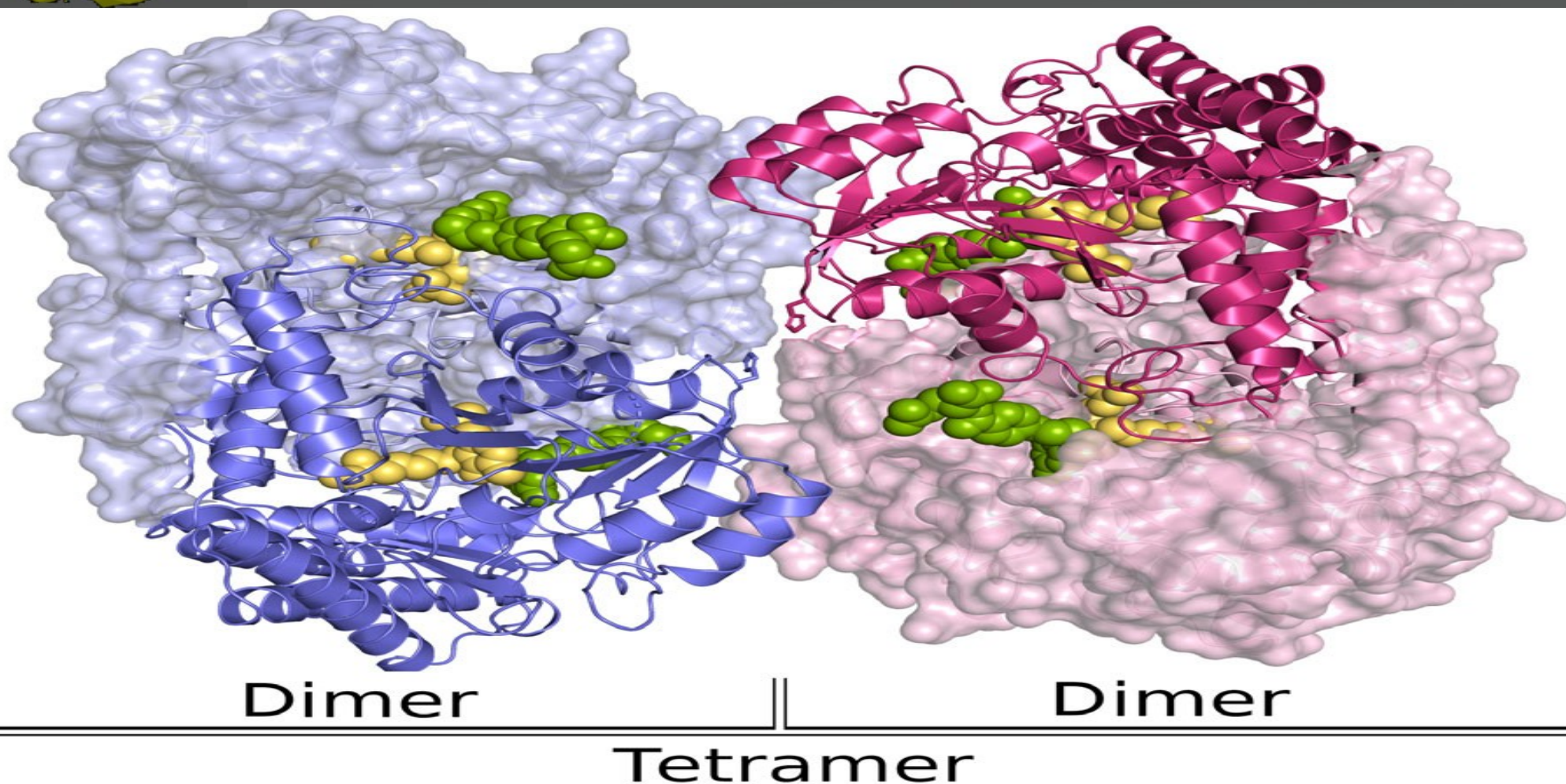
Structure

Stereoview of the tetramer centre showing the central role of His135. The carbon atoms of the A,B,C and D subunits are coloured in purple, green, cyan and black, respectively. For the sake of clarity, only two of the four hydrogen-bond networks involving His135 and its symmetry-related mates are drawn (dashed lines).

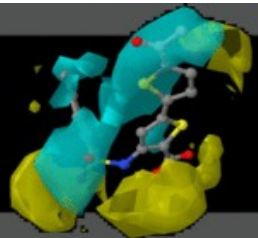


SHMT2 TETRAMER

by www.RCMD.it



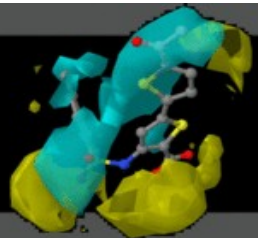
The crystal structure of lometrexol bound hSHMT2. Crystallographic structure of tetrameric hSHMT2 with individual monomers shown as ribbon representations. hSHMT2 is a 'dimer of dimers' and is comprised of two tight dimers which are related by two perpendicular two-fold axes, passing through the centre of the His158 cluster. The two tight dimers of the tetramer are coloured blue and pink, respectively. Single monomers from each tight dimer are shown as surface representations. The histidines from the His158 cluster located at the centre of the tetramer are shown as sticks. The PLP cofactor (yellow) and lometrexol (green) are depicted as space-filling representations.



SHMT Monomer Structure

by www.RCMD.it

- The monomer fold can be described in terms of three domains: **The N-terminus, the ‘large’ domain and the ‘small’ domain.**
- The first domain, the N-terminus, mediates **intersubunit contacts** and folds into two α helices and one β strand.
- The second (large) N-terminal domain **binds PLP**. It folds into an $\alpha\beta$ sandwich containing nine α helices wrapped around a seven-stranded mixed β sheet. **The large domain in the eukaryotic form also contains a histidine that is essential for tetramer stability**
- The C-terminal small domain folds into an $\alpha\beta$ sandwich. This sheet packs on one side against the large domain and is shielded from the solvent by four helices on the other side.



Monomer Structure

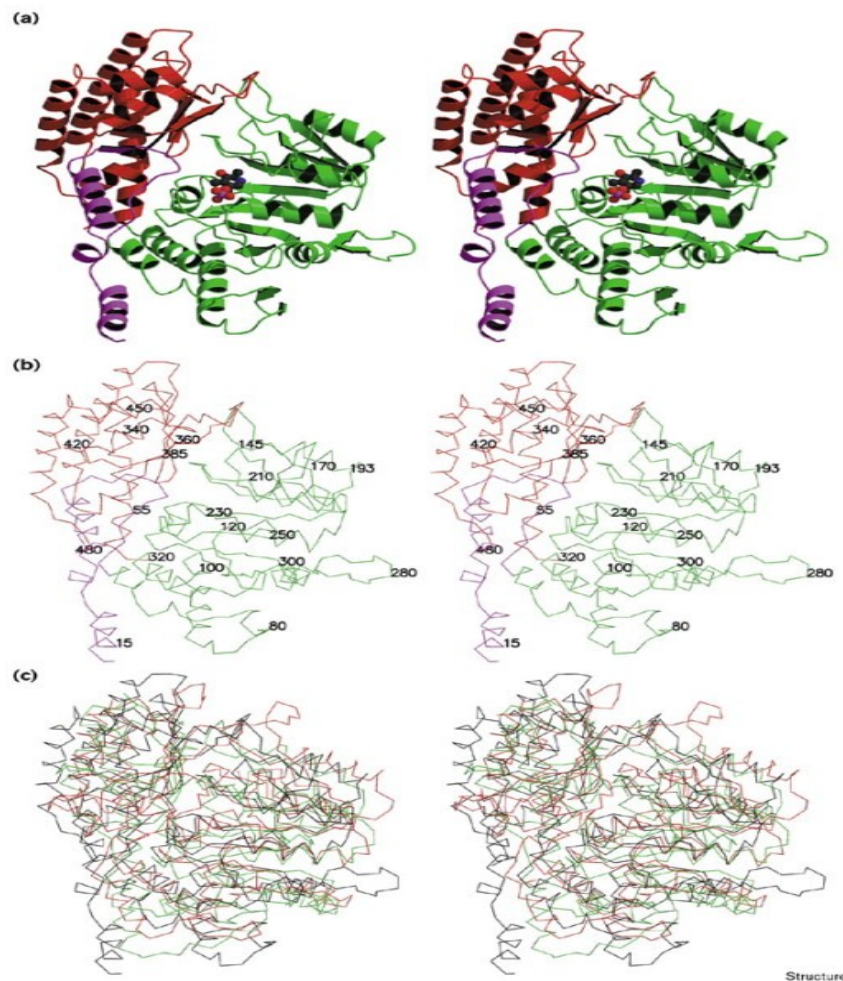
by www.RCMD.it



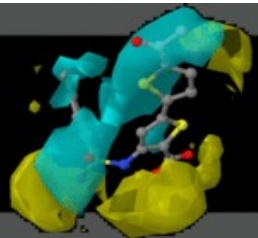


Monomer Structure

by www.RCMD.it



The overall fold of the SHMT monomer. (a) Stereoview ribbon diagram of the monomer. The N terminus is shown in purple, the small domain in red and the large domain in green. The cofactor PLP is shown in ball-and-stick representation. (The figure was prepared using MOLSCRIPT and Raster3D .) (b) Stereoview $C\alpha$ plot of the monomer with residue numbering. The domains are coloured as in (a). (c) Stereoview $C\alpha$ overlay of SHMT (black), dialkylglycine decarboxylase (DKB; red) and aspartate aminotransferase (AAT; green).



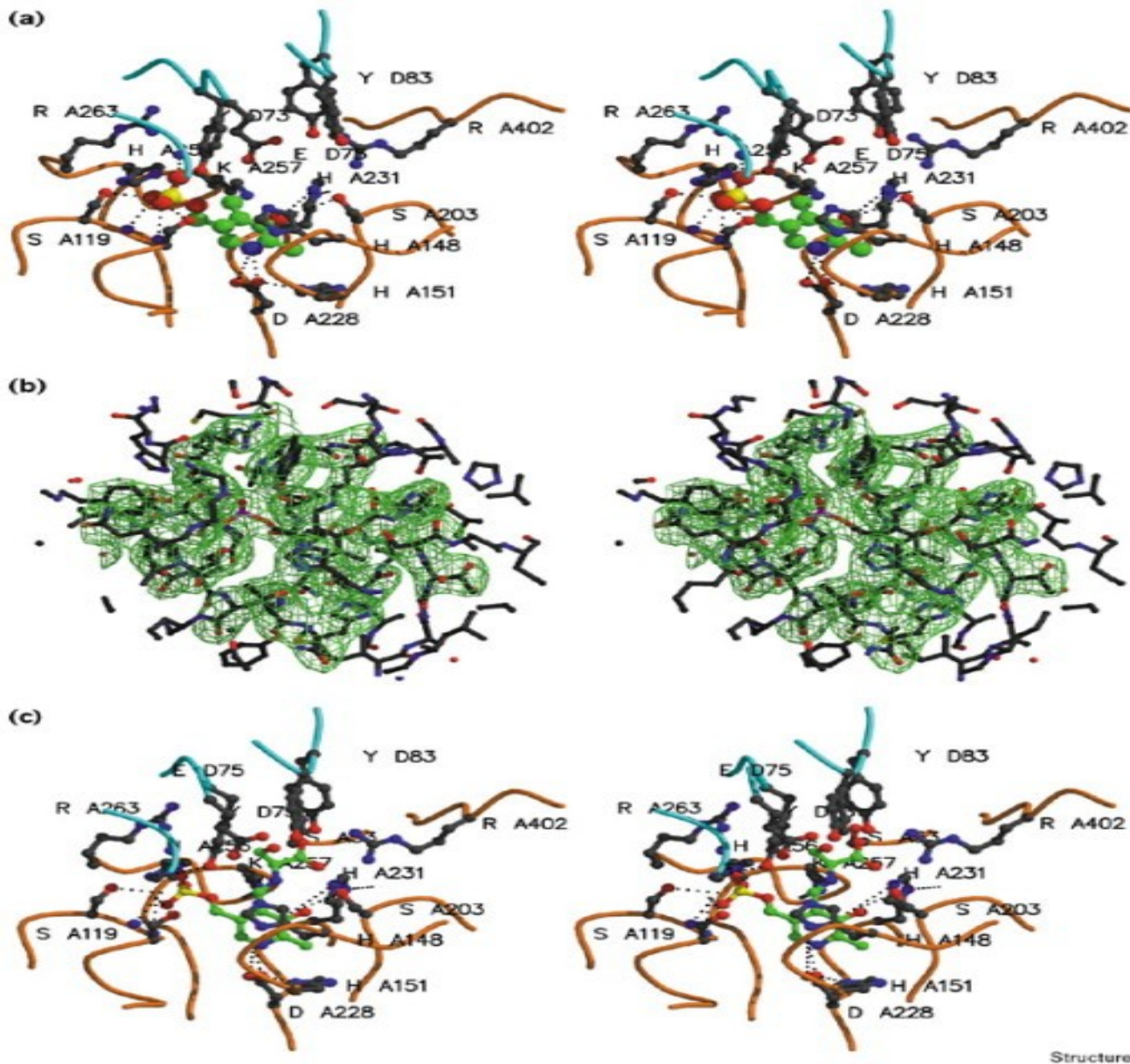
The active site

by www.RCMD.it

- The active site is located **at the interface of the domains** and is delimited by amino acid residues **contributed by both subunits** of the dimer.
- The cofactor **PLP** is covalently **bound to Lys257** in the active site of the molecule .
- The two subunits forming the active site are the same two that form the tight dimer (A–D).

Active site of SHMT

by www.RCMD.it



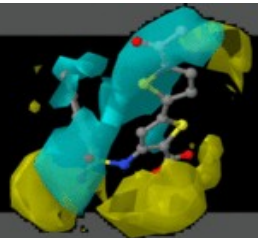
The active site of SHMT. (a) Stereoview active site cartoon depicting key residues. The A and D subunits are shown as orange-brown and cyan traces, respectively. PLP carbon atoms are shown in green, carbon atoms in black, oxygens in red, nitrogens in blue and phosphorus in yellow. Hydrogen bonds are shown as dotted lines. (b) Stereoview Fo-Fc 'omit' electron-density map overlaid on the final model. The contour level is 3σ . (c) Stereoview showing a tentative model of the serine-PLP complex.



SHMT Mechanism of reaction

by www.RCMD.it

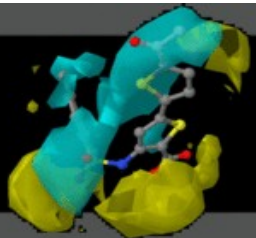
- The mechanism commonly ascribed to SHMT enzymatic activity is a transamidation followed by a cleavage of amino acid side chain from the backbone.
- 1) The N-terminal amine of **serine** makes a **nucleophilic attack** on the aldimine between the SHMT lysine (Internal Aldimine) and the PLP aldehyde to form a gem-diamine, and then the N-terminal amine lone pair comes down to displace the lysine, forming a new aldimine, this time with the serine (External Aldimine).
 - 2) Once the serine is bonded to PLP, **PLP triggers the α -elimination of the hydroxymethyl group of the substrate (serine)**. This group is released as a **formaldehyde molecule** because a nearby glutamate abstracts the proton from the hydroxyl group.
 - 3) The **nucleophilic amine on THF attacks the free formaldehyde** intermediate to make the carbinolamine intermediate.
 - 4) In the second case, the nucleophilic amines on THF attack the serine side chain carbon, **simultaneously forming a carbinolamine intermediate on the THF and a quinoid intermediate with the PLP**.



Catalytic mechanism

by www.RCMD.it

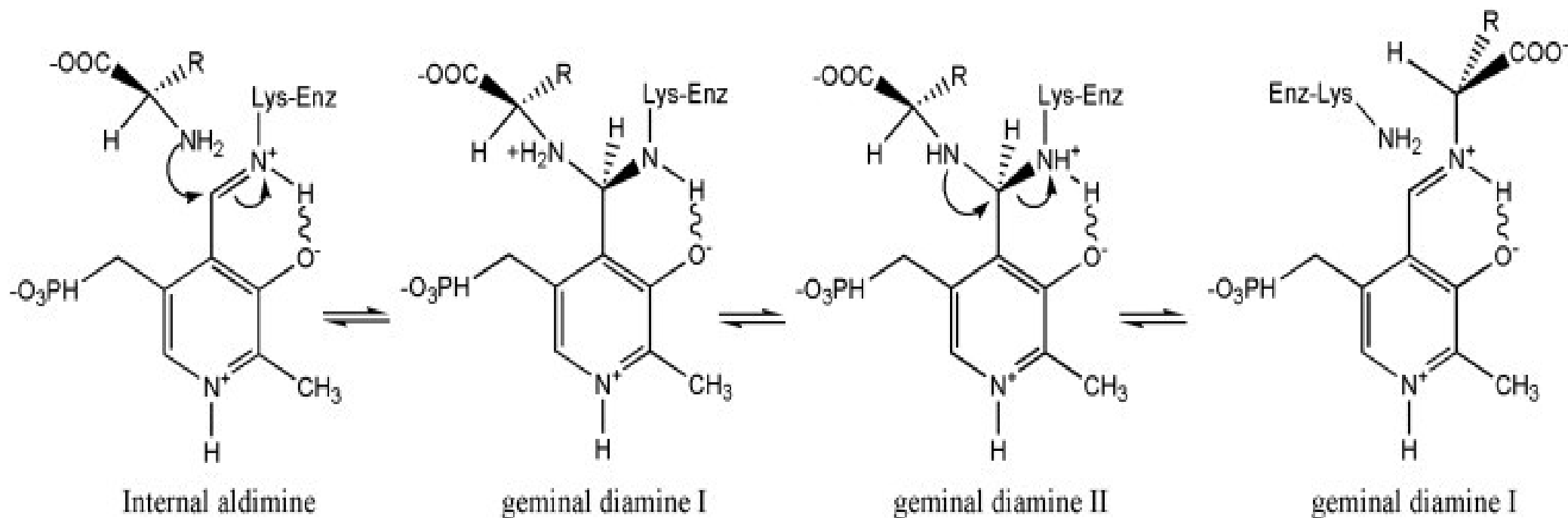
- The catalytic mechanism of the **transaldimination reaction** is a **poorly investigated** aspect of PLP-based catalysis
- The unliganded enzyme exists as an internal aldimine in which **an active site lysine forms a Schiff base with the C4' aldehyde of PLP**. The labialization of the substrate C α bond requires the formation of the external aldimine intermediate, in which the amino group of the substrate is bound to PLP through a Schiff base linkage.
- **Internal and external aldimines interconvert through two geminal diamine intermediates**, which differ by the position of a proton on the two nitrogens .



Retroaldol cleavage mechanism

by www.RCMD.it

The currently accepted mechanism for the hydroxymethyltransferase reaction consists of a modified folate-dependent retroaldol cleavage via direct nucleophilic attack of N5 of 5,10-CH₂-THF to C β of serine, which results in the elimination of the quinonoid intermediate.



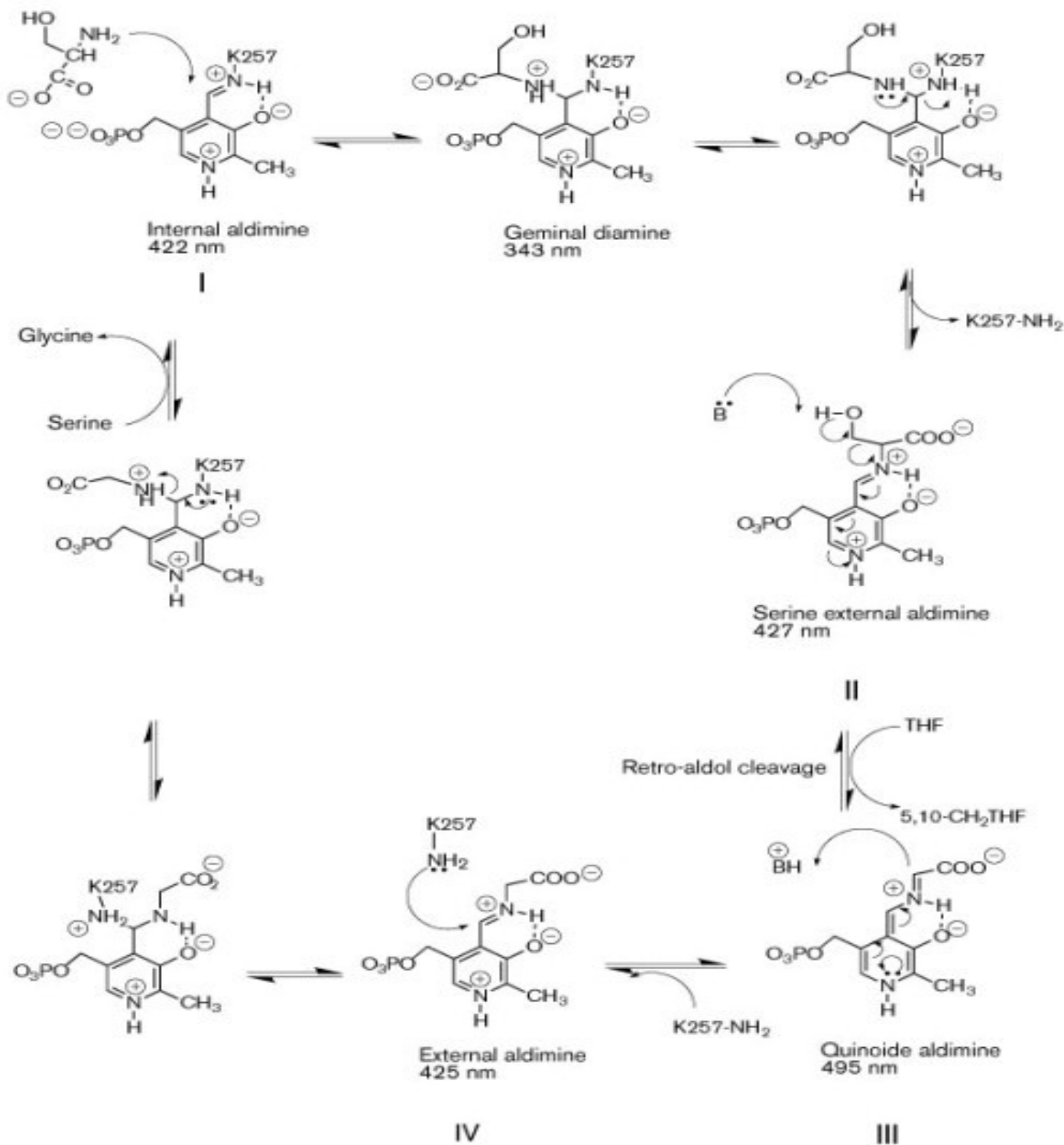


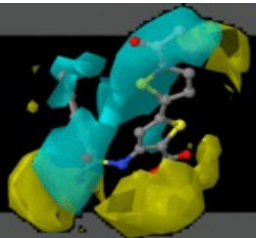
Figure 1. Proposed reaction cycle catalysed by SHMT. Initially, the cofactor PLP is covalently bound as a Schiff base to the sidechain of Lys257. The retro-aldol cleavage is the reaction step leading from intermediate II to III and involves deprotonation of the serine external aldimine by an unidentified base (B). The second product of this step, formaldehyde, reacts with tetrahydrofolate to form 5,10-methylene-tetrahydrofolate. The maximum absorption of some intermediates are indicated in nm.



Clinical significance

by www.RCMD.it

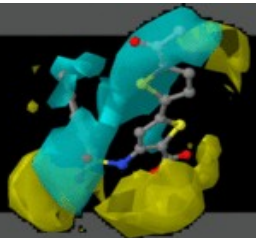
- **Malaria is, besides tuberculosis and AIDS, with more than 250 million clinical cases causing over 600 000 deaths per year, one of the most devastating infectious diseases worldwide.**
- **Widespread resistance has developed against almost all available antimalarials.**
- **The “last resort” artemisinin derivatives, which constitute the backbone of most new combination therapies in development, the emergence of resistance becomes a major concern.**



Potent Anti-malarial drugs

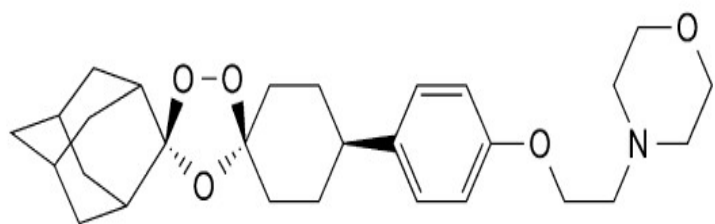
by www.RCMD.it

- OZ439 is in phase IIa clinical trials.
- NITD609 , a spiroindolone derivative, for parasitemia in adults is in phase II clinical Trials
- KAF156 based on an imidazolopiperazine core, has just finished phase II,
- DSM265 an inhibitor of the enzyme dihydroorotate dehydrogenase (DHODH), which is currently in phase IIb clinical trials
- Pyrimethamine and cycloguanil, inhibitors of DHFR, are currently undergoing preclinical testing.

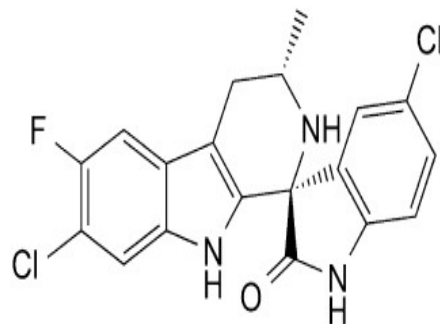


Portfolio of potentially new therapeutic drugs

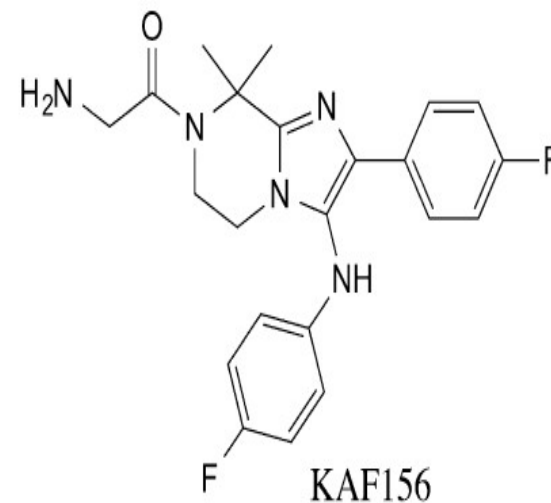
by www.RCMD.it



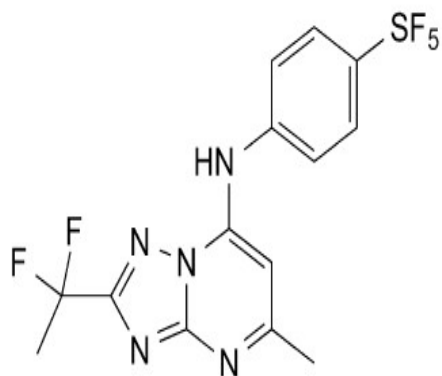
OZ439



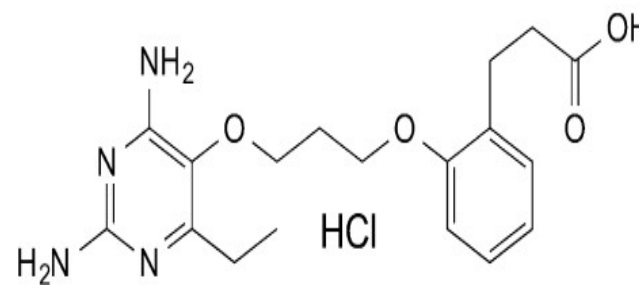
NITD609



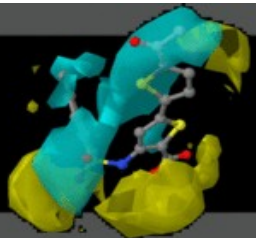
KAF156



DSM265



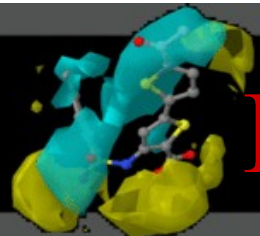
P218



Pyrazolopyran scaffold discovery

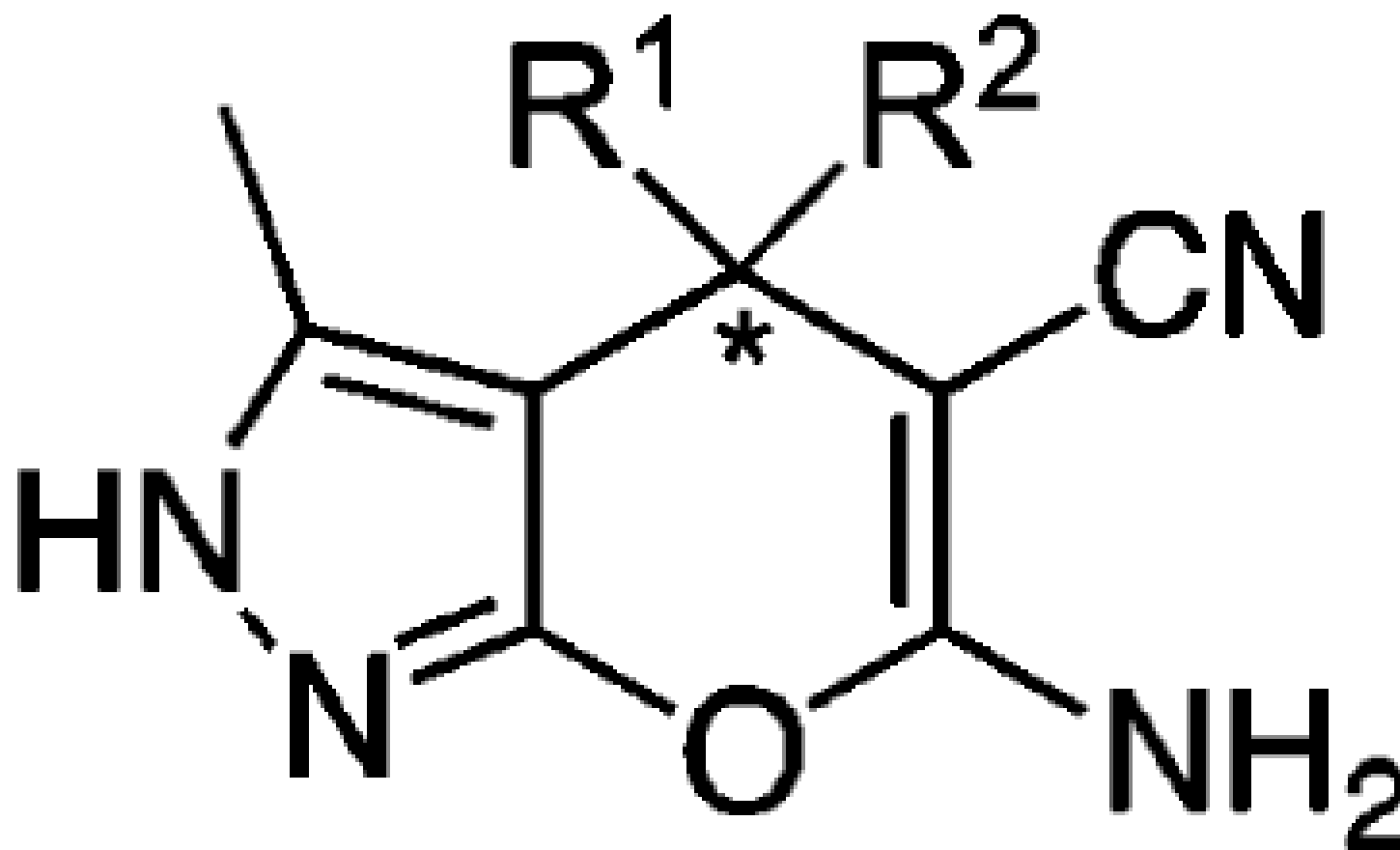
by www.RCMD.it

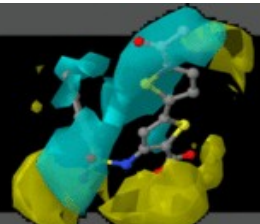
- Plasmodium parasites have **several essential enzymatic pathways in common with plants** so that herbicides potentially can serve as lead structures for new antimalarials.
- This has been shown in a **systematic screen of commercial agrochemicals against different protozoans**, which resulted in a high number of promising hits.
- Systematically examination of antiplasmodial activity of lead structures from **target-based herbicide programs**
- The **key role** of the enzyme serine hydroxymethyltransferase (SHMT) raised particular interest.
- In a **screen of 100.000 compounds**, two compound with a **pyrazolopyran scaffold showed IC50 values in the micromolar range**, which could further be optimized to activities in the nanomolar range against plant SHMT.



Pyrazolopyran scaffold

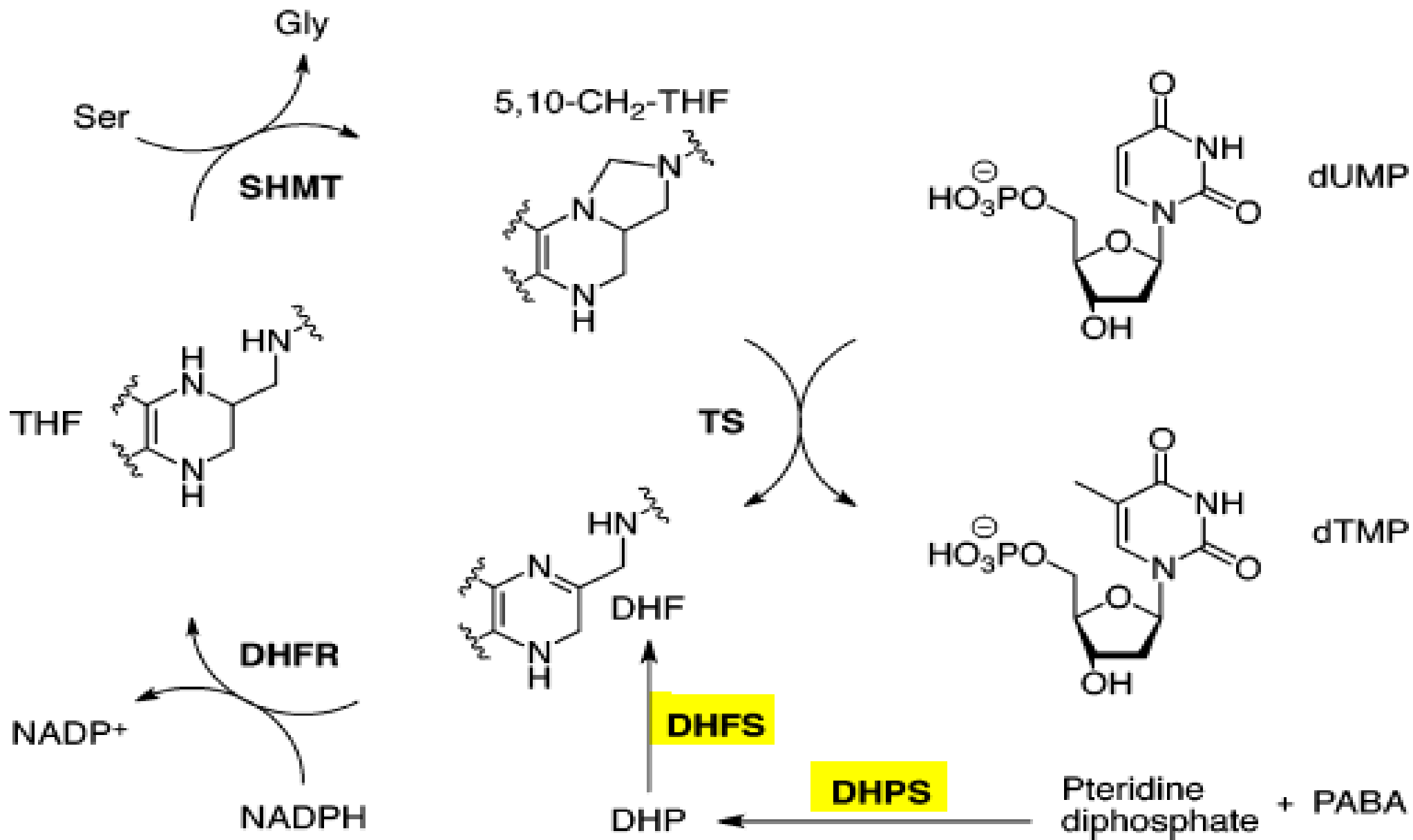
by www.RCMD.it



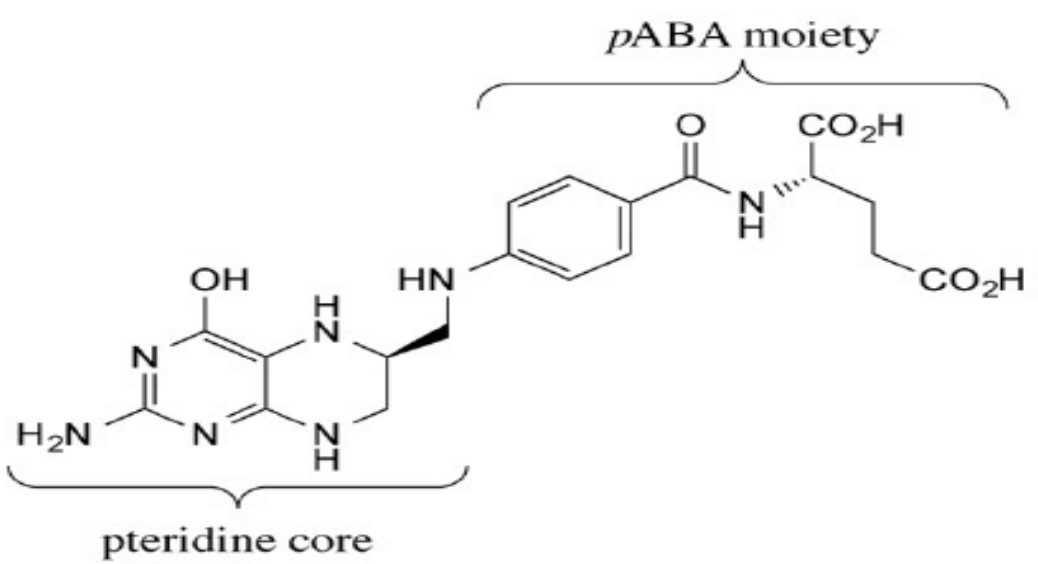


Folate cycle

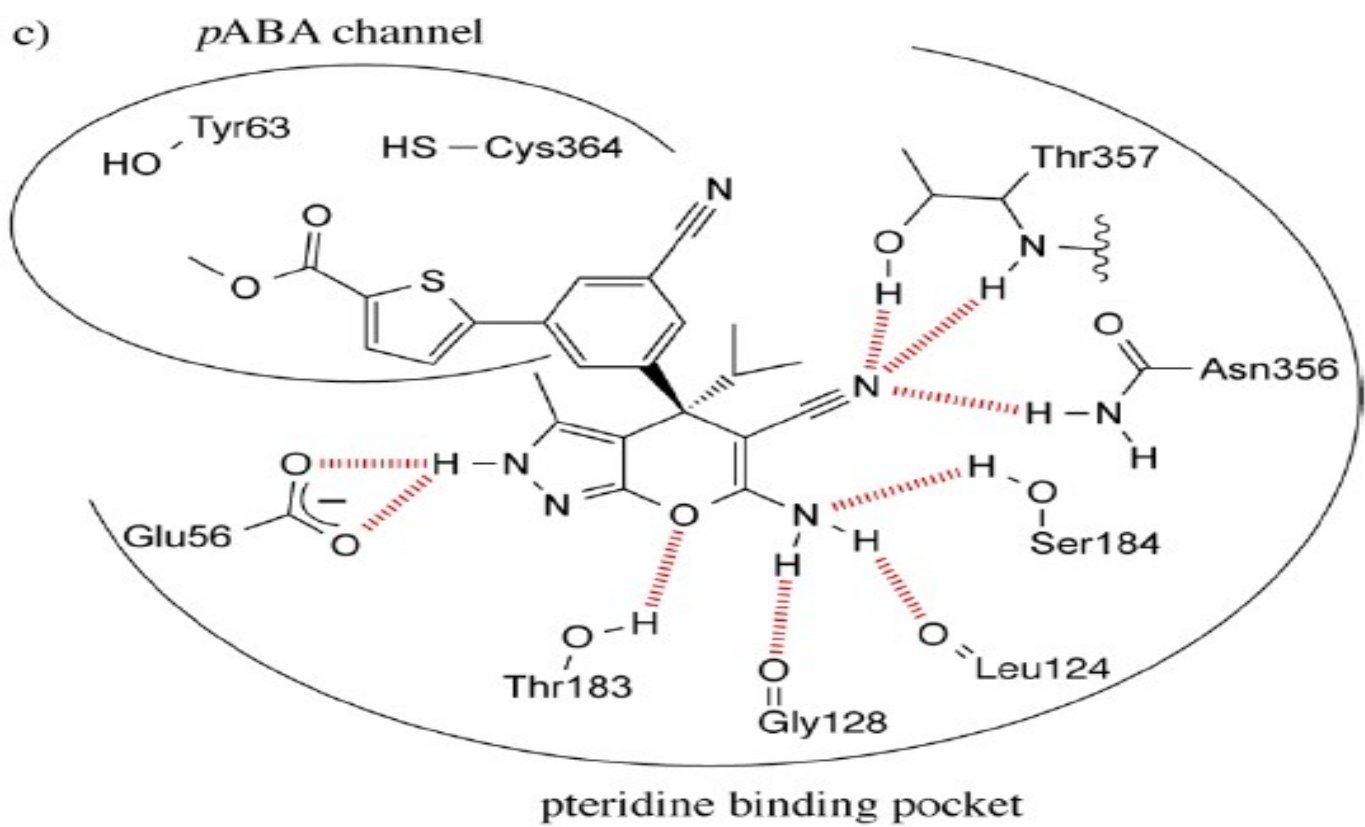
by www.RCMD.it



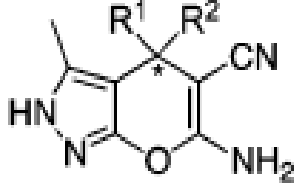
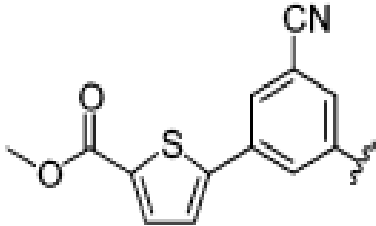
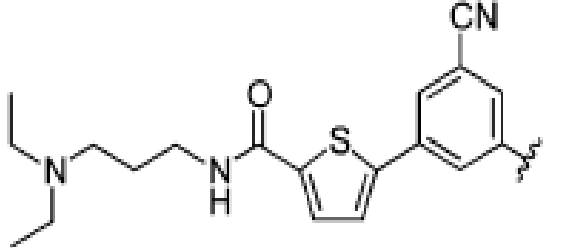
b)



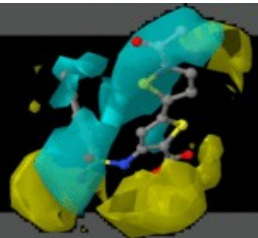
c)



EC_{50} *Pf* NF54: (±)-**1** = 3 nM; (+)-**1** = 2 nM
 IC_{50} *Pf* SHMT: (±)-**1** = 370 nM; (+)-**1** = 60 nM

Num.	R ¹		R ²	EC ₅₀ /nM				IC ₅₀ /nM	
				<i>Pf</i> NF54	<i>Pf</i> TM90C2B	<i>Pf</i> K1	<i>Pf</i> V1/S	Rat L6	<i>Pf</i> SHMT
(±)-1				3	5	5	9	31100	370
(-)-1	49			31	35	41400	5420		
(+)-1	2			2	3	25000	60		
(±)-3				1160	1850	1640		96800	
(±)-4 • 2 TFA	620			1080	1010	91400			
(4 <i>R</i> / <i>S</i> ,2'' <i>S</i>)-7 • TFA	2520			5560	4970	>145200			
(±)-8 (-)-8 (+)-8	3 300 2			3 240 1	3 261 1	4	12700 11200 9000	420 170	

(±)-9			700	1250	1060	>224500		
(±)-10			59		130	92	270	
(±)-16			1210				210	
(-)-16			2300		2200		94000	370
(+)-16			2880		3630			470
(±)-17			340				220	
(±)-18			80				210	
(±)-19			600				480	
(±)-20			920				560	
(±)-21			2018				290	
(±)-22			250					
(±)-23			4150					



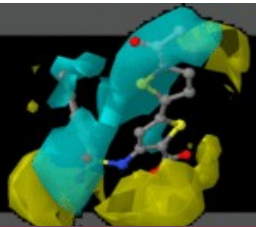
SAR Results

by www.RCMD.it

- Methyl (\pm)-1 and benzyl ester (\pm)-8 show by far the most potent activity within the low single-digit nanomolar range.
- Replacing the thienyl against a phenyl ring (in (\pm)-18) reduces the activity to 80 nM.
- The N,Ndimethylamide (\pm)-10 is 20-fold less active than (\pm)-1.
- The thienyl ring is critical for high affinity and far superior to phenyl rings
- The enantiomers of (\pm)-1 and (\pm)-8 were separated .The (+)-enantiomers showed a higher activity compared to their racemic mixture, whereas the activity of the (-)-enantiomers is markedly reduced (25-and 150-fold, respectively).



- Compound (+)-1 was also tested on PvSHMT, showing an **IC₅₀ value of 98 ± 2 nM**.
- The most active pyrazolopyran (±)-1 has also been tested **against P. berghei** in the liver-stage assay. In this assay, (±)-1 also showed a high potency with an **IC₅₀ value of 9 nM**.
- Cytotoxicity was tested for compound (±)-1 in the **human HepG2 cell line** (human hepatocellular liver carcinoma cell line). **No effects were observed** up to the highest concentration (20 000 nM) tested.
- The two methyl groups of the isopropyl residue form **well aligned interactions**, one pointing at the edge of **Tyr64 at close distance** and the other at the face of **the hydrogen bonding array between Arg371 and the cofactor pyridoxal 5'-phosphate (PLP)**. In general, substitution of the isopropyl group by the **cyclobutyl group leads to a decrease in activity**.



Bindind of compound (\pm)-1

by www.RCMD.it

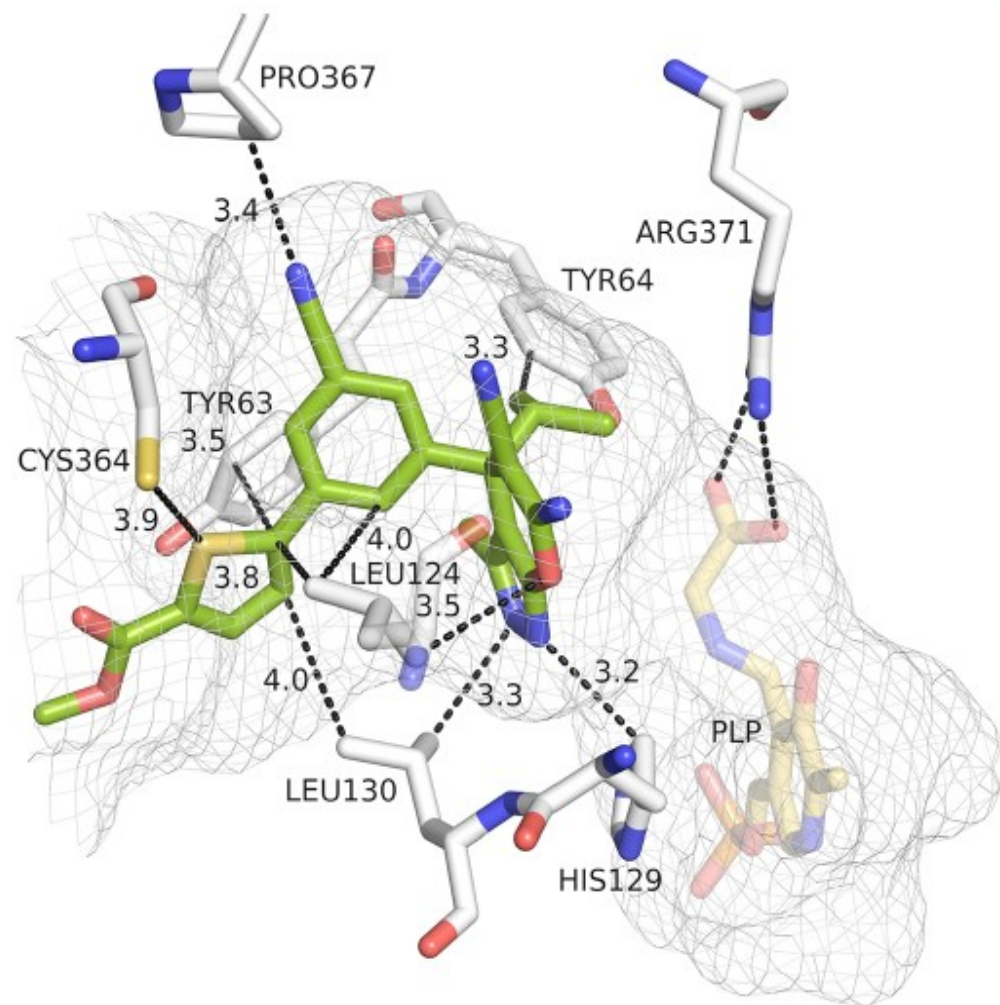
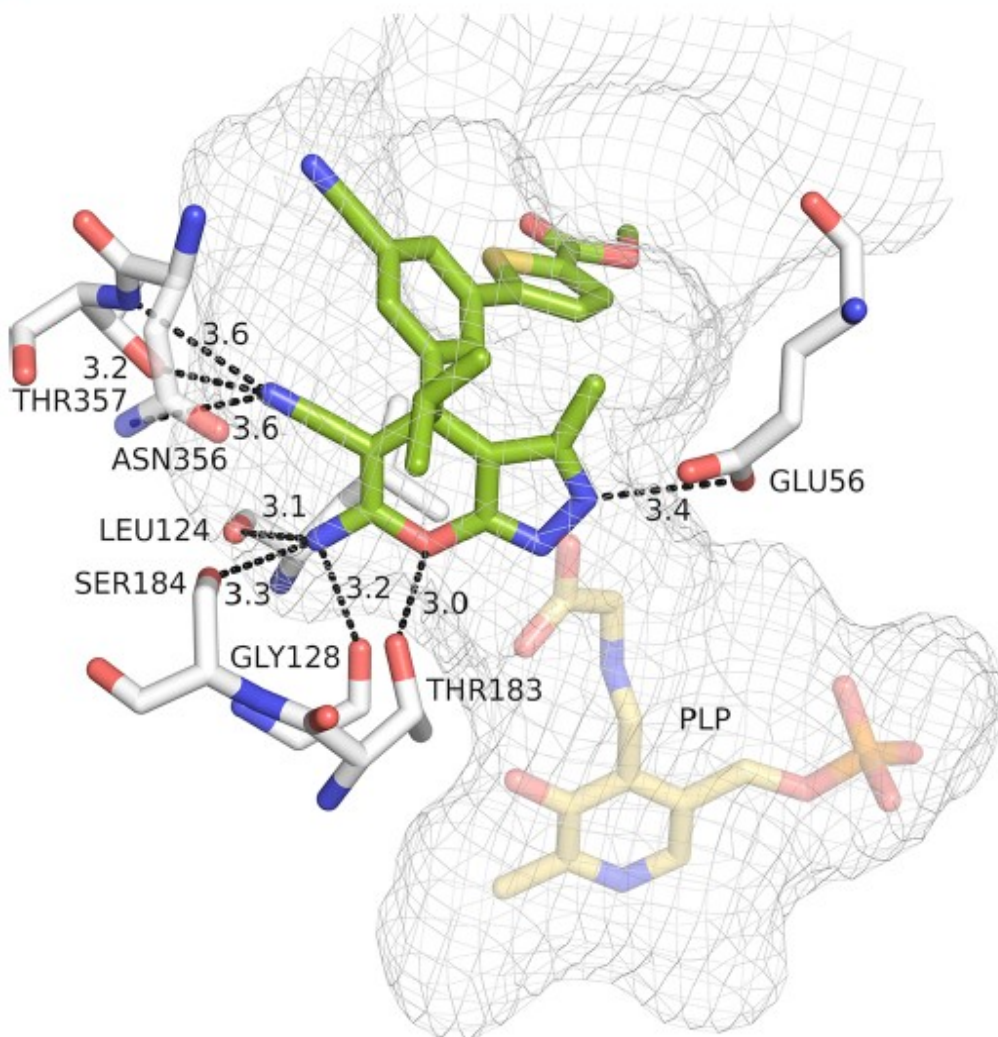
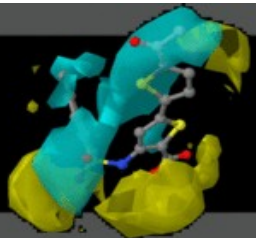


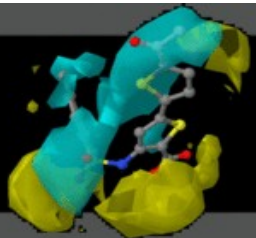
Figure 1. Cocrystal structure (PDB code 4TMR) showing protein–ligand interaction of pyrazolopyran (+)-1 (green) and *Pv*SHMT (white). Left image shows polar (hydrogen bonding) interactions, right image nonpolar contacts. The mesh surface spans the volume of the binding pocket, and cofactor PLP is shown in yellow. Distances are given in Å. Atom coloring is the following: N blue, O red, P orange, S yellow.



Animal models and pharmacokinetics

by www.RCMD.it

- In initial animal models with *P. berghei* infected mice, **no significant activity of (±)-1 or (±)-8 been observed.**
- After oral and intraperitoneal dosing of (±)-8 with 100 and 10 mg/kg, respectively, plasma levels were **below the limit of detection at all tested time points** (1, 4, 24 h after treatment). There was evidence of **rapid conversion of the ester group into the acid** in the plasma samples.
 - . This potential lability of the ester group may lead into the formation of **metabolite (±)-9 with more than 200-fold reduced activity** and thus could explain the lack of in vivo activity.
- In **liver microsomes**, a rapid degradation of **ester (±)-8 and N,N-dimethylamide (±)-10 by ester/amide hydrolysis or monooxygenation was observed**. The closely related **biphenyl analogue (±)-17 showed improved stability**
- Despite its rapid metabolism, **(±)-10 showed a reduction of parasitemia of 38% (po) and 41% (ip)** in a 4-day-test SCID mice model with *P. falciparum* 3D7 infected SCID mice at 4 × 30 mg/kg. Considering the **very short half-life** of the compound, **the significant reduction of parasitemia validates the activity of pyrazolopyrans in vivo.**



Binding of (+)-1 and (+)-16

by www.RCMD.it

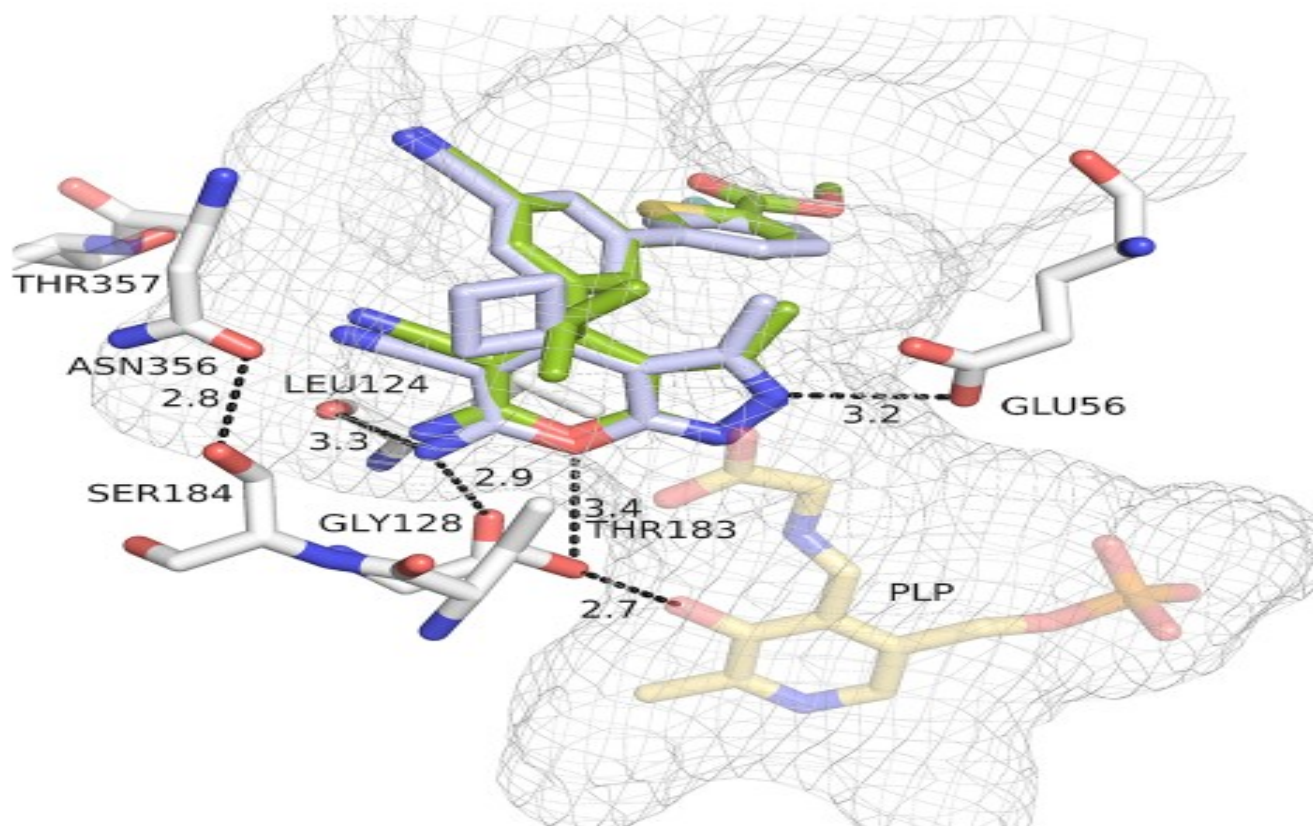


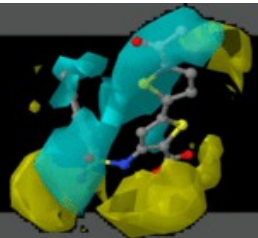
Figure 2. Cocystal structure (PDB code 4TN4) showing polar protein–ligand interaction of pyrazolopyran (+)-16 (blue) and *Pv*SHMT (white). Ligand (+)-1 (green) of superimposed structure 4TMR is shown for comparison. The mesh surface spans the volume of the binding pocket, and cofactor PLP is shown in yellow. Distances are given in Å. Atom coloring is the following: F cyan, N blue, O red, P orange, S yellow.



Differences in binding

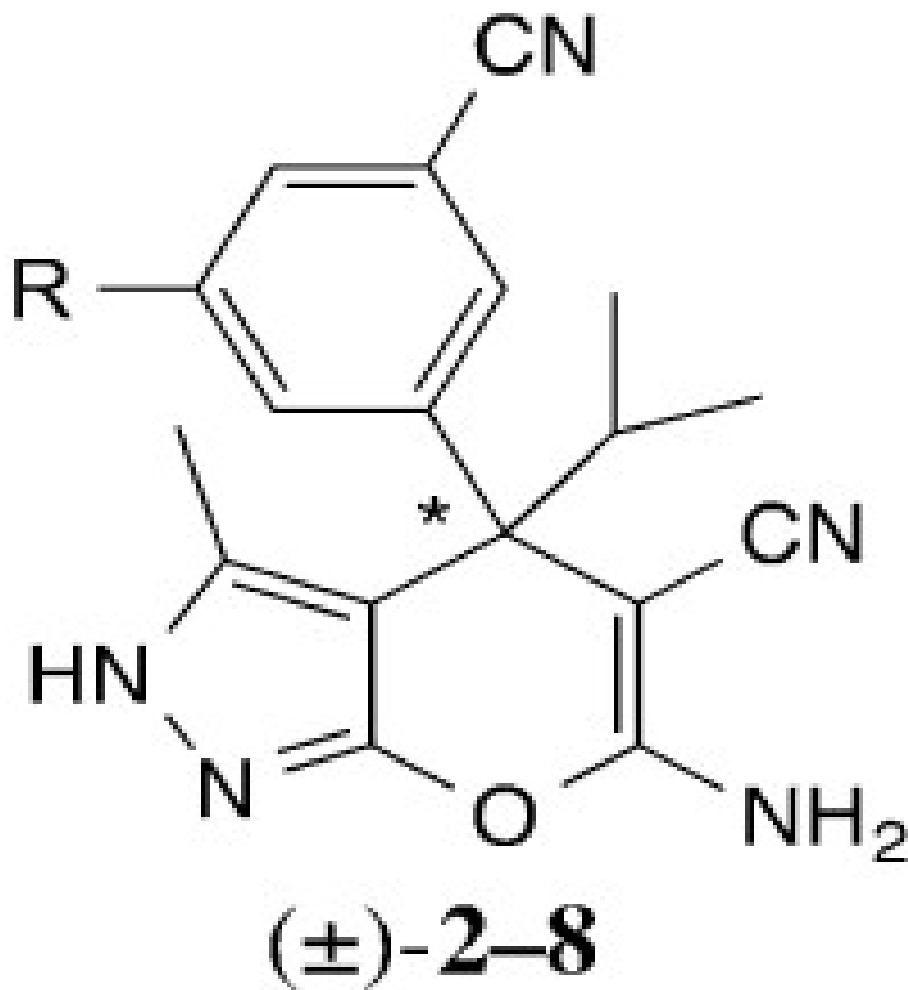
by www.RCMD.it

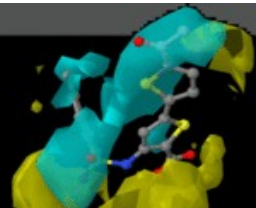
- Binding mode and conformation of (+)-16 and (+)-1 are very similar. The pyrazolopyran core adopts a nearly **superimposable position** in the two complexes, but some **polar interactions differ** because of different conformations of amino acid side chains, such as those of **Thr183 and Ser184**.
- The biphenyl substituent in (+)-16 extending into the pABA channel assumes a conformation similar to the phenylthienyl residue in (+)-1. The F-substituent points into the same direction as the C=O of methyl ester (+)-1.
- The lipophilic pocket, which hosts the isopropyl substituent at the stereogenic center of (+)-1, is now filled by the cyclobutyl substituent of (+)-16 but in a **different orientation**.
- **Lack in chiral recognition of (±)-16 by the enzyme.** In sharp contrast to the large difference in binding affinity measured for (+)-1 and (-)-1, the two enantiomers of 16 exhibit similar inhibition.
- **In the cellbased assay, the two ligands differ strongly, with EC50 values of 2 nM (+)-1 and 2880 nM (+)-16.**



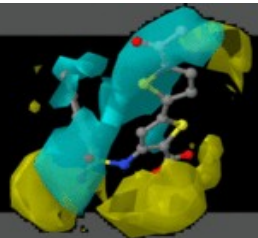
Thiophene Derivatives

by www.RCMD.it





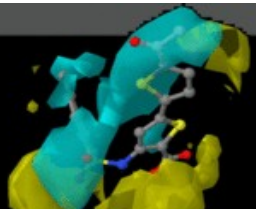
Num.	R	EC ₅₀ Pf NF54 [nM]	IC ₅₀ Pf SHMT ± SD [nM] ^a
(±)-2		594	388 ± 5
(±)-3		410	323 ± 43
(±)-4		228	42 ± 1
(±)-5		501	202 ± 9
(±)-6		212	133 ± 6
(±)-7		151	99 ± 2
(±)-8		197	60 ± 1



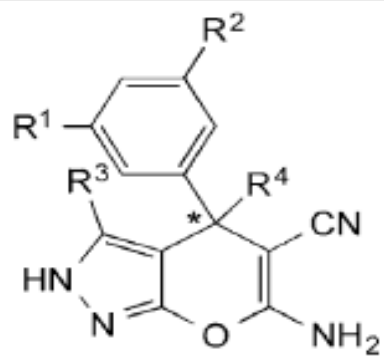
Thiophene substitution

by www.RCMD.it

- In this assay, the best inhibitor of the series was **sulfonamide (\pm)-7** with an EC50 value of 151 nM .
- No good explanation became apparent for the higher target affinity of (\pm)-4 as compared to (\pm)-3
- Because the cell-based affinity of this series of thiophene derivatives was **still 2 orders of magnitude lower** than that of (\pm)-1 (EC50 value = 3 nM), modifications at other positions of the molecule were evaluated to improve biological activity.



Num.



EC₅₀ PfNF54
[nM]

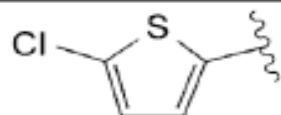
R¹

R²

R³

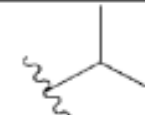
R⁴

(±)-13



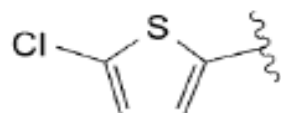
Cl

Me



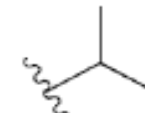
485

(±)-14



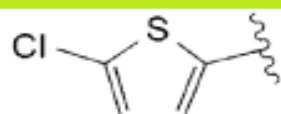
Br

Me



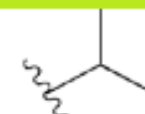
892

(±)-15



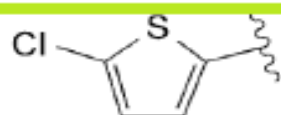
CF₃

Me



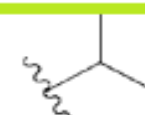
226

(±)-16



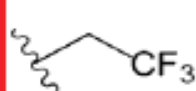
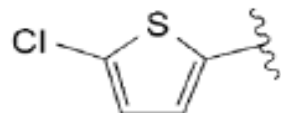
OCF₃

Me

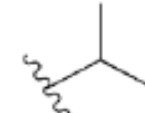


3760

(±)-17

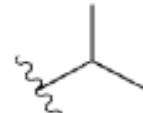
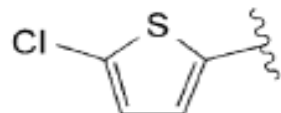


Me

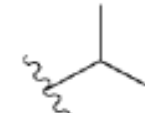


7106

(±)-18

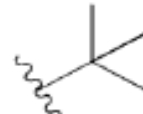
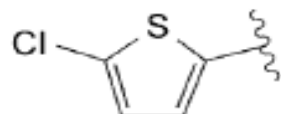


Me

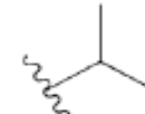


4511

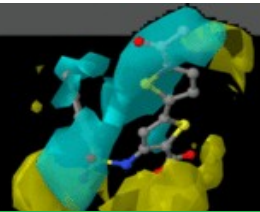
(±)-19



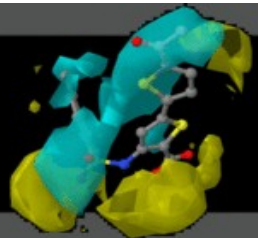
Me



5501



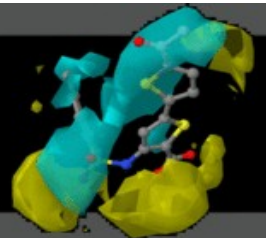
(±)-20	 <chem>CN(C)C1=CC=C(S1)S(=O)(=O)C2=CC=CC=C2C3=CC=CC=C3</chem>	CF ₃	Me		18
(±)-21	 <chem>CN(C)C1=CC=C(S1)S(=O)(=O)C2=CC=CC=C2C3=CC=CC=C3</chem>	CF ₃	CD ₃		11
(±)-22	 <chem>CN(C)C1=CC=C(S1)S(=O)(=O)C2=CC=CC=C2C3=CC=CC=C3</chem>	CF ₃	Et		172
(±)-23	 <chem>CN(C)C1=CC=C(S1)S(=O)(=O)C2=CC=CC=C2C3=CC=CC=C3</chem>	CF ₃	cyPr		576
(±)-24	 <chem>CN(C)C1=CC=C(S1)S(=O)(=O)C2=CC=CC=C2C3=CC=CC=C3</chem>	CF ₃	H		29
(±)-25	 <chem>CN(C)C1=CC=C(S1)S(=O)(=O)C2=CC=CC=C2C3=CC=CC=C3</chem>	CF ₃	Me		340
(±)-26	 <chem>CN(C)C1=CC=C(S1)S(=O)(=O)C2=CC=CC=C2C3=CC=CC=C3</chem>	CF ₃	Me		1202
(±)-27	 <chem>CN(C)C1=CC=C(S1)S(=O)(=O)C2=CC=CC=C2C3=CC=CC=C3</chem>	CF ₃	Me		498



Biaryl phenyl ring substitution

by www.RCMD.it

- Substitution of the nitrile in (±)-5 by a chloride (±)-13 or bromide (±)-14 **did not have significant effect** .
- Introduction of a CF₃ group (±)-15 resulted in an **improved in vitro potency** by a factor of 2 (EC₅₀ = 226 nM).
- With **larger substituents**, the potency was **significantly reduced** and EC₅₀ values in the single-digit micromolar range were measured (±)-16–19. The larger groups **interfere** with the conformationally flexible **Cys364-loop**.
- Applying the **CF₃-substitution** to the sulfonamide ligand (±)-7, a **low nM cell-based activity reached**, giving more than a 10-fold boost in potency (EC₅₀ (±)-20 = 18 nM).
- Substitution of the isopropyl in (±)-20 (EC₅₀ = 18 nM) by **ethyl, cyclopropyl, and cyclobutyl** (±)-25–27 **strongly reduced** the cell-based activity .



Num.	R	EC ₅₀ Pf NF54 [nM]
(±)-29		350
(±)-30		44
(±)-31		56
(±)-32		59
(±)-33		25
(±)-34		49
(±)-35		26
(±)-36		193
(±)-37		65
(±)-41		454
(±)-46		523
(±)-52		610
(±)-53		65

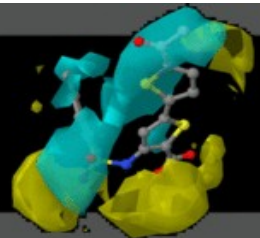
by www.RCMD.it

Best derivatives

Try63 H-Bond

Failed to
establish Cys364
interactions

Try63 H-Bond



Heterocyclic Rings as Thiophene Replacements

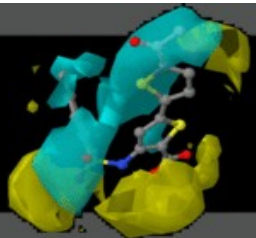
by www.RCMD.it

- The **highest cellular potency** was measured for the fused N-heterocyclic derivatives(±)-30–35,suggesting the establishment of **good hydrophobic interactions with the apolar surface at the exit of the pABA channel**, formed by Leu124, Leu130, Phe134, and Val141 within the active site.In the AtSHMT assay,compound (±)-33 was the most potent with an IC50 value of 17.7 nM.
- Attempts to gain affinity by interacting with Cys364 apparently **remained unsuccessful** ((±)-41, (±)-46, and (±)-52) according to both EC50 and IC50 values.
- Sulfone (±)-37 and sulfonamide (±)-53 gave both promising EC50 (65 nM) and IC50 values , establishing **H-bonding interactions with Tyr63**.



Num.	R	EC ₅₀ PfNF54 [nM]
(±)-59		115
(±)-60		4.8
(±)-61		3.2
(±)-62		10
(±)-63		27
(±)-64		125
(±)-65		18
(±)-66		52
(±)-67		4.2
(±)-68		5.1
(±)-69		6.4
(±)-70		14
(±)-71		66

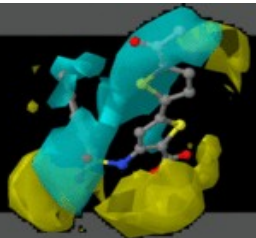
by www.RCMD.it



Aromatic N-Heterocyclic Ligands

by www.RCMD.it

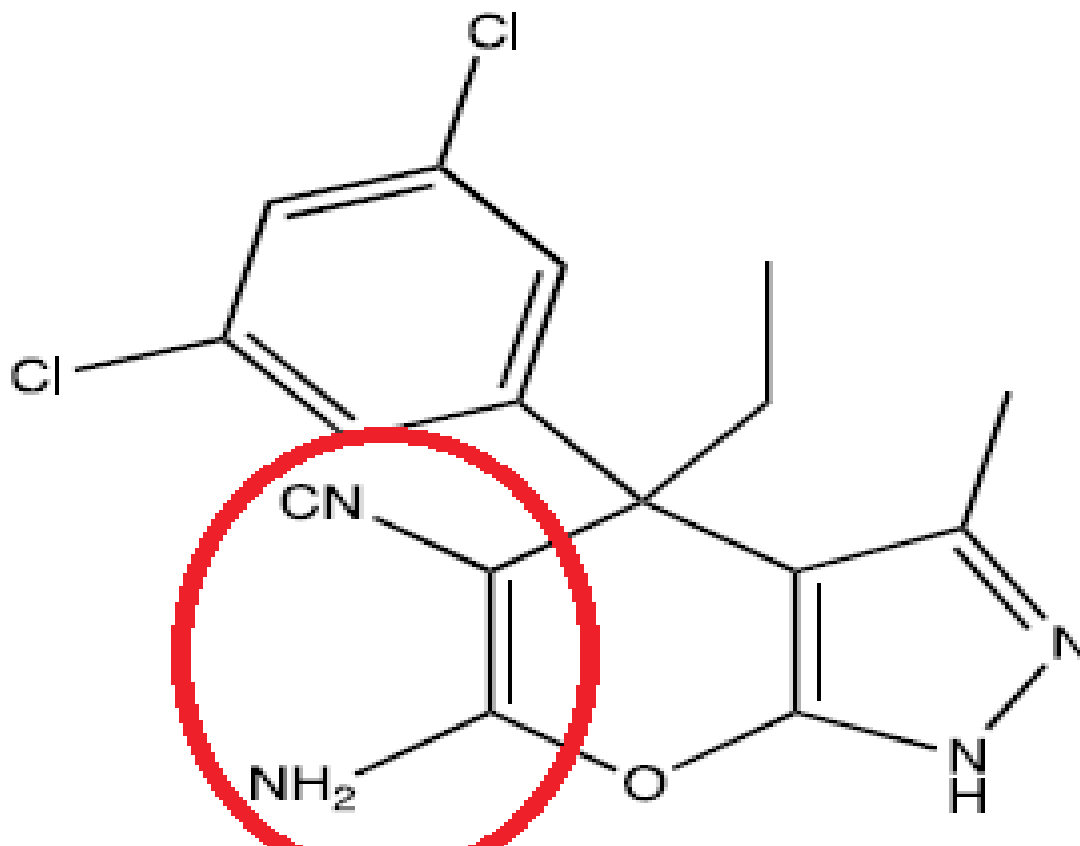
- Five of the prepared pyridine derivatives gave **desired EC50 values in the single-digit nanomolar range ((±)-60, (±)-61, and (±)-67–69)** and similar activity was also measured in the AtSHMT assay .
- **No apparent cytotoxicity** for (±)-60 and (±)-61 was measured on rat myoblast cell line (L6) and human HepG2 cell line, with IC50 values only in the high micromolar range . hERG inhibition was also assessed for (±)-60, resulting in an IC50 of 29 μ M, which highlights once again the safeness of this series .
- The potential of these ligands however was greatly diminished by their **very short halflife when incubated with human liver microsomes (<10 min)**



Pyrazolopyrans metabolism

by www.RCMD.it

The main metabolite arises from oxidation on the pyrazolopyran core, possibly by oxidation of the vinylogous cyanamide. Probably the metabolism is compound-specific and the vinylogous cyanamide moiety might be a liability.

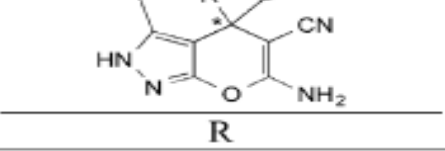
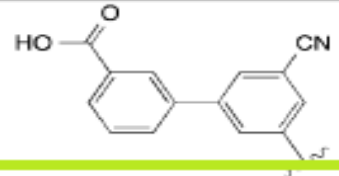
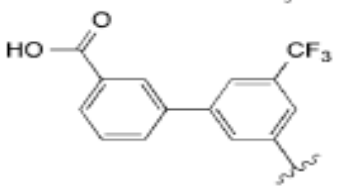
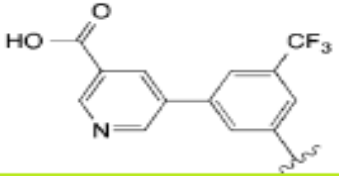
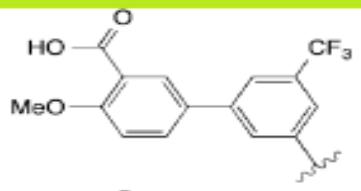
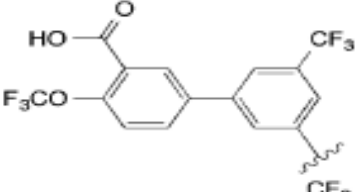
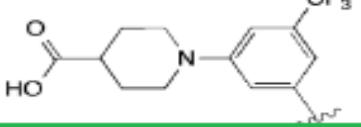
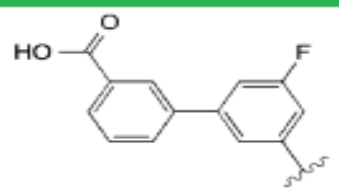
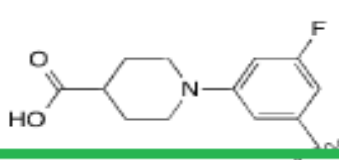


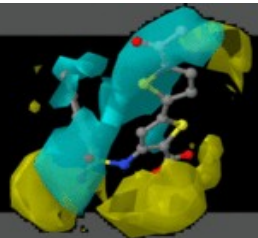


Amino acids sequence

by www.RCMD.it

- *Arabidopsis thaliana* SHMT, the plant counterpart, and PfSHMT share **45% sequence identity**, and only very few amino acid residues differ within each active site.
- The two *Arabidopsis thaliana* isoforms, mitochondrial AtSHMT2 and cytosolic AtSHMT4 are counterparts of hmSHMT and hcSHMT respectively. **Amino acids sequence identities between corresponding plant and human isoforms are 60%** , whereas hmSHMT and hcSHMT share 66% identity and AtSHMT2 with AtSHMT4 share 56% identity.

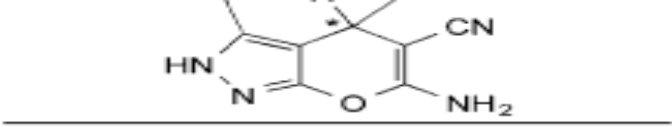
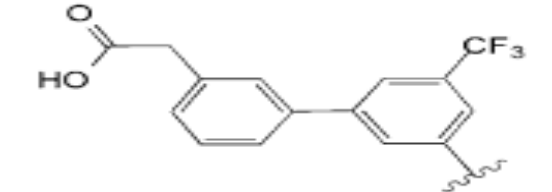
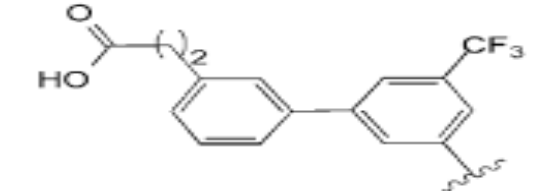
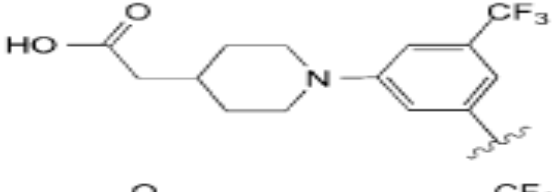
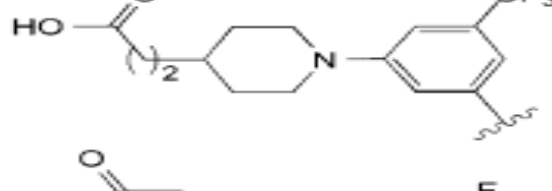
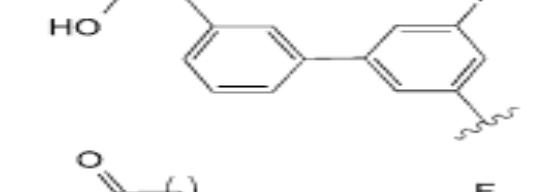
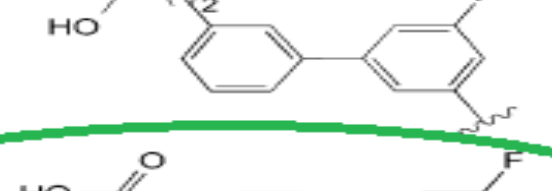
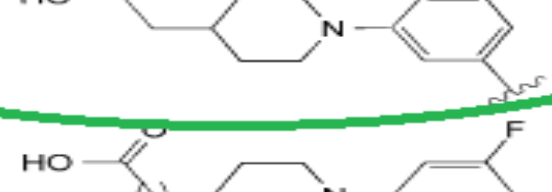
Num.		EC_{50} <i>Pf</i> NF54 [nM]	IC_{50} <i>Pf</i> SHMT \pm SD [nM] ^a	IC_{50} <i>At</i> SHMT [nM]	$\log D_{7.4}$ ^b	$t_{1/2}$ [min] ^c
(±)-72		340	220 ± 70	0.088	1.4	137
(±)-73		54	189 ± 7	19.1	1.8	41
(±)-74		632	119 ± 6	n.d. ^d	n.d.	64
(±)-75		822	77 ± 1	n.d.	1.7	59
(±)-76		172	268 ± 15	n.d.	n.d.	70
(±)-77		116	312 ± 10	41.9	1.6	55
(±)-78		194	56 ± 1	27.8	1.5	157
(±)-79		154	75 ± 1	26.2	1.2	226



Carboxylic Acid Series

by www.RCMD.it

- Acid derivative (\pm)-72 drew attention because of **reasonably stable in the microsomal test system ($t_{1/2} = 137$ min)** but had only moderate potency (EC_{50} Pf NF54 = 340 nM)
- The piperidine derivatives **showed good solubility**.
- The meta-fluoro derivative (\pm)-78 has a moderate activity on Pf NF54 ($EC_{50} = 194$ nM), but it surpassed all ligands studied so far with a microsomal **half-life of 157 min**. Ligand (\pm)-78 was also incubated in rat liver microsomes, resulting in a comparable half-life of 95 min.
- Applying the $CF_3 \rightarrow F$ replacement strategy to piperidine derivative (\pm)-77 led to a **slight potency loss**, which was compensated by a **large stability gain** (\pm)-79. In addition, (\pm)-78 and (\pm)-79 had **high target affinity** in both PfSHMT and AtSHMT assays.

Num.	 R	EC ₅₀ <i>Pf</i> NF54 [nM]	IC ₅₀ <i>Pf</i> SHMT ± SD [nM] ^a	IC ₅₀ <i>At</i> SHMT [nM]	t _{1/2} [min]
(±)-80		22	186 ± 9	59.0	54
(±)-81		10	165 ± 7	27.0	31
(±)-82		84	186 ± 7	13.5	36
(±)-83		17	168 ± 11	18.2	12
(±)-84		52	172 ± 10	22.4	159
(±)-85		19	90 ± 4	33.6	95
(±)-86		55	97 ± 1	37.1	194
(±)-87		17	130 ± 4	13.8	50

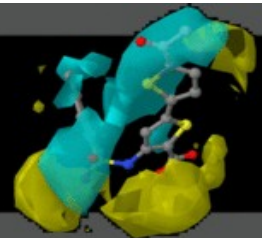


Carboxylic Acid Series

by www.RCMD.it

- Extension of the carboxylate side chain has a **beneficial effect on cellular potency** in both CF3- and F-series. Activity gain came **along with a loss in metabolic stability**, which became unacceptable in the CF3 series.
- Taking all parameters into account, (±)-86 is clearly the compound with the most attractive profile and the **best balance between potency and metabolic stability**.
- As observed previously with enantiomerically pure pyrazolopyran-based ligands, (+)-86 is considerably more potent than (–)-86 in all in vitro assays. Additionally, (+)-86 is roughly 2-fold more potent than the racemic mixture. Remarkably, (+)-86 also has an improved metabolic stability with a in vitro half-life greater than 255 min.

compd	EC ₅₀ PfNF54 [nM]	IC ₅₀ PfSHMT ± SD [nM] ^a	IC ₅₀ AtSHMT [nM]	t _{1/2} ^b [min]
(±)-86	55	97 ± 1	37.1	194
(+)-86	35	110 ± 2	12.6	>255 ^c
(–)-86	6143	1581 ± 49	977	206



Binding of (+)-85

by www.RCMD.it

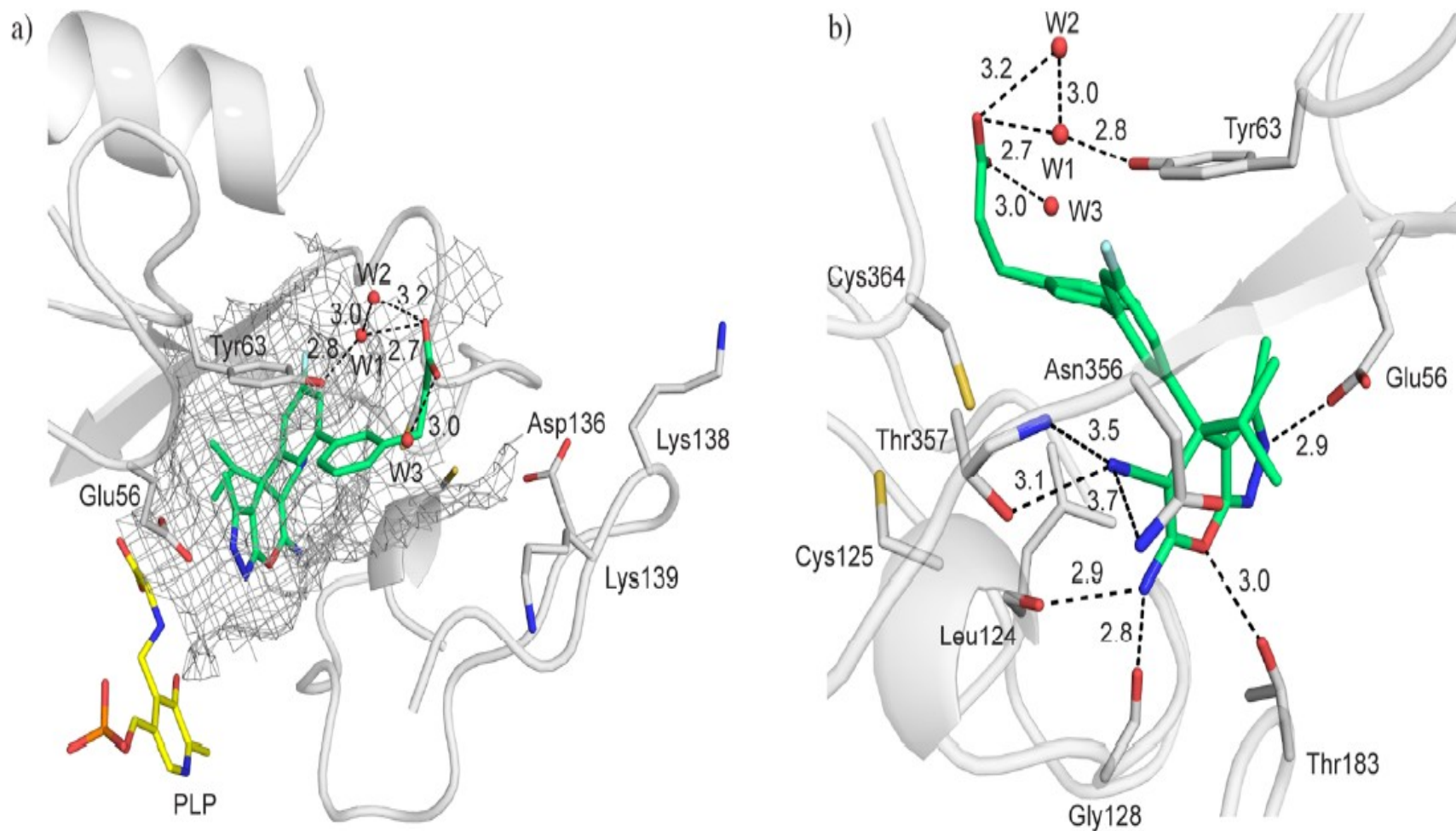


Figure 3. Cocystal structure (PDB 5GVN, 2.3 Å) showing the protein–ligand interactions of pyrazolopyran (+)-85 (lime) and PvsHMT (gray). (a) Occupancy of the active site by (+)-85, the water-mediated interaction with Tyr63, and the cofactor (pyridoxal 5'-phosphate, PLP). The mesh spans the volume of the binding pocket. (b) Polar interactions between (+)-85 and the protein; PLP is omitted for clarity. The water molecules (W1, W2, and W3) are represented as red spheres. Distances are given in Å. Color code: C_{protein} gray, C_{Ligand} lime, C_{PLP} yellow, F light cyan, N blue, O red, P orange, S yellow.



Binding of (+)-85

by www.RCMD.it

- The **N(2) atom** of the pyrazole ring is **protonated** and forms a **short ionic H-bond** with the side chain of **Glu56**.
- The biaryl moiety is located in the pABA channel and directs the carboxylate side chain toward the periphery of the protein where **Tyr63** adopts a **conserved position** in all structures.
- The **carboxylate of (+)-85** in a gauche conformation of the side chain is actually engaged in a **water-mediated interaction with Tyr63** via W1 ($d(\text{O} \cdots \text{OW1}) = 2.7 \text{ \AA}$ and $d(\text{OW1} \cdots \text{OTyr}) = 2.8 \text{ \AA}$). Two additional water molecules (W2 and W3) participate in solvating the carboxylate; no other protein residues are in their close proximity.
- The **isopropyl and methyl groups** attached to the core provide an **optimal filling of small lipophilic pockets**.
- The **meta-fluorine atom** is involved into **hydrophobic contacts with Lys355 and Pro367**.

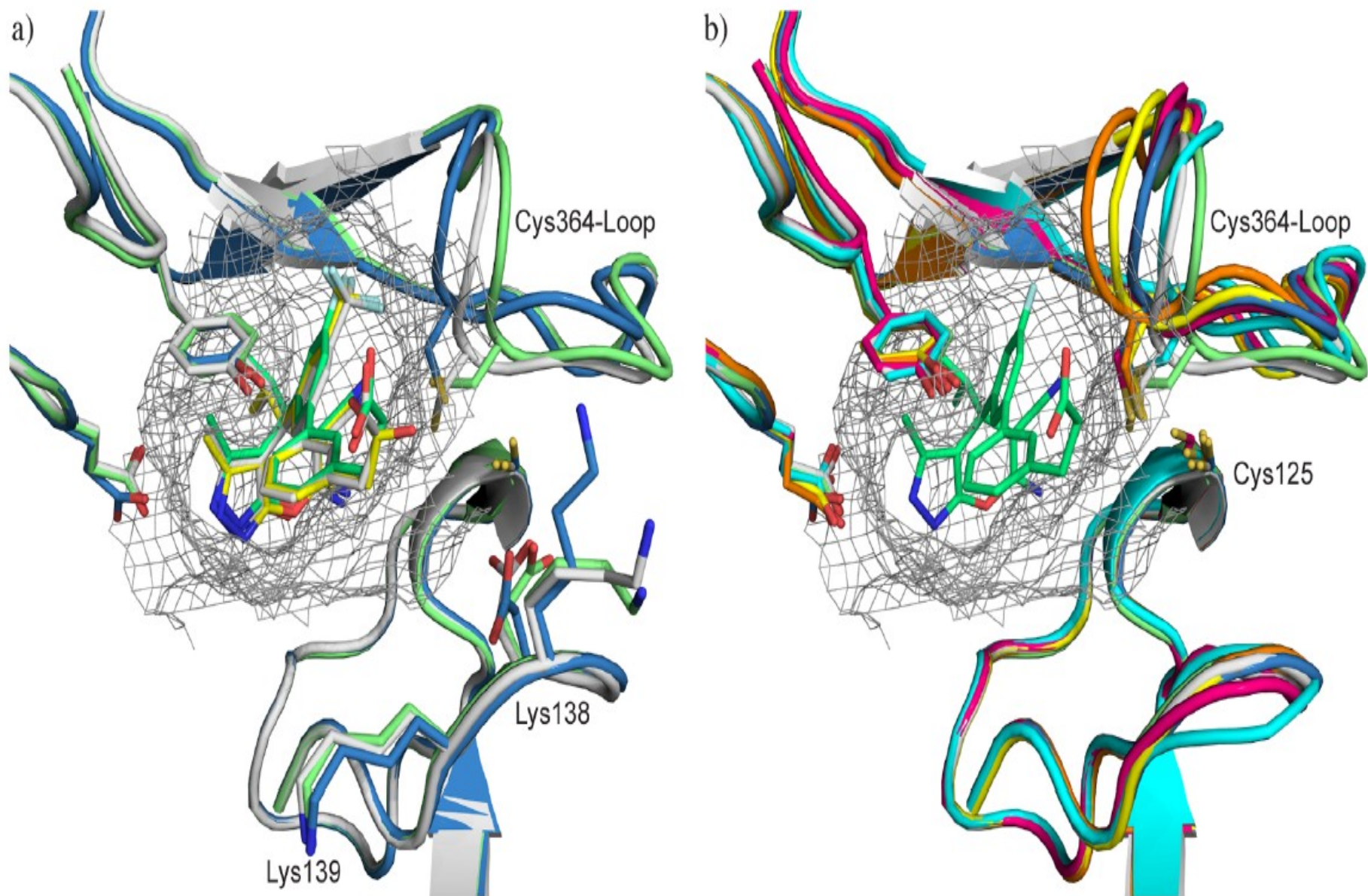
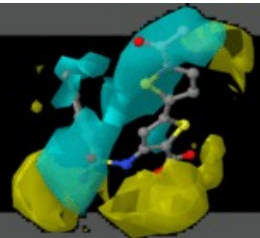
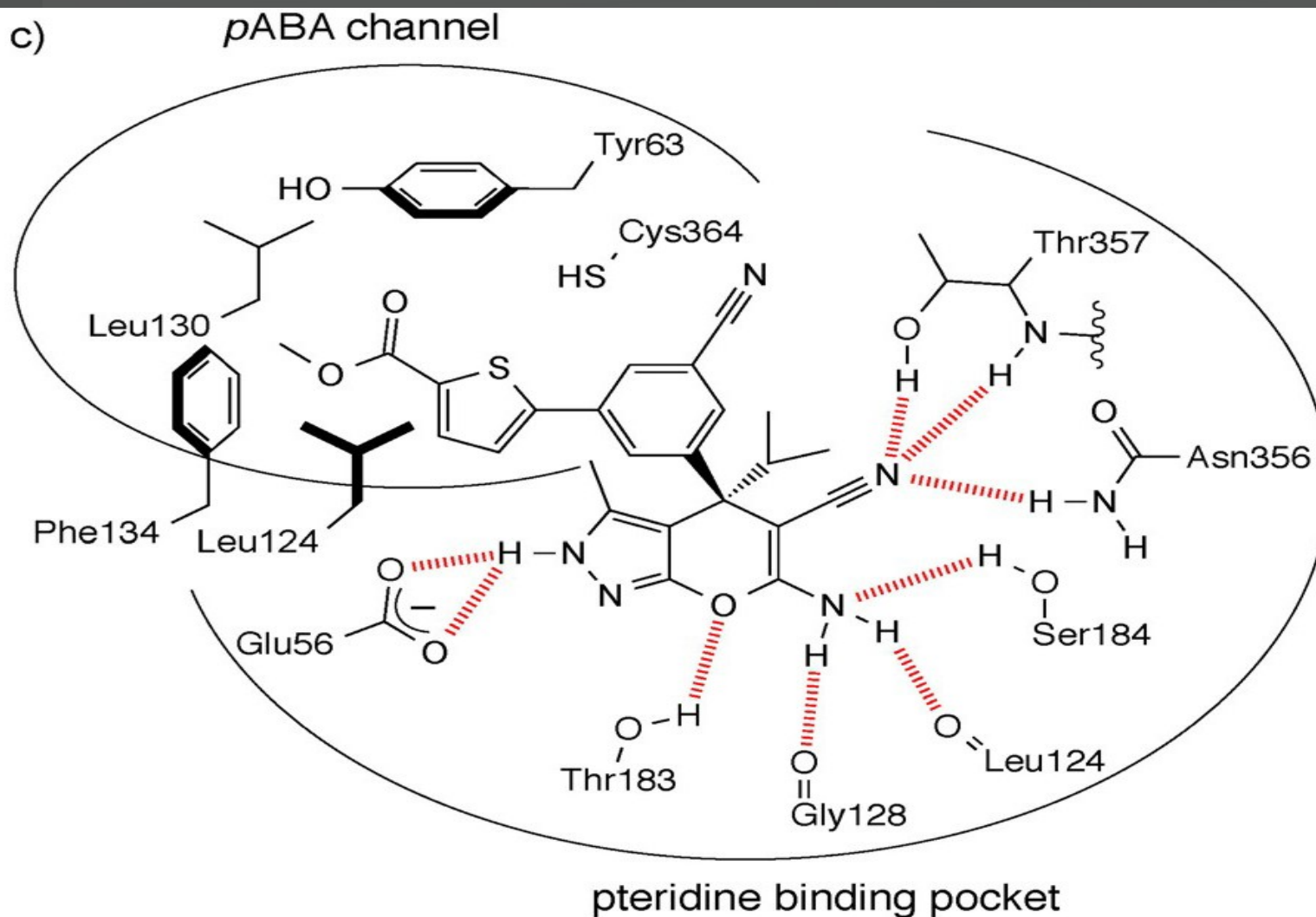


Figure 5. (a) Superimposition of the complexes of *PvSHMT* with (+)-80, (+)-81, and (+)-85. (b) Superimposition of the complexes with (+)-1, (+)-4, (+)-7, (+)-80, (+)-81, (+)-85, and (+)-89 (the structure of (+)-89 is shown in the SI, Section S4.3, Figure S23). Only ligand (+)-85 is shown for clarity. The protein loops and β -strands are represented as cartoon; the active site surface is represented as gray mesh. PLP and water molecules omitted for clarity. Color code: $C_{(+)-1-PvSHMT}$ pink, $C_{(+)-4-PvSHMT}$ orange, $C_{(+)-7-PvSHMT}$ yellow, $C_{(+)-80-PvSHMT}$ marine blue, $C_{(+)-81-PvSHMT}$ green, $C_{(+)-85-PvSHMT}$ gray, $C_{(+)-89-PvSHMT}$ cyan, $C_{(+)-80}$ yellow, $C_{(+)-81}$ gray, $C_{(+)-85}$ lime, F light cyan, N blue, O red, S yellow.

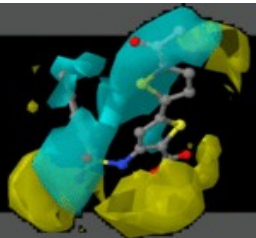


Biphenyl Series

by www.RCMD.it

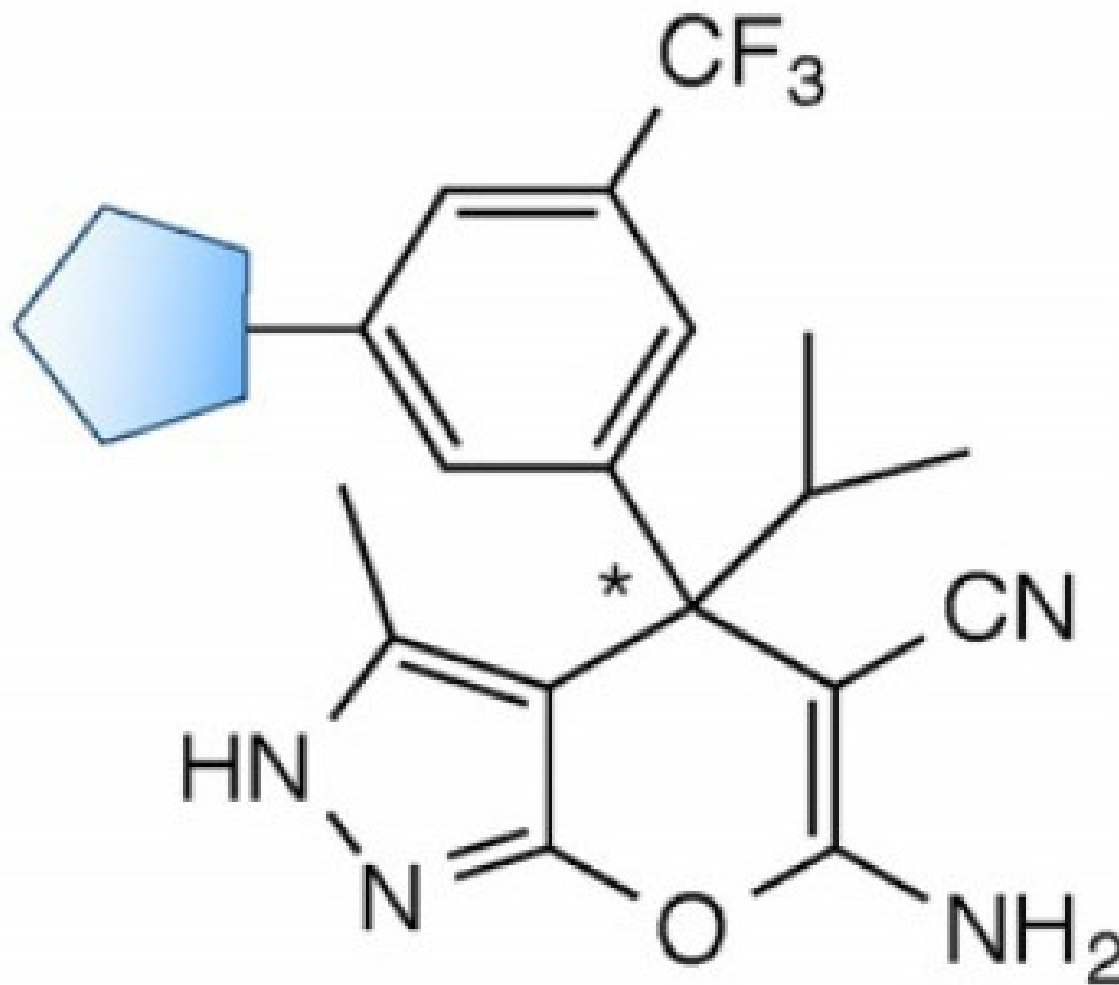


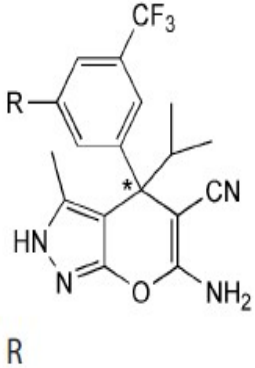
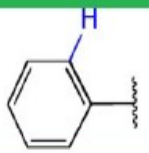
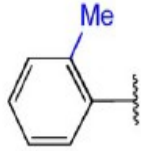
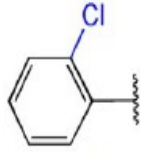
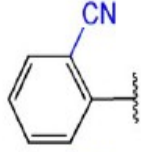
EC₅₀ *Pf* NF54: (±)-**1** = 3 nM; (+)-**1** = 2 nM
 IC₅₀ *Pf* SHMT: (±)-**1** = 370 nM; (+)-**1** = 60 nM

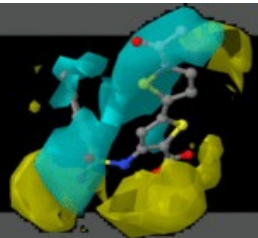


Ortho-substituted biphenyl series

by www.RCMD.it



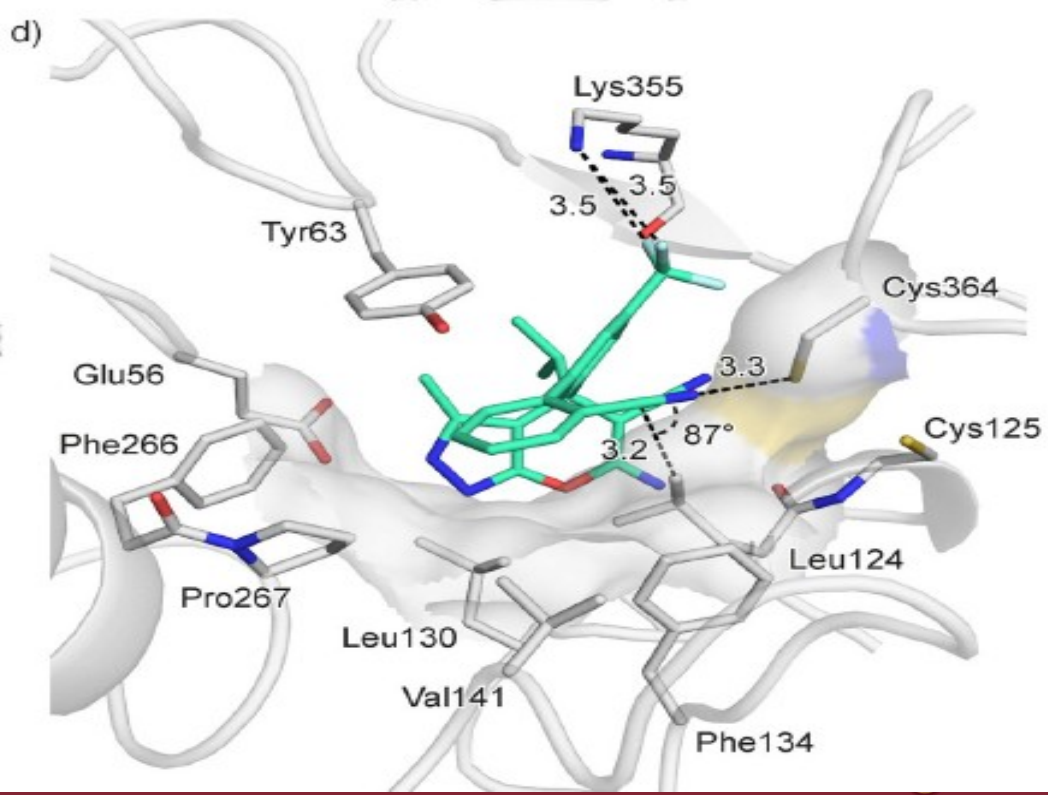
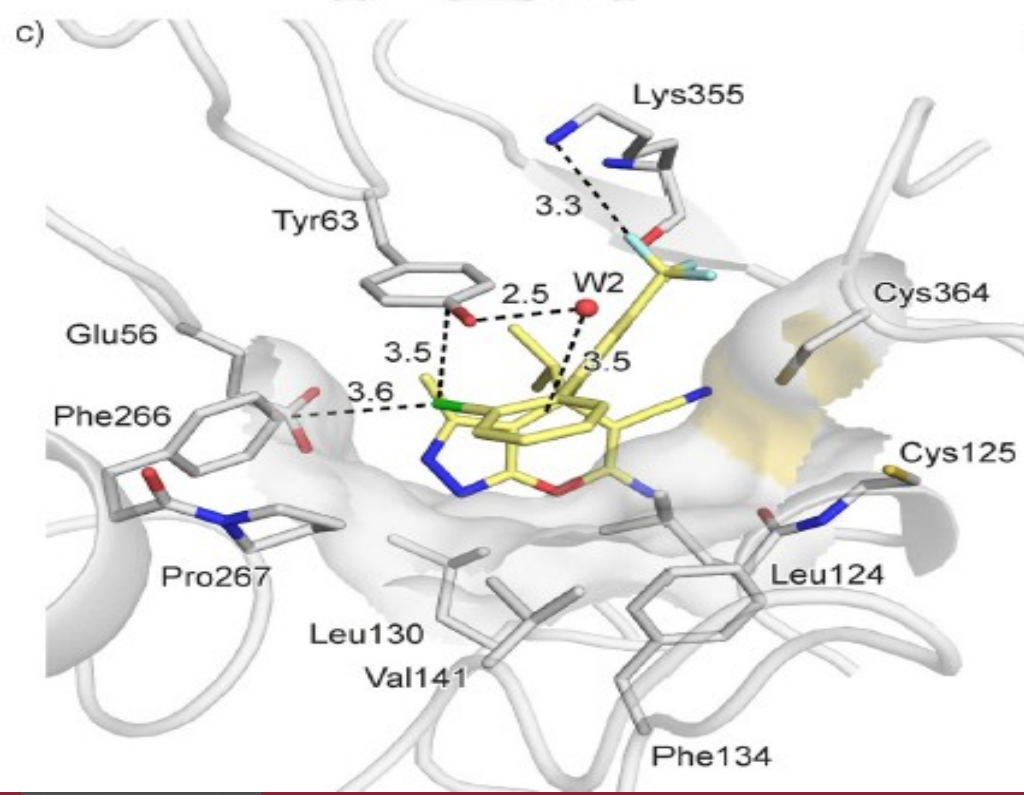
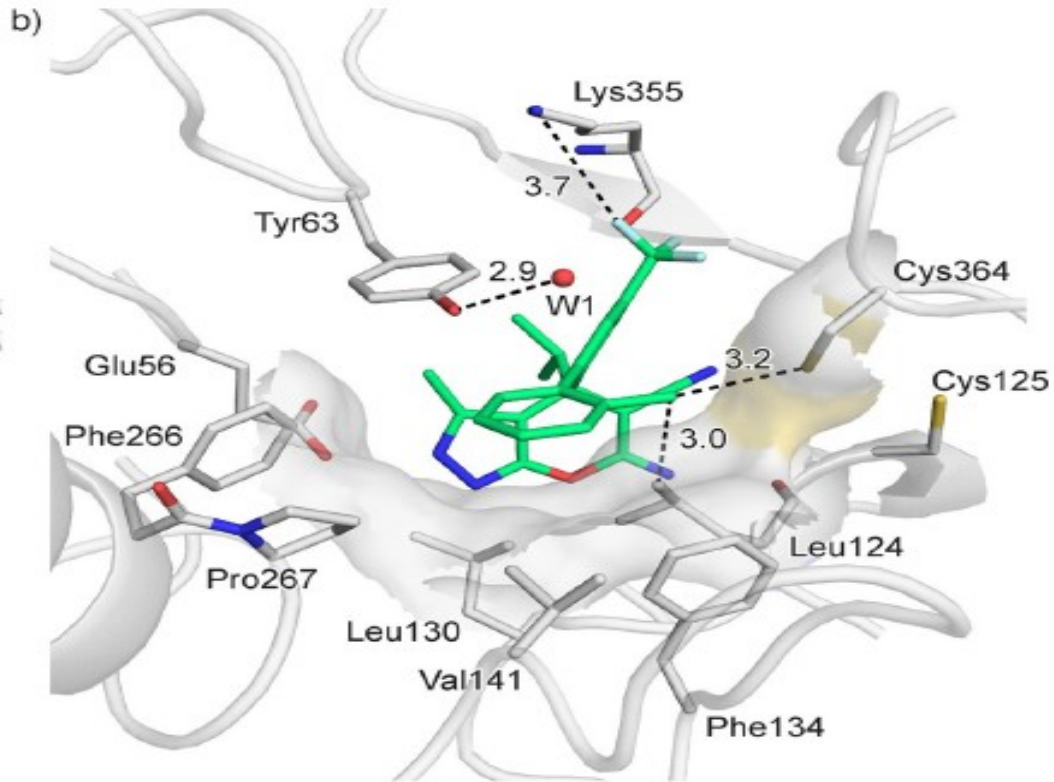
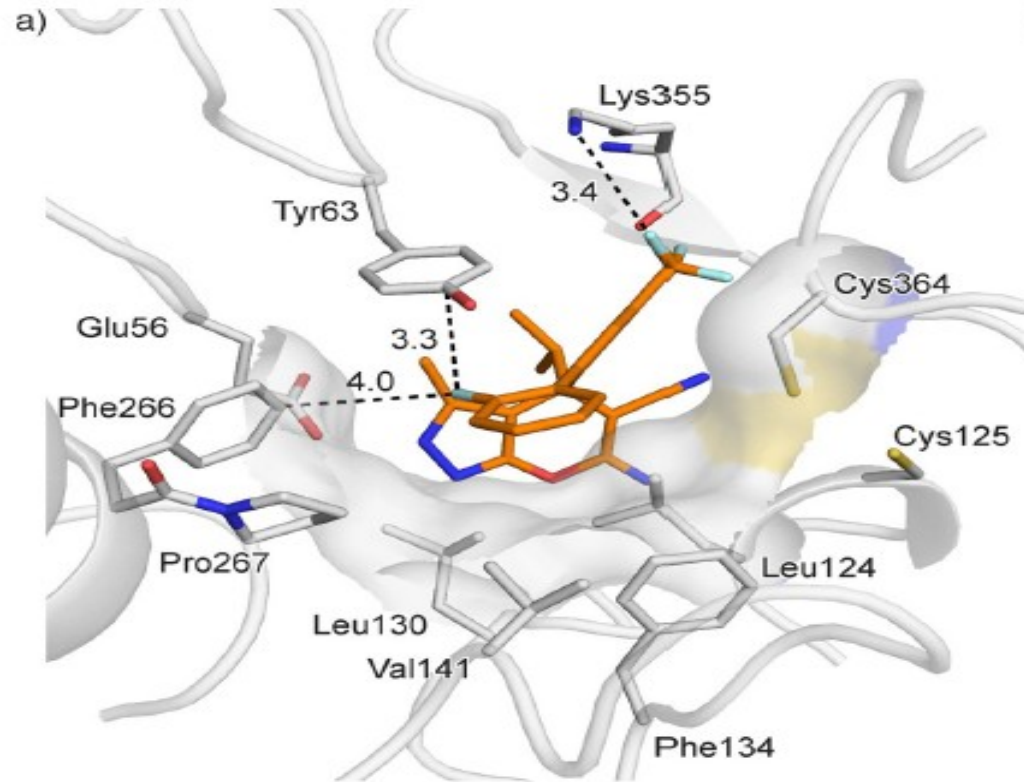
Cpd.		EC ₅₀ <i>PfNF54</i> [nM]	IC ₅₀ <i>PfSHMT</i> ± SD [nM] ^[a]	IC ₅₀ <i>AtSHMT</i> [nM]	Biphenyl Median τ [°] ^[b]	clogP ^[c]
(±)- 2		18	111 ± 5	18.6	30.3	5.2
(±)- 3		20	144 ± 0	7.3	43.2	4.9
(±)- 4		27	263 ± 11	30.9	55.5	5.3
(±)- 5		51	165 ± 4	20.9	51.3	5.5
(±)- 6		81	471 ± 8	32.0	56.8	5.5
(±)- 7		356	289 ± 13	26.2	46.1	4.7
(±)- 8		665	330 ± 22	18.5	71.8	6.0



BIPHENYL SERIES

by www.RCMD.it

- The **unsubstituted analogue (\pm)-2** was the most active ligand of the series in the target assay against PfSHMT (IC₅₀=111:5 nm, Table 1) and introduction of **larger substituents led to weaker binding**.
- The nature of the ortho-substituent exerted a significant influence on the cell-based potency (EC₅₀). **Increase in size of the ortho-substituent led to considerable decrease in antiparasitic efficacy** from EC₅₀=18 nm (\pm)-2 to 665 nm (\pm)-8. No direct correlation between cellular potency and lipophilicity (clogP) is distinguishable.
- It is **likely** that the substituent-dependent conformation of the biphenyl moiety **influences the cell-based efficacy by affecting cell permeation**. Cell permeation occurs by means of passive diffusion, carrier proteins (transporters), and channel proteins.

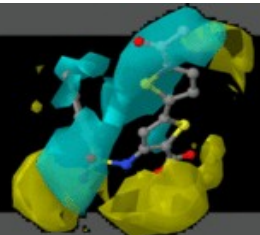




- There are **two distinct dihedral angles** in aryl sulfonamides and one in aryl sulfones that determine the conformational preferences of these fragments.

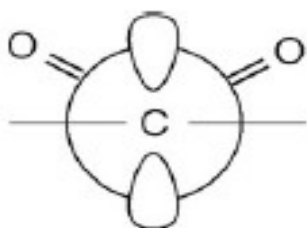
- 1) The first is the torsion angle about the Csp²-S bond in both moieties. The **favoured conformation** of aryl sulfonamides and aryl sulfones, in which the π -orbital of the ipso-carbon atom bisects the SO₂ angle.

- 2) The second dihedral angle of interest in aryl sulfonamides is the Csp²-S-N-Csp³ angle. This angle can adopt **either an eclipsed or a staggered conformation**. In most of the molecules the Csp²-S-N-Csp³ torsion angles are in a range between 60° and 90° meaning a **clear preference for the staggered conformation** with the **nitrogen lone pair bisecting the SO₂ angle**.

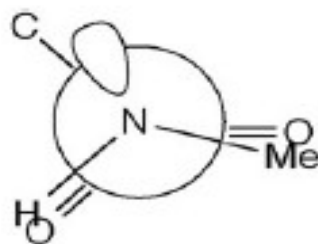


Conformation of aryl sulfonamides and aryl sulfones

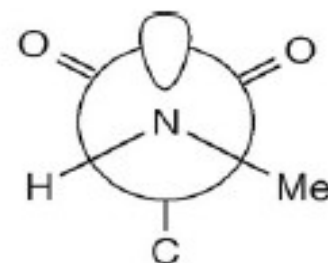
by www.RCMD.it



a) C-S bond

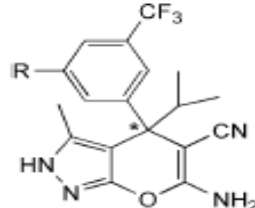
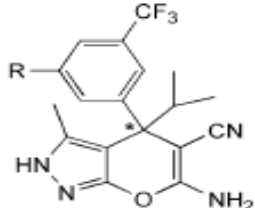
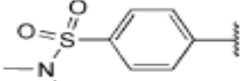
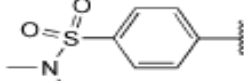
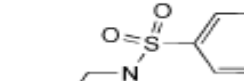
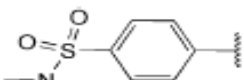
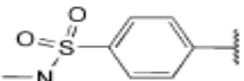
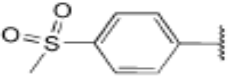
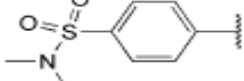
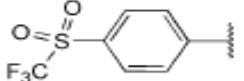
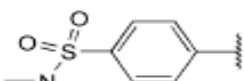
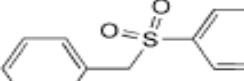
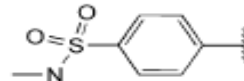
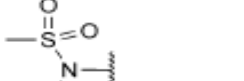
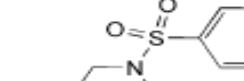
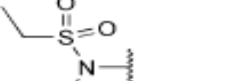


b) Eclipsed



c) Staggered

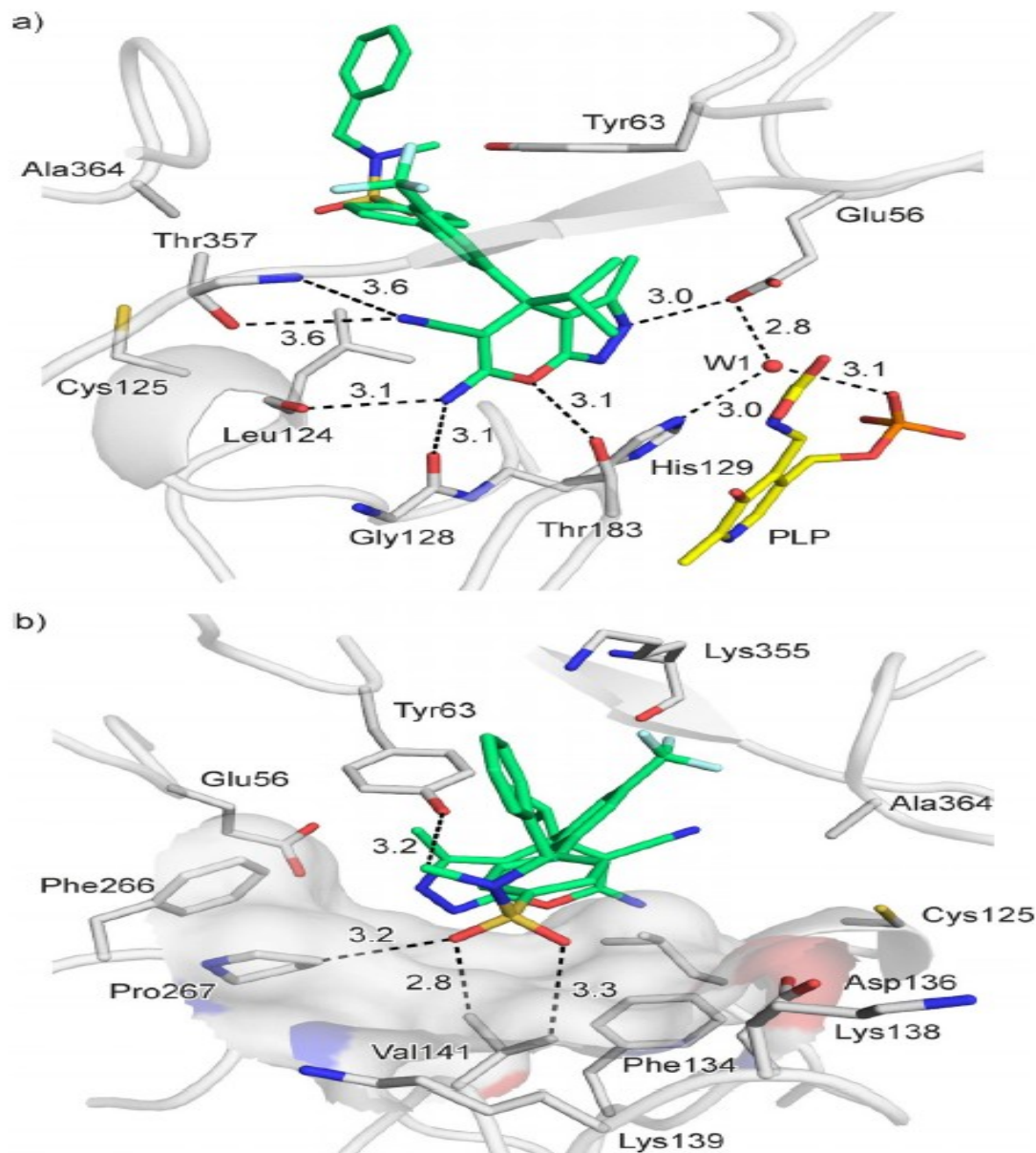
Figure 5. a) Stable conformation of aryl sulfonamides/aryl sulfones relative to the C_{sp^2} -S bond. b) and c) Two energetically stable conformations of sulfonamides relative to the N-S bond.

Cpd.		EC ₅₀ P/NF54 [nM]	IC ₅₀ ArSHMT [nM]	Cpd.		EC ₅₀ P/NF54 [nM]	IC ₅₀ ArSHMT [nM]
	R				R		
(±)- 9		114	22.8	(±)-17		104	73.9
(±)- 10		210	74.4	(+)-17		56	n.d. ^[a]
(±)- 11		657	43.0	(-)-17		1584	n.d.
(±)- 12		400	39.1	(±)-18		91	16.8
(±)- 13		391	29.0	(±)-19		1399	n.d.
(±)- 14		374	87.7	(±)-20		557	24.5
(±)- 15		872	79.1	(±)-21		200	22.4
(±)- 16		838	85.6	(±)-22		186	19.2



Binding of (+)-17

by www.RCMD.it



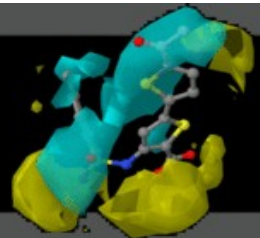
Co-crystal structure (PDB ID code: 5XMQ) showing the protein–ligand interactions of pyrazolopyran (+)-17 (lime) and C364A-PvSHMT mutant (grey). a) Polar interactions between (+)-17 and the protein. b) Interactions, largely dipole-dipole type, involving the sulfonamide moiety in the pABA channel. The surface spans the volume of the pABA channel. The water molecule (W1) is represented as a red sphere. PLP is omitted for clarity in b). Distances are given in a. Color code: Cprotein grey, C(+)-17 lime, CPLP gold, F light cyan, N blue, O red, P orange, S yellow.



SAR Results

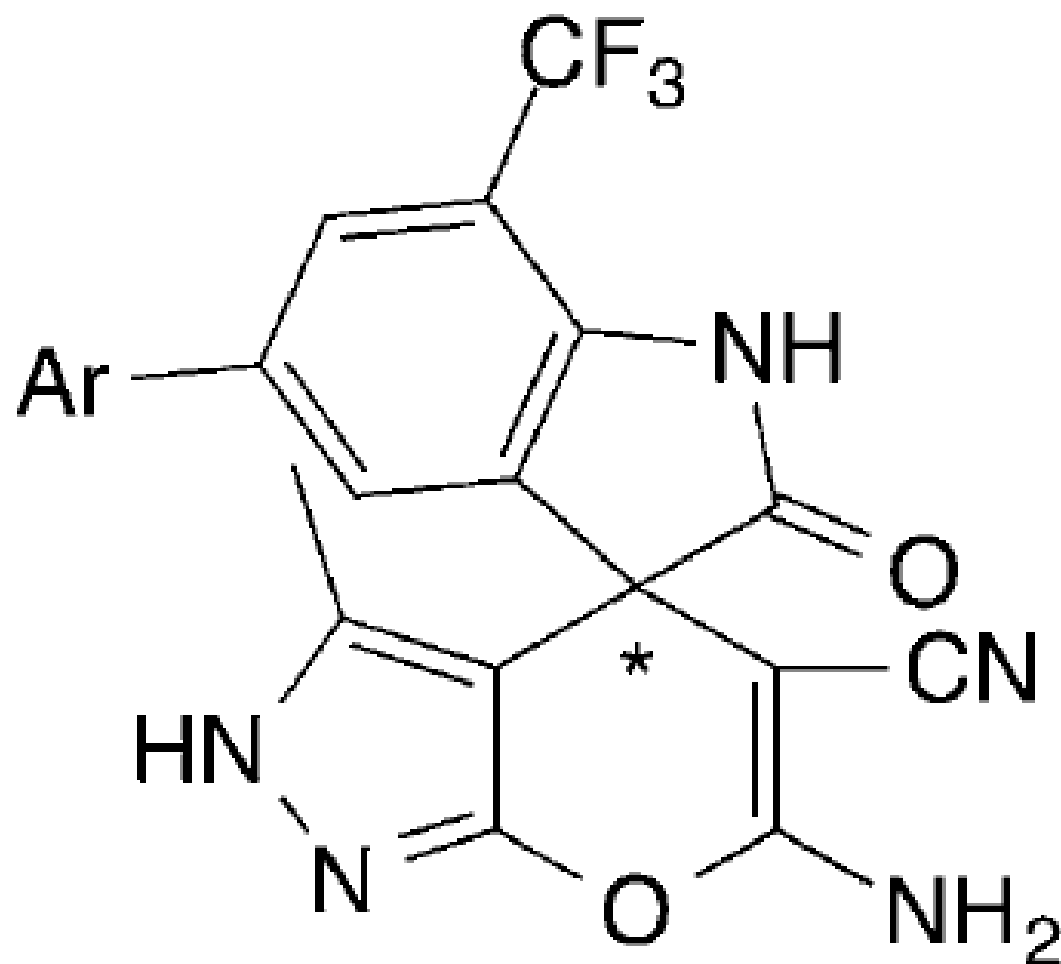
by www.RCMD.it

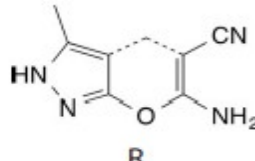
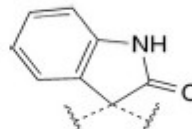
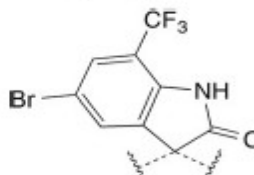
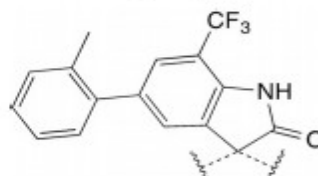
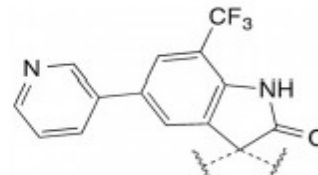
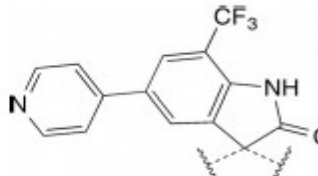
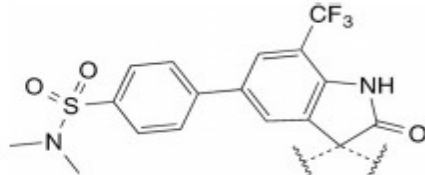
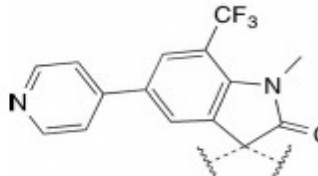
Several ligands of both biphenyl and aryl sulfonamide/ aryl sulfone series proved to be **highly potent** in our in vitro assays, they were not studied further due to their **limited metabolic stability in human liver microsomes ($t_{1/2} < 10$ min)**. The **terminal fragments** on the phenyl ring departing from the core **are presumably responsible for this intrinsic instability** and not the pyrazolopyran core (series of pyrazolopyran-based ligands with half-lives up to 4 h.)



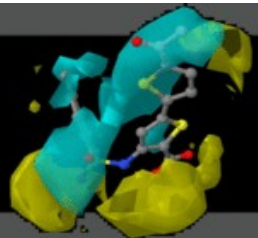
2-Indolinone series

by www.RCMD.it



Compound		EC ₅₀ P/NF54 [μM]	IC ₅₀ P/SHMT [μM] ^[a]	IC ₅₀ A/SHMT [μM]
(±)-29		> 34	> 250	12% inhibition at 100 μM
(±)-30		22.7	> 250	14.3
(±)-19		22.1	5.2 ± 0.4	1.2
(±)-20		22.8	> 250	48% inhibition at 100 μM
(±)-21		11.6	> 250	34.2
(±)-22		16.7	n.d. ^[b]	n.d.
(±)-31		1.5	> 250	9.6

[a] Data are the mean ± SD of $n=3$ experiments performed in duplicate. [b] n.d.: not determined.

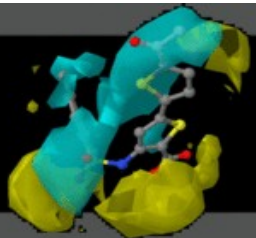


SAR Results

by www.RCMD.it

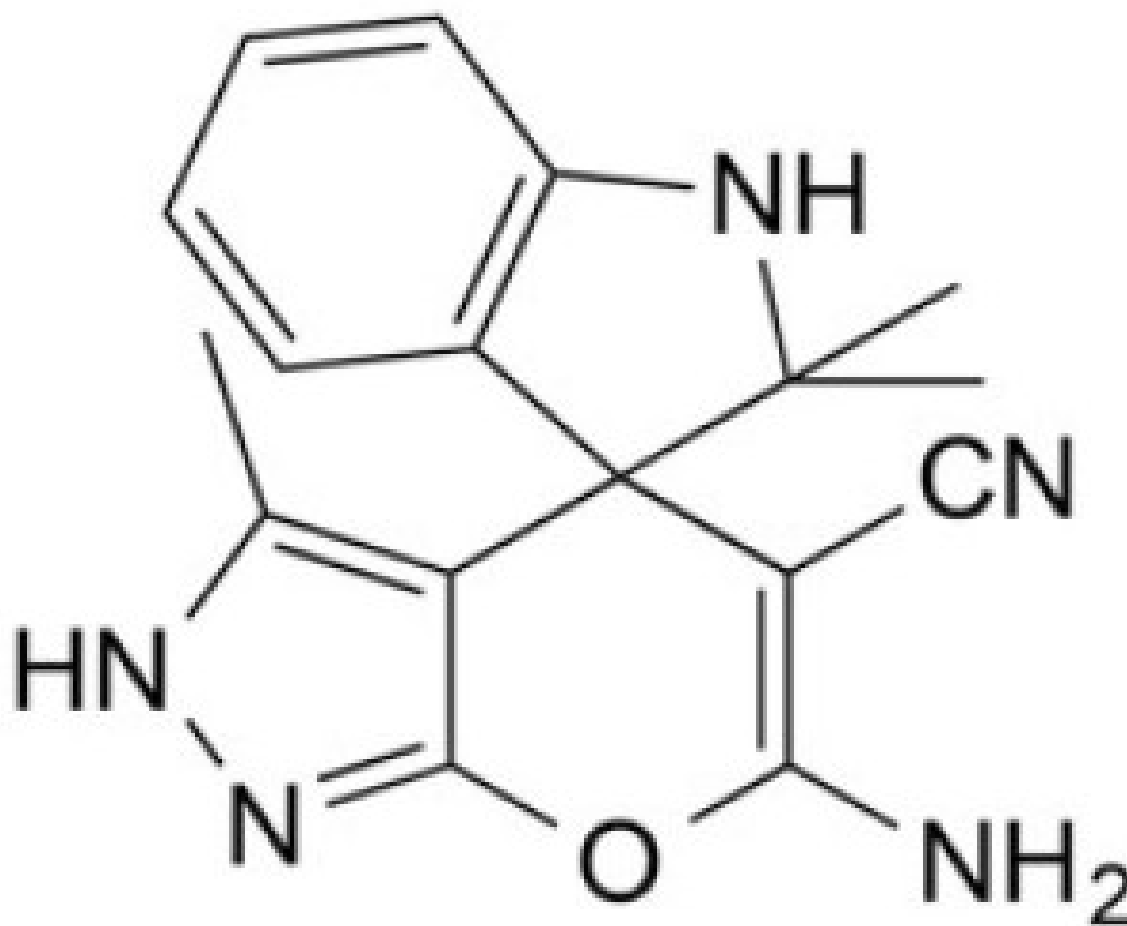
- **The core alone (\pm)-29 did not exhibit any efficacy** in any assays, whereas its functionalization at both meta positions led to minor improvements (target affinities still remained in the high micromolar range)
- With the exception of **orthotolyl derivative (\pm)-19**, which could decrease the enzymatic activities in the **low micromolar range** , **all other ligands (\pm)-20–22 and (\pm)-30 were inactive** in the target assays. Cell-based efficacies were also unsatisfactory, with measured EC50 values in the two-digit micromolar range.
- **N-Methylation of (\pm)-21 resulted in (\pm)-** with **sevenfold enhanced potency** in the cell-based assay (EC50=1.5 μ m), which **might be the result of better cell permeation**.

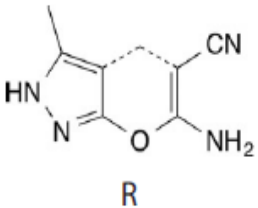
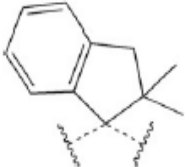
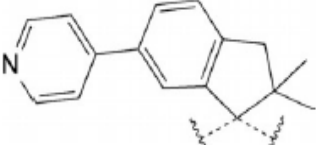
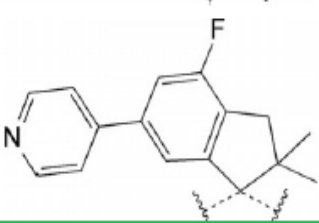
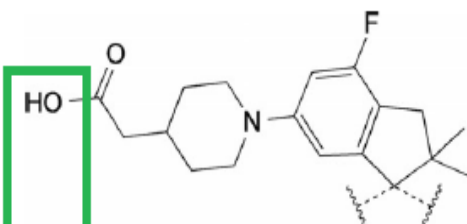
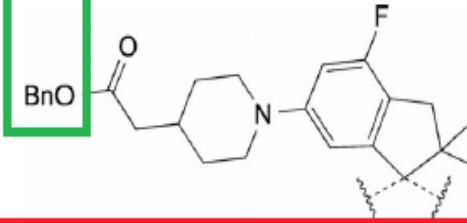
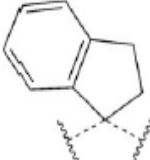
The poor activity values observed with this series reflect that a polar fragment at this position of the molecule, such as the lactam ring in the 2-indolinone analogues, is not suitable for binding to SHMT.



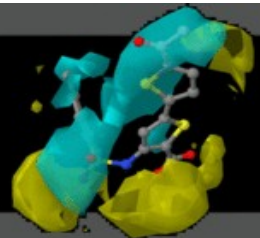
Spiro-dihydroindene series

by www.RCMD.it



Compound		EC ₅₀ <i>PfNF54</i> [μM]	IC ₅₀ <i>PfSHMT</i> [μM] ^[a]	IC ₅₀ <i>AtSHMT</i> [μM] ^[a]	IC ₅₀ <i>hSHMT1</i> [μM] ^[a]	SF ^[b]	
(±)-42		25.5	0.201 ± 0.004	2.86 ± 0.280	8.86 ± 0.68	44.1	
(±)-43		2.358	0.030 ± 0.001	0.173 ± 0.009	0.047 ± 0.002	1.6	
(±)-57		0.619	0.039 ± 0.001	0.195 ± 0.004	0.047 ± 0.001	1.2	
(+)-57		0.334	0.014 ± 0.002	0.281 ± 0.016	0.027 ± 0.001	1.9	
(-)-57		10.213	0.339 ± 0.006	2.27 ± 0.156	0.125 ± 0.003	0.4	
(±)-59		2.131	0.061 ± 0.001	0.112 ± 0.006	0.057 ± 0.001	0.9	
(+)-59		0.861	0.043 ± 0.002	0.163 ± 0.007	0.019 ± 0.001	0.4	
(-)-59		> 21.5	2.51 ± 0.03	4.69 ± 0.200	0.440 ± 0.010	0.2	
(±)-63			0.252	0.076 ± 0.002	0.648 ± 0.038	0.029 ± 0.001	0.4
(+)-63			0.165	0.060 ± 0.002	0.494 ± 0.043	0.029 ± 0.001	0.5
(-)-63			2.487	> 25.0	4.79 ± 0.861	0.248 ± 0.005	< 0.1
(±)-64		> 36.0	4.36 ± 0.72	47% inhibition at 100 μM	> 250	57.3	

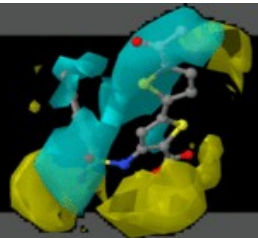
[a] Data are the mean ± SD of *n* = 3 experiments performed in duplicate. [b] Selectivity factor: (IC₅₀ *hSHMT1*)/(IC₅₀ *PfSHMT*).



SAR Results

by www.RCMD.it

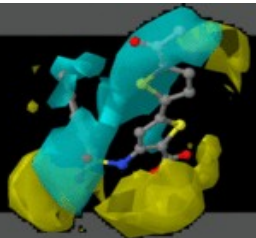
- The **core shows good sub-micromolar affinity** for PfSHMT, which is in contrast to the inactive 2-indolinone analogues .
- Affinity gained for (\pm)-43, which featured a terminal 4-pyridyl moiety highlighting the importance of filling the pABA channel to inhibit PfSHMT activity efficiently.
- Introducing a fluoride into ligand(\pm)-57 did not substantially affect the target affinity, whereas replacing the pyridyl ring with a carboxypiperidyl moiety in compounds(\pm)-59 and (\pm)-63 also resulted in activity in the two-digit nanomolar range .
- **More than 10-fold potency improvement** was obtained upon occupying the pABA channel with a **4-pyridyl fragment** .
- The **addition of a fluoride** to the meta position of the fused phenyl ring had a significant impact, as exemplified by the **sub-micromolar potency** measured for (\pm)-57
- A better EC50 value was measured for **benzyl ester** (\pm)-63, presumably as a result of **improved cellular permeation** due to its significant lipophilic character, because the corresponding carboxylate (\pm)-59 is 10-fold less potent.
- **It is noteworthy that the gem-dimethyl moiety on the dihydroindene scaffold is essential for activity** because its removal led to a considerable loss of affinity .



Binding of (+)-59

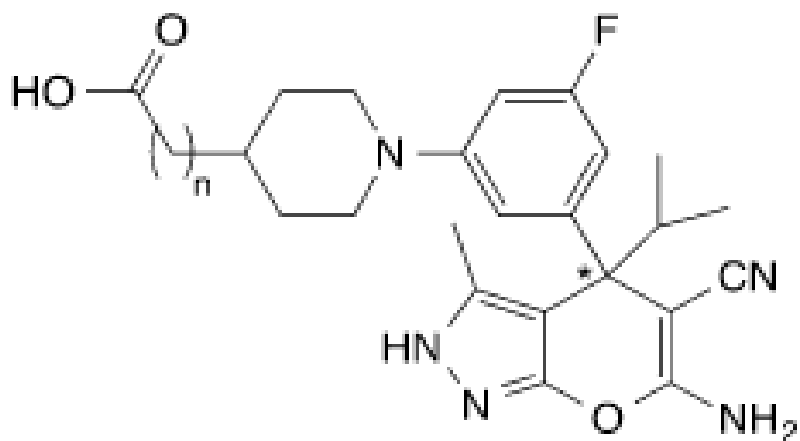
by www.RCMD.it

- The pyrazolopyran core forms three strong hydrogen-bonding interactions through the vinylogous cyanamide with the side chain of Thr357 and the backbone C=O of Leu124 and Gly128
- In addition, the nitrile moiety of the ligands is engaged in favorable parallel stacking with the side chain of Asn356 .
- The sp³-oxygen atom of the pyran ring is at a short distance from Thr183, establishing a favorable hydrogen bond, but it is also in proximity to the backbone C=O of Gly128 .
- The small lateral pocket lined by the Cys364 loop is not properly filled by the meta-fluoro-substituted phenyl ring of the dihydroindene fragment of (+)-59, leading to a small void, which allows the insertion of a water molecule.
- The pyrazole ring is oriented in such a way that the pyrazole NH cannot interact directly with Glu56 . The pyrazolopyran core was not aligned with Glu56 to form a strong direct ionic hydrogen bond with its side chain.
- The gem-dimethyl fragment on the spirodihydroindene scaffold and the methyl moiety on the pyrazole ring provide optimal filling of the binding pocket. The methyl group is loosely surrounded by the lipophilic side chains of Tyr63 and Phe266, while the gem-dimethyl moiety interacts with both Tyr64 and the polarizable hydrogen-bonding array between the side chain of Arg371 and the carboxylate of the PLP-Gly Schiff base.



Non-spirocyclic analogue (+)-65

by www.RCMD.it



(+)-**65** (n = 1): EC_{50} *Pf* NF54 = 35 nM
 IC_{50} *Pf* SHMT = 110 nM
 IC_{50} *At* SHMT = 12.6 nM

(±)-**66** (n = 2): EC_{50} *Pf* NF54 = 17 nM
 IC_{50} *Pf* SHMT = 130 nM
 IC_{50} *At* SHMT = 13.8 nM

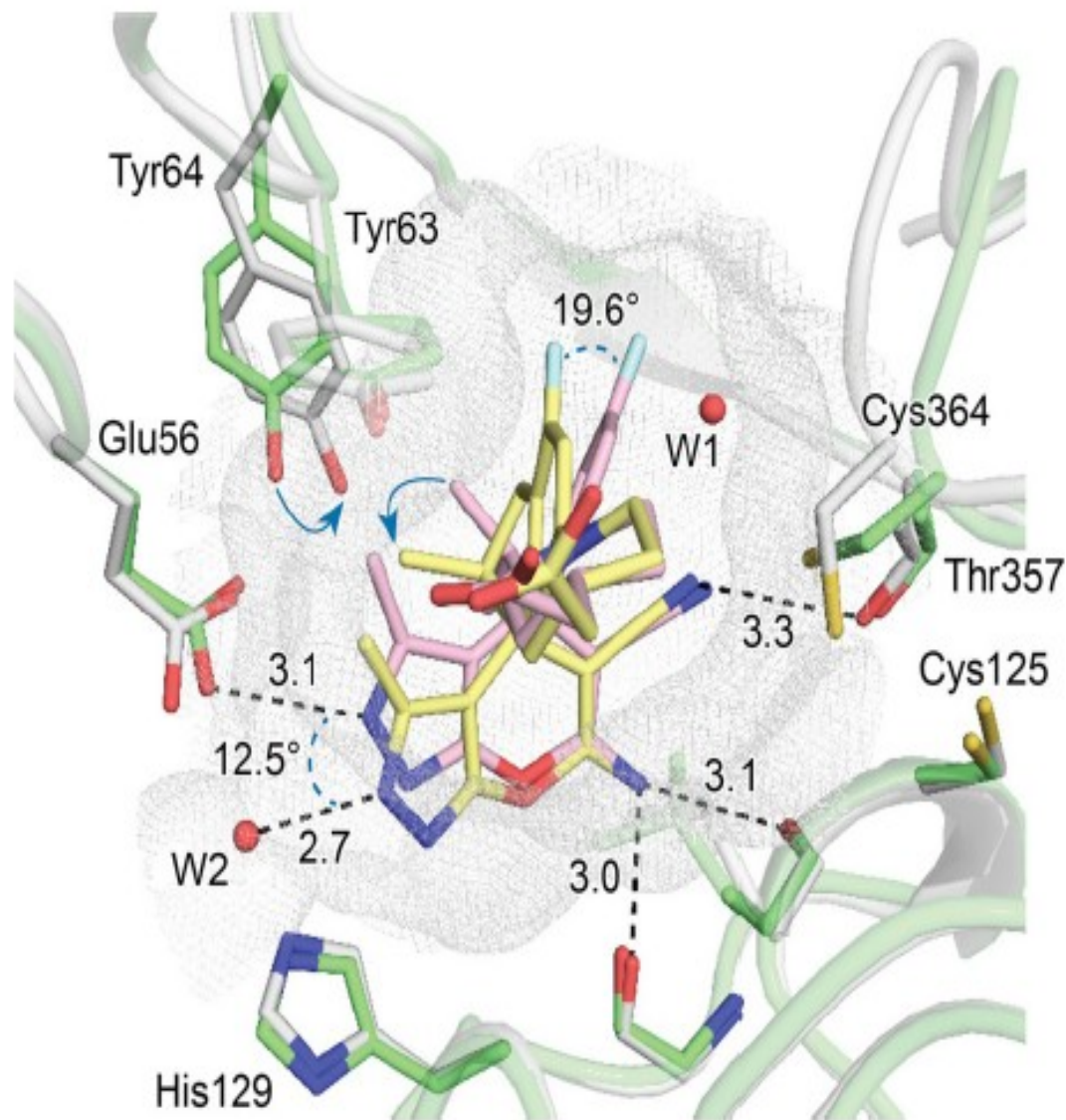


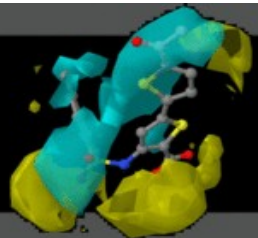
Figure 4. Overlay of the PvSHMT–ligand complexes obtained with (+)-59

(PDB ID: 5YG4, 2.3 a) and (+)-65 (PDB ID: 5YFZ, 2.2 a). The water molecules

are represented as red spheres. PLP-Gly is omitted for clarity. The mesh

spans the volume of the binding pocket. Distances are given in a. Color

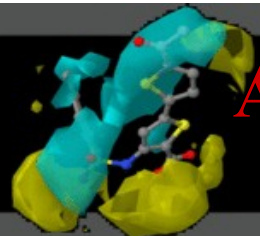
code: CPvSHMT–(+)-59 gray, CPvSHMT–(+)-65 green, C(+)-59 gold, C(+)-65 pink, F light cyan, N blue, O red, S yellow.



Comparison between (+)-59 and its non-spirocyclic analogue (+)-65

by www.RCMD.it

- The spirocyclic motif in (+)-59 enforces a more tetrahedral arrangement at the stereogenic center, leading to a significantly **less planar conformation** of the pyrazolopyran core than that in (+)-65 .
- The pyrazole fragment of (+)-59 **does not point toward Glu56** and deviates by 12.58 compared with the original binding mode.
- The positioning of one **CH3 group** (from the gem-dimethyl moiety in (+)-59 and the isopropyl moiety in (+)-65) in the back of the pocket **varies markedly**. Tyr64 swings away to compensate for the small void created by the different positioning of this methyl moiety in the PvSHMT–(+)-59 complex.
- These two co-crystal structures **underline the paramount importance of the vinylogous cyanamide in the binding mode of both ligand classes to PvSHMT.**
- They suggest that the **pyrazole fragment can possibly be replaced by alternative heterocyclic moieties without affecting the target affinity much**. Interactions of the ligand core with the side chain of Glu56, as in the non-spirocyclic series, **are not essential for strong binding of the spirocyclic scaffolds.**



Affinity of spiro-dihydroindene analogues for hSHMT1

by www.RCMD.it

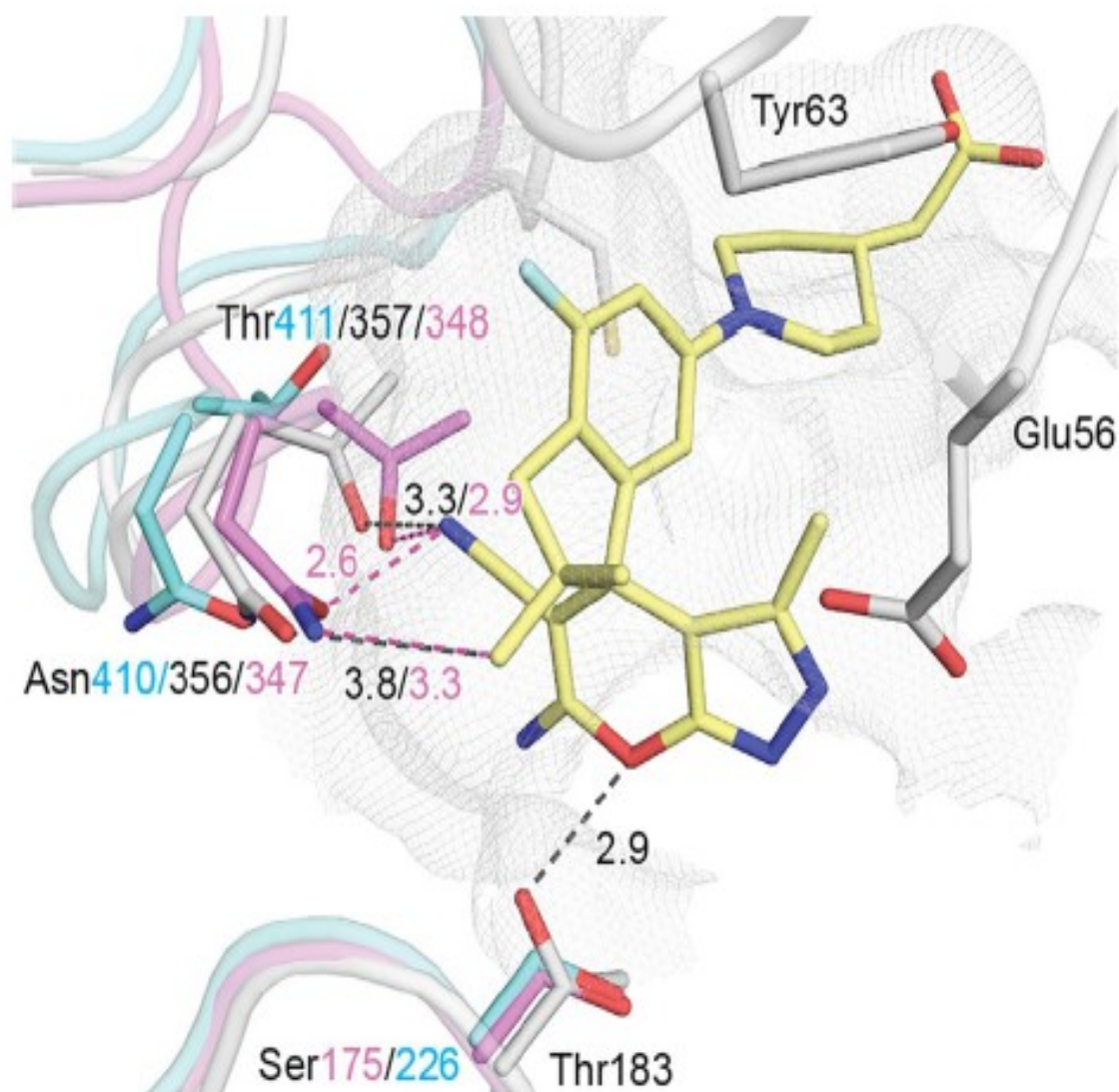
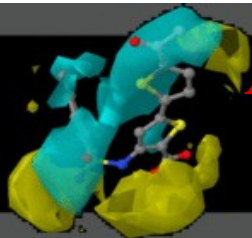


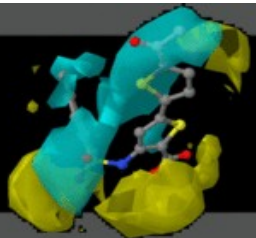
Figure 6. Superposition of the PvSHMT-(+)-59 complex (gray; PDB ID: 5YG4,) with rabbit SHMT1 (purple; from PDB ID: 1LS3, 2.7 a)[64] and human SHMT2 (cyan; from PDB ID: 5V7I, 2.5 a).[62] Only relevant residues are shown as stick representation. The mesh spans the volume of the binding pocket. PLP-Gly is omitted for clarity. Distances are given in a. Color code: C(+)-59 gold, F light cyan, N blue, O red, S yellow.



Affinity of spiro-dihydroindene analogues for hSHMT1

by www.RCMD.it

- Ligands (\pm)-42 and (\pm)-64 are highly selective for PfSHMT, whereas other ligands of this series have similar affinities for both species (e.g. (\pm)-57 or (\pm)-59). **The SAR is identical for both species:** occupying the pABA channel with a terminal fragment significantly enhancing the activity and **adding a fluoride on the fused phenyl ring having no effect on target affinity.**
- It is noteworthy that **chiral recognition is less pronounced with hSHMT1.** There is a 23-fold difference in affinity for hSHMT1 between (+)-59 and (-)-59, whereas the affinity discrepancy is considerably larger (58-fold) for PfSHMT.
- There are **three major differences** between the three structures that could possibly explain the observed selectivity.
 - 1) First, the **threonine residue (Thr183)** in Plasmodial SHMT, which establishes a strong hydrogen bond with the pyran ring of (+)-59, is **replaced by a serine residue (Ser175/ 226) in mammalian SHMTs** that cannot interact with the ligand in the observed conformation.
 - 2) Second, the position of the **asparagine side chain fluctuates notably.** Asn410 from hSHMT2 is too far away to establish any attractive interaction. Conversely, Asn356 from PvSHMT is at an ideal position for interacting with (+)-59 and avoiding repulsion.
 - 3) Residue Thr411 from hSHMT2 is turned away from the ligand, which prevents the formation of a hydrogen bond with the nitrile moiety of the ligand.



Antifolate Inhibitors

by www.RCMD.it

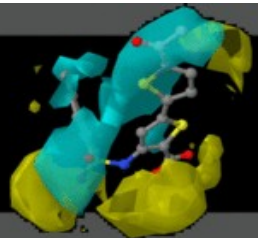
- Methotrexate (MTX) , a methylated derivative of aminopterin, was the **first selective chemotherapeutic targeting 1C metabolism**.
- Methotrexate has gradually increased and now it is used to cure millions of cancer patients annually. Methotrexate treatment, as a single agent or as a part of multidrug chemotherapy, is **effective against leukemia, non-Hodgkin lymphomas and a number of other cancer types**. As a chemotherapeutic Methotrexate is used in high doses over a short period of time and its efficacy depends on the duration of infusion and on intracellular drug concentration
- In low doses, Methotrexate is generally well tolerated, and **prolonged low-dose therapy is given to patients suffering from autoimmune diseases**, such as lupus, psoriasis, sarcoidosis, and rheumatoid arthritis.



Antifolate Inhibitors

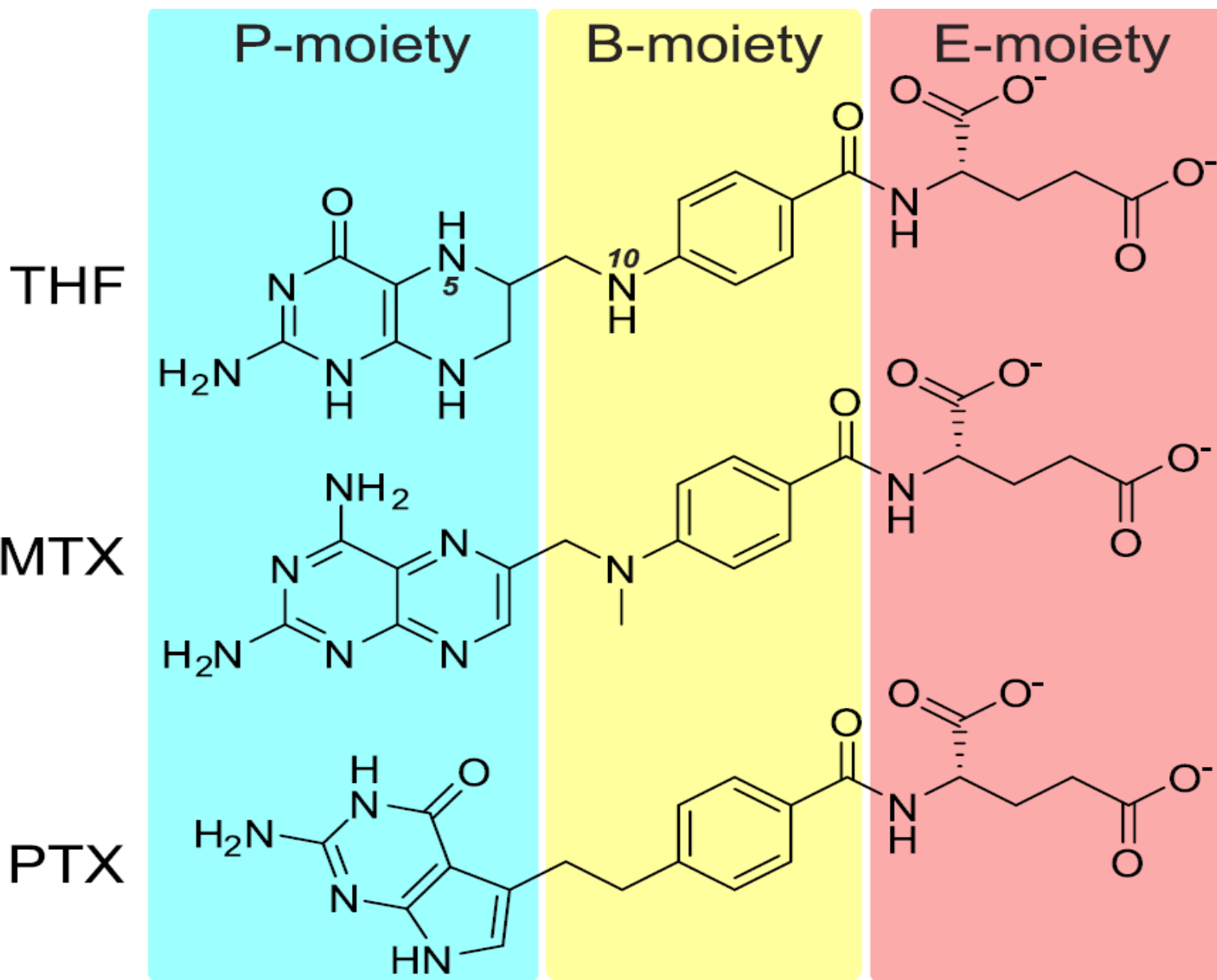
by www.RCMD.it

- Pemetrexed represents a recently discovered antifolate approved by the Food and Drug Administration for the **treatment of mesothelioma (in combination with cisplatin) and non-small cell lung cancer (as a stand-alone agent)**.
- Instead of targeting a single enzyme, like many other antifolates, pemetrexed acts by **inhibiting several enzymes** involved in folate-dependent biosynthetic pathways, i.e. TS, glycinamide ribonucleotide formyltransferase (GARFT) and, to a lesser extent, 5-aminoimidazole-4-carboxamide ribonucleotide formyltransferase (AICARFT), DHFR, the 5,10-CH₂-THF dehydrogenase and 10-CHO-THF synthetase activities of C1 tetrahydrofolate synthase.



Moieties of THF

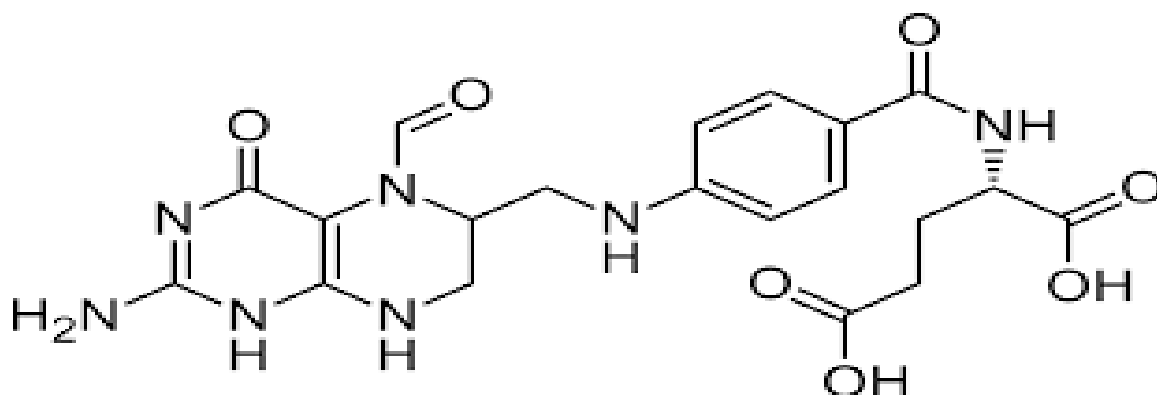
by www.RCMD.it



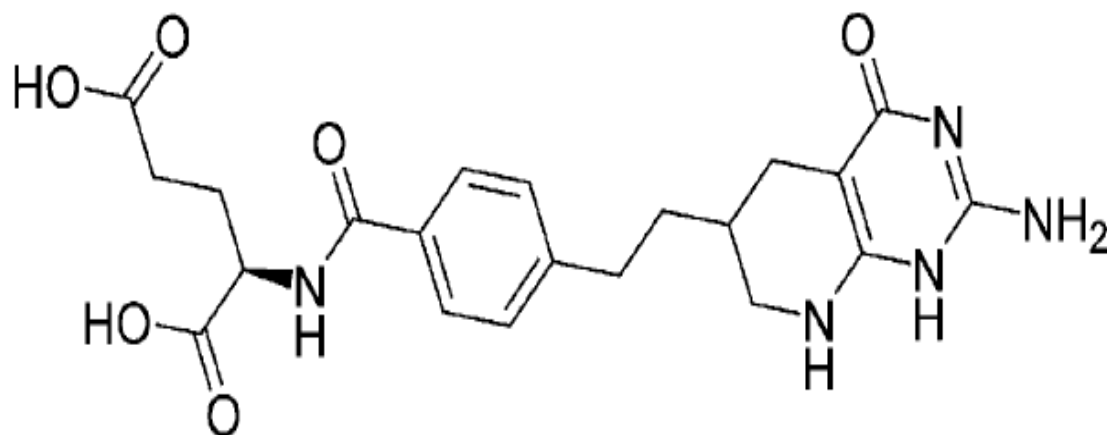


Leucovorin and Lometrexol structures

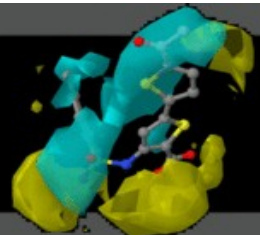
by www.RCMD.it



Leucovorin



Lometrexol

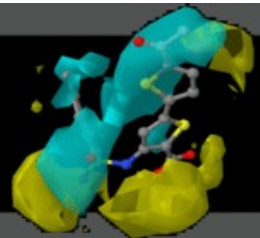


Inhibition of Lometrexol

by www.RCMD.it

Table 3. Inhibition data of hSHMT1 and hSHMT2 with antifolates

	SHMT1		SHMT2	
	Activity (%) at 100 μM compound	<i>n</i>	Activity (%) at 100 μM compound	<i>n</i>
Pemetrexed	71.9 \pm 11.6	3	79.2 \pm 6.8	3
Lometrexol	36.5 \pm 4.1	3	49.7 \pm 4.7	3
Methotrexate	59.1 \pm 8.2	3	87.4 \pm 8.3	3
Raltitrexed	72.7 \pm 5.9	3	94.0 \pm 11.5	3



SHMT Inhibition by Lometrexol

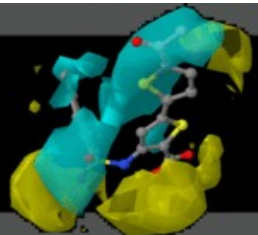
by www.RCMD.it

Table 2. Thermodynamic parameters of the interactions characterized in this work derived from the curve fit obtained through microcalorimetric titrations of *hcSHMT* and different ligands.

Ligand	$\Delta H^{[a]}$ [kcal mol ⁻¹]	ΔS [cal mol ⁻¹ /deg]	K_d [μM] ^[a]	$n^{[a]}$
LTX	3.50 ± 0.06	38.0	1.99 ± 0.99	0.53 ± 0.05
Leucovorin	4.64 ± 0.39	42.4	1.36 ± 0.49	0.51 ± 0.03
Leucovorin ^[b]	– ^[c]	– ^[c]	– ^[c]	– ^[c]

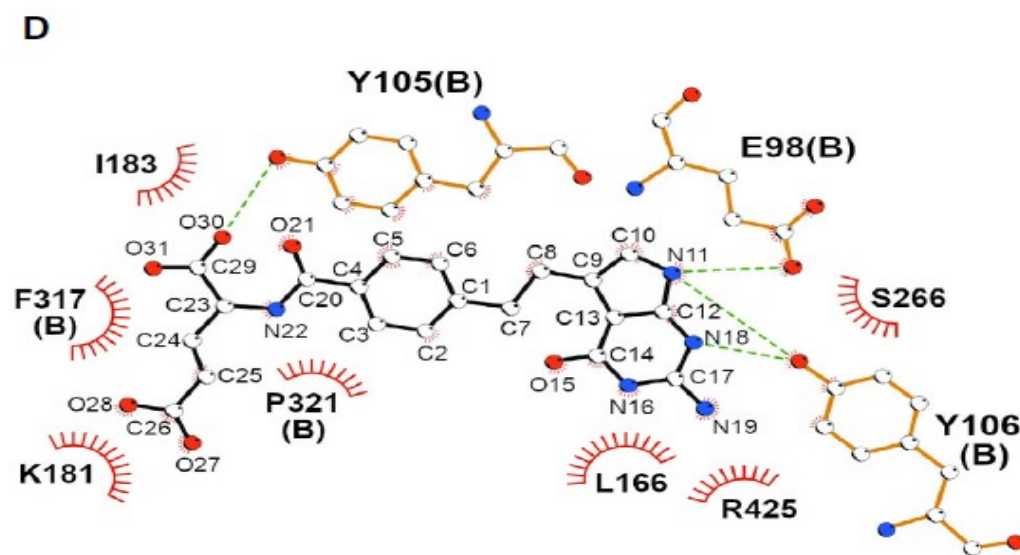
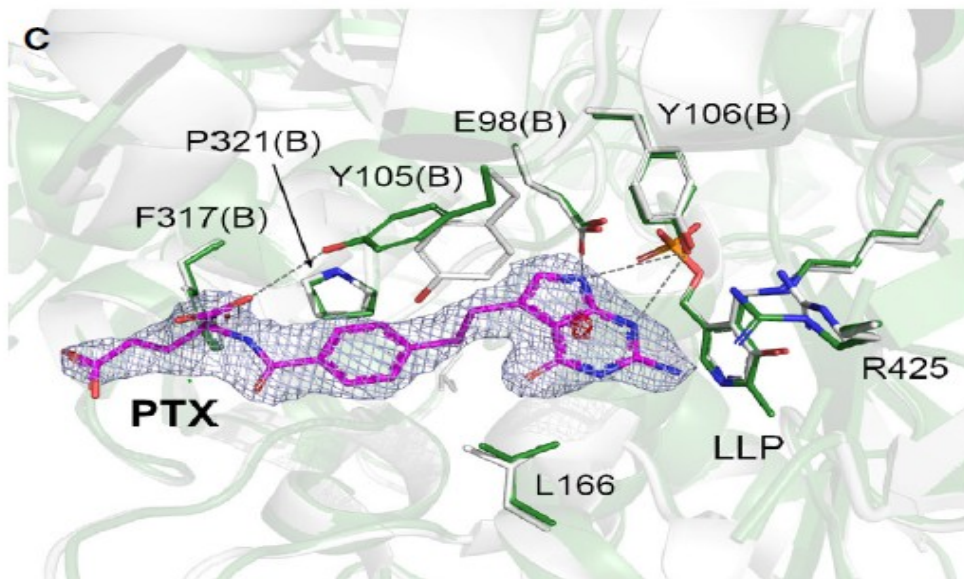
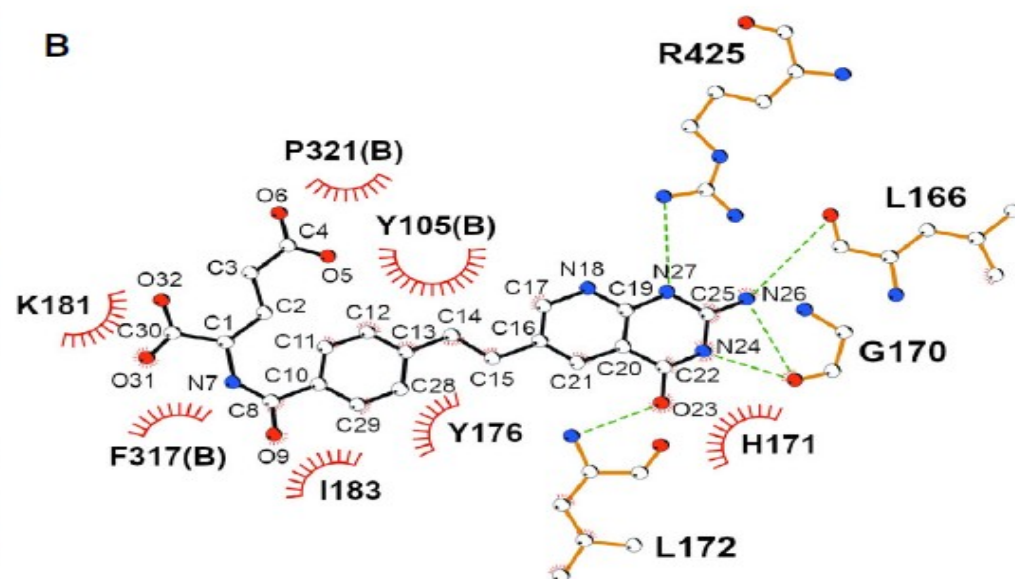
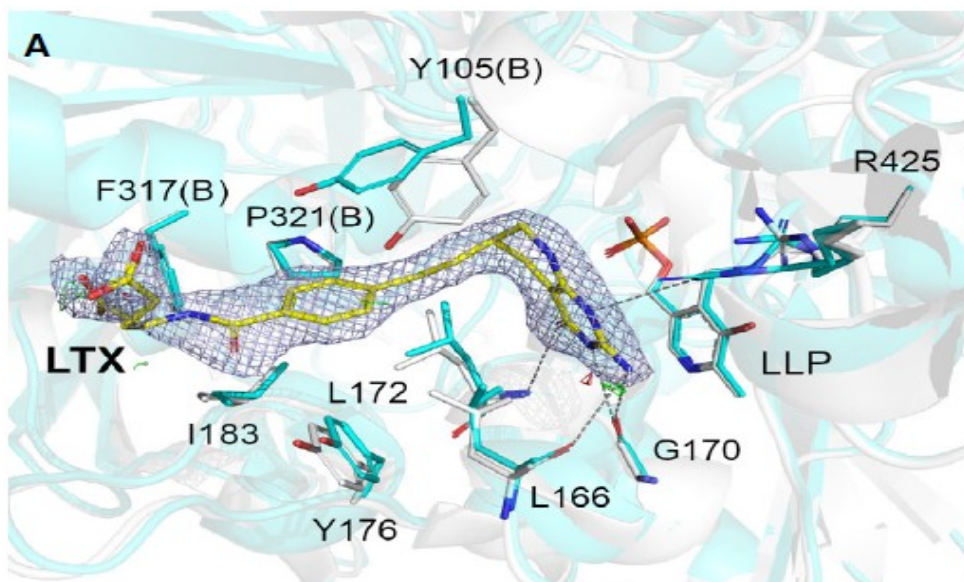
[a] Heat of binding (ΔH), the stoichiometry (n), and the dissociation constant (K_d) were calculated from plots of the heat evolved per mole of ligand injected versus the molar ratio of ligand to protein (for further details see Experimental Section); data represent the mean \pm SD of at least two independent experiments. [b] Experiment carried out in the presence of 200 μM lometrexol (LTX) in both *hcSHMT* and leucovorin solutions. [c] No binding observed; the signal measured superposes with that of the dilution of leucovorin into buffer (data not shown).

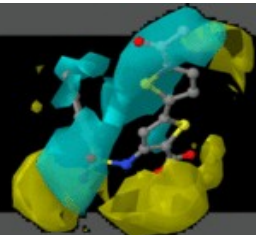
Lometrexol competitively inhibits SHMT with respect to leucovorin, with a measured K_i value of 204 μM , this value compares with the K_d value of 21 μM measured by ITC.



Lometrexol and Pemetrexed binding

by www.RCMD.it





Pyrazolopyran derivatives

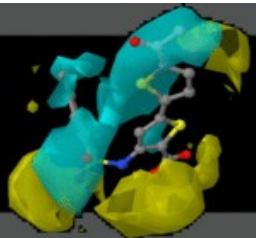
by www.RCMD.it

Table 2
Analysis of 2.12 and its analogues.

Compound	Structure	Assay	IC ₅₀ SHMT1 (μM)	IC ₅₀ SHMT2 (μM)
2.12		Quinonoid formation SHMT activity	44 ± 4 0.65 ± 0.05	256 ± 28 1.38 ± 0.11
2.2		Quinonoid formation SHMT activity	111 ± 30 12.7 ± 1	263 ± 48 17.4 ± 0.9
^a STL042011		Quinonoid formation SHMT activity	80% inhibition at 63 μM 69% inhibition at 63 μM	n.d. n.d.
^a STL054794		Quinonoid formation SHMT activity	81% inhibition at 63 μM 47% inhibition at 63 μM	77% inhibition at 63 μM 46% inhibition at 63 μM
^a STL371478		Quinonoid formation SHMT activity	61% inhibition at 63 μM 49% inhibition at 63 μM	80% inhibition at 63 μM 76% inhibition at 63 μM

nd., not determined.

^a Not soluble above 63 μM concentration in the conditions used in the assay.



Most efficient compound

by www.RCMD.it

Structure

Assay

IC₅₀ SHMT1 (μM)

IC₅₀ SHMT2 (μM)

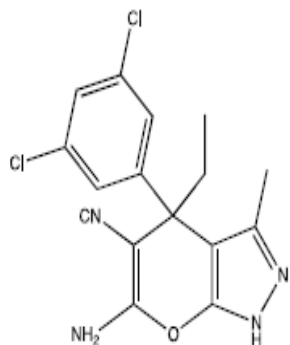
Quinonoid formation
SHMT activity

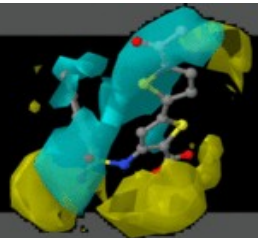
44 ± 4

0.65 ± 0.05

256 ± 28

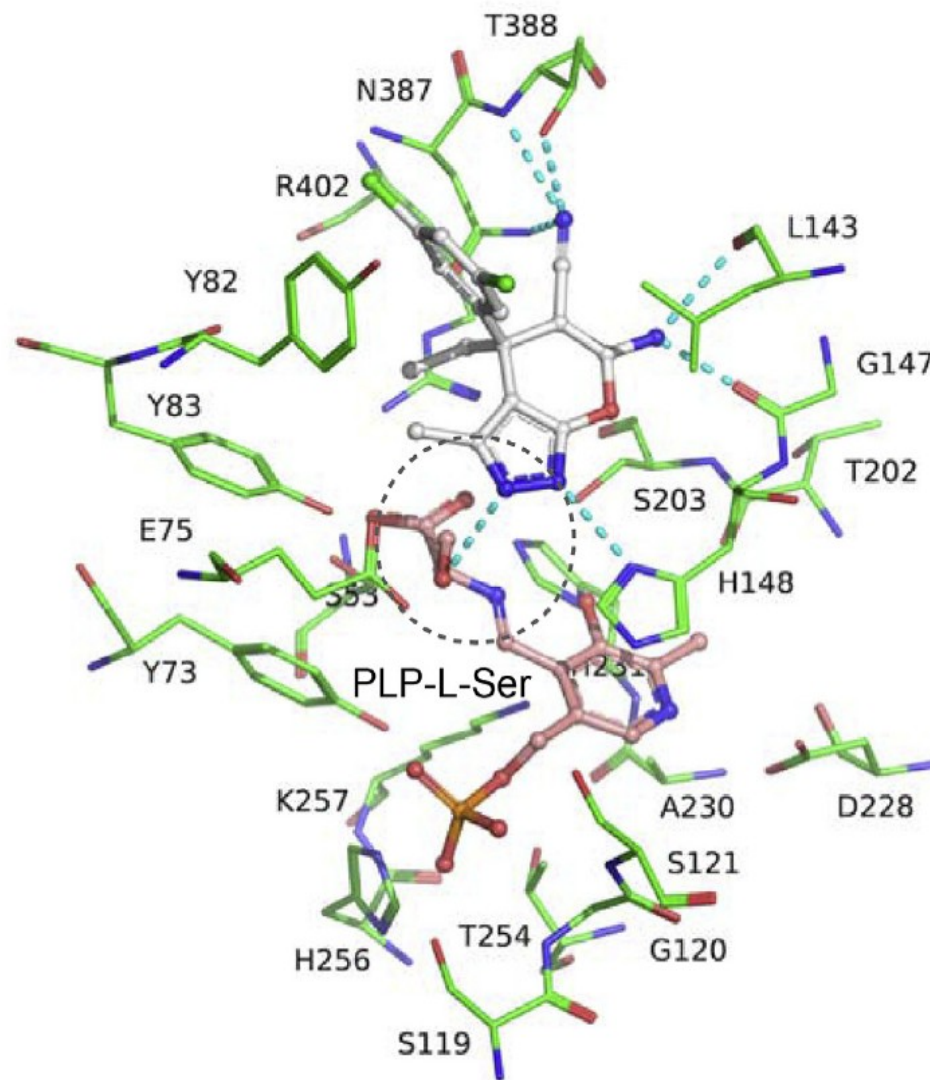
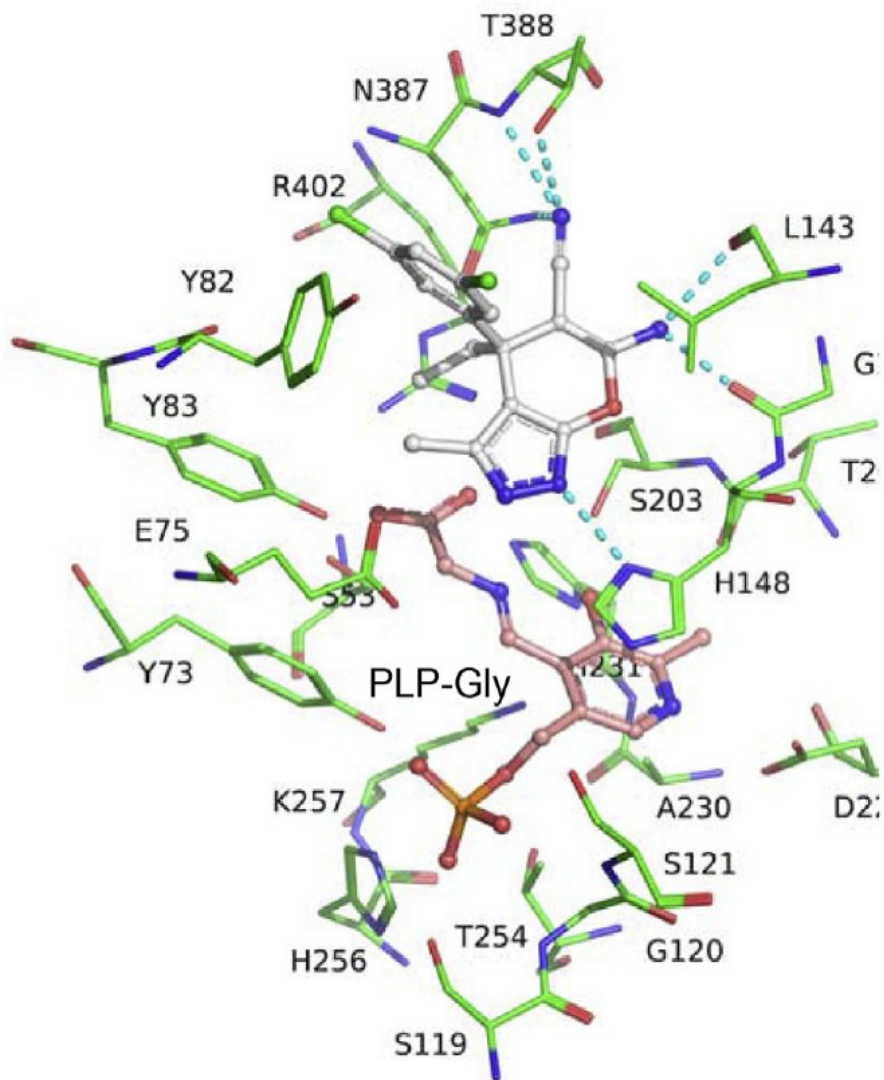
1.38 ± 0.11

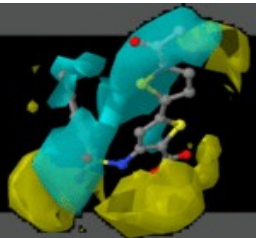




2.12 Binding

by www.RCMD.it





**THANK YOU FOR YOUR
ATTENTION!**